DEVELOPMENT OF NOVEL HOMOGENEOUS AND MAGNETIC HETEROGENEOUS CATALYSTS USING PARACETAMOL-BASED DEEP EUTECTIC SOLVENTS FOR ESTERIFICATION OF FREE FATTY ACIDS

ANDREW YEOW TZE HAO

FACULTY OF ENGINEERING
DEPARTMENT OF CHEMICAL ENGINEERING
UNIVERSITI MALAYA
KUALA LUMPUR

2024

DEVELOPMENT OF NOVEL HOMOGENEOUS AND MAGNETIC HETEROGENEOUS CATALYSTS USING PARACETAMOL-BASED DEEP EUTECTIC SOLVENTS FOR ESTERIFICATION OF FREE FATTY ACIDS

ANDREW YEOW TZE HAO

THESIS SUBMITTED IN FULFILMENT OF THE REQUIREMENTS FOR THE DEGREE OF MASTER OF ENGINEERING SCIENCE

FACULTY OF ENGINEERING
DEPARTMENT OF CHEMICAL ENGINEERING
UNIVERSITI MALAYA
KUALA LUMPUR

2024

UNIVERSITI MALAYA

ORIGINAL LITERARY WORK DECLARATION

Name of Candidate: Andrew Yeow Tze Hao

Matric No: S2149667

Name of Degree: Master of Engineering Science

Title of Thesis ("this Work"):

Development of Novel Homogeneous and Magnetic Heterogeneous Catalysts Using Paracetamol-Based Deep Eutectic Solvents for Esterification of Free Fatty Acids Field of Study: Chemical and Process

I do solemnly and sincerely declare that:

(1) I am the sole author/writer of this Work;
(2) This Work is original;
(3) Any use of any work in which copyright exists was done by way of fair dealing and for permitted purposes and any excerpt or extract from, or reference to or reproduction of any copyright work has been disclosed expressly and sufficiently and the title of the Work and its authorship have been acknowledged in this Work;
(4) I do not have any actual knowledge nor do I ought reasonably to know that the making of this work constitutes an infringement of any copyright work;
(5) I hereby assign all and every rights in the copyright to this Work to the Universiti Malaya ("UM"), who henceforth shall be owner of the copyright in this Work and that any reproduction or use in any form or by any means whatsoever is prohibited without the written consent of UM having been first had and obtained;
(6) I am fully aware that if in the course of making this Work I have infringed any copyright whether intentionally or otherwise, I may be subject to legal action or any other action as may be determined by UM.

Candidate's Signature Date: 25/11/2024

Subscribed and solemnly declared before,

Witness's Signature Date: 25/11/2024

Name:

Designation:

ABSTRACT

Oil palm milling processes generate large quantities of byproducts such as low-quality crude palm oil (LPO) that contain high free fatty acid (FFA) content. The use of these high FFA raw materials present major challenges as feedstocks for biodiesel production due to saponification reactions. Therefore, esterification reaction is the typical pretreatment process for high FFA feedstocks using methanol and acidic catalysts (such as sulphuric acid). In the works of this thesis, new homogeneous and heterogeneous acidic catalysts were developed. The homogeneous acid catalysts were developed based on deep eutectic solvents (DESs). Herein, paracetamol (PCM) was reported as a novel DES formed with Brønsted acids (5-sulfosalicylic acid (SSA) and benzenesulfonic acid (BZSA)) at a 3:1 molar ratio. At the optimized reaction conditions of 1.5 wt% DES catalyst dosage, 8:1 methanol-to-oil molar ratio, 50 °C reaction temperature for 50 min reaction time, the [3BZSA:PCM] DES achieved high FFA conversion at 86.4 %. On the other hand, at the optimized conditions of 2.5 wt% DES catalyst dosage, 16:1 methanol-to-oil molar ratio, 60 °C reaction temperature for 90 min reaction time, the [3SSA:PCM] DES achieved similarly high FFA conversion at 86.0 %. The activation energy was determined for the catalytic reaction using [3BZSA:PCM] and [3SSA:PCM] DESs, as 40.91 and 50.89 kJ/mol respectively, following the pseudo first order rate of reaction. Through the Eyring-Polanyi thermodynamic study, the DES-catalysed esterification reactions were endothermic, non-spontaneous and endergonic. However, the homogeneous DES catalysts exhibit challenges in recyclability and separation despite its high catalytic efficiency. Magnetic composites (Fe_3O_4/PVA) as support materials for acid catalysts is a viable protocol in improving the recyclability and separation performances. Therefore, SSA, BZSA, *p*-toluenesulfonic acid (PTSA) and their DES counterparts (formed with paracetamol at 3:1 molar ratio) were investigated to be supported on Fe_3O_4/PVA to yield heterogeneous catalysts for FFA esterification in LPO. From the

screening results, Fe_3O_4/PVA/PTSA was determined as the best catalytic activity for FFA esterification reaction. The optimized reaction conditions were determined: 10 wt% catalyst loading, 20:1 methanol-to-oil molar ratio, 5 h of contact time and at 60 °C, resulting in an FFA conversion of 79.81 %. Fe_3O_4/PVA/PTSA exhibited fair recyclability performances and stability with > 65 % FFA conversion after five successive runs. FFA esterification reaction using Fe_3O_4/PVA/PTSA was determined to require an activation energy of 43.72 kJ/mol following the pseudo first order rate of reaction. By comparing the operating conditions of both types of catalysts, the heterogeneous Fe_3O_4/PVA/PTSA magnetic catalyst required double the reaction conditions compared to the homogeneous DESs in catalysing the esterification reaction. However, from the perspective of catalyst recyclability, the magnetically recoverable Fe_3O_4/PVA/PTSA catalyst can be recycled for five times with improved stability, while the homogeneous DESs exhibited significant challenges in catalyst recycling. Additionally, the pristine sulphonic acids exhibited better compatibility to be supported on Fe_3O_4/PVA magnetic composite than their DES counterpart, with Fe_3O_4/PVA/PTSA being a viable catalyst for the pretreatment of low-quality oils through FFA esterification.

Keywords: Deep eutectic solvents, esterification, free fatty acid, magnetic support, sulfonic acids.

ABSTRAK

Proses pengilangan kelapa sawit menjana produk sampingan yang berlebihan seperti minyak sawit mentah berkualiti rendah (LPO) yang mengandungi kandungan asid lemak bebas (FFA) yang tinggi. Penggunaan bahan mentah yang mengandungi FFA yang tinggi memberikan cabaran utama dalam proses pengeluaran biodiesel akibat tindak balas saponifikasi. Oleh itu, tindak balas pengesteran adalah proses prarawatan biasa untuk bahan mentah FFA yang tinggi menggunakan metanol dan pemangkin berasid (seperti asid sulfurik). Dalam kerja-kerja tesis ini, pemangkin berasid homogen dan heterogen baru telah dibangunkan. Pemangkin asid homogen telah dibangunkan berdasarkan pelarut eutektik (DES). Parasetamol (PCM) digunakan sebagai penjana DES dengan asid Brønsted (asid 5-sulfosalisilik (SSA) dan asid benzenasulfonik (BZSA)) pada nisbah molar 3:1. Pada keadaan tindak balas yang dioptimumkan sebanyak 1.5 wt% dos pemangkin DES, nisbah molar metanol-ke-minyak 8:1, suhu tindak balas 50 °C selama 50 minit masa, DES [3BZSA:PCM] mencapai penukaran FFA yang tinggi pada 86.4 %. Sebaliknya, pada keadaan optimum sebanyak 2.5 wt% dos pemangkin DES, nisbah molar metanol-ke-minyak 16:1, suhu tindak balas 60 °C selama 90 minit masa, DES [3SSA:PCM] mencapai FFA yang setinggi penukarannya pada 86.0 %. Tenaga pengaktifan ditentukan untuk tindak balas pemangkin menggunakan [3BZSA:PCM] dan [3SSA:PCM] DESs, masing-masing sebagai 40.91 dan 50.89 kJ/mol, mengikuti kadar tindak balas tertib pertama pseudo. Melalui kajian termodinamik Eyring-Polanyi, tindak balas pengesteran berpemangkin DES adalah endotermik, tidak spontan dan endergonik. Walau bagaimanapun, pemangkin DES homogen mempamerkan cabaran dalam kebolehkitar semula dan pengasingan walaupun kecekapan pemangkinnya yang tinggi. Komposit magnetik (Fe_3O_4/PVA) sebagai bahan sokongan untuk pemangkin asid adalah protokol yang berdaya maju dalam meningkatkan prestasi kitar semula dan pemisahan. Oleh itu, SSA, BZSA, asid p-toluenasulfonik (PTSA) dan komponen DES (dibentuk

dengan parasetamol pada nisbah 3:1 molar) telah disiasat untuk disokong pada Fe_3O_4/PVA untuk menghasilkan pemangkin heterogen untuk pengesteran FFA dalam LPO. Daripada keputusan saringan, Fe_3O_4/PVA/PTSA telah ditentukan sebagai aktiviti pemangkin terbaik untuk tindak balas pengesteran FFA. Keadaan tindak balas yang optimum ditentukan sebagai: 10 wt% pemuatan pemangkin, nisbah molar metanol-ke-minyak 20:1, 5 jam masa dan pada 60 °C suhu tindak balas, menghasilkan penukaran FFA sebanyak 79.81 %. Fe_3O_4/PVA/PTSA mempamerkan prestasi kebolehkitar semula yang baik dan kestabilan dengan > 65 % penukaran FFA selepas lima kali berturut-turut. Tindak balas pengesteran FFA menggunakan Fe_3O_4/PVA/PTSA ditentukan untuk memerlukan tenaga pengaktifan 43.72 kJ/mol mengikut kadar tindak balas tertib pertama pseudo. Dengan membandingkan keadaan operasi kedua-dua jenis pemangkin, pemangkin magnet Fe_3O_4/PVA/PTSA heterogen memerlukan dua kali ganda keadaan tindak balas berbanding DES homogen dalam mepemangkinkan tindak balas pengesteran. Walau bagaimanapun, dari perspektif kebolehkitar semula pemangkin, pemangkin Fe_3O_4/PVA/PTSA yang boleh dipulihkan secara magnetik boleh dikitar semula sebanyak lima kali dengan kestabilan yang baik, manakala DES yang homogen mempamerkan cabaran yang ketara dalam kitar semula pemangkin. Selain itu, asid sulfonik tulen mempamerkan keserasian yang lebih baik untuk disokong pada komposit magnet Fe_3O_4/PVA berbanding dengan komponen DES, dan Fe_3O_4/PVA/PTSA dipilih sebagai pemangkin yang berdaya maju untuk prarawatan minyak berkualiti rendah melalui pengesteran FFA.

Keywords: Asid lemak bebas, asid sulfonik, pengesteran, pelarut eutektik, bahan sokongan magnetik.

ACKNOWLEDGEMENTS

I would like to sincerely thank my esteemed supervisors – Dr. Adeeb Hayyan and Dr. Mohd Usman Mohd Junaidi, for their invaluable supervision, continuous support and unwavering guidance during the course of my research work and studies. I would like to give a significant acknowledgement and appreciation to Dr. Chan Mieow Kee at the Department of Chemical Engineering, SEGi University for her unconditional technical support during the period of my laboratory investigations. Additionally, I would like to express gratitude to Emeritus Prof. Mohd Ali Hashim for his treasured support and advisory that was influential in the direction of my results and thesis. I also thank my lab colleagues, including Dr. Shahira, Dr. Khalid and Dr. Mohamed for their mentorship and being part of the research team. My appreciation also goes out to my family and friends for their encouragement and support all through my studies.

TABLE OF CONTENTS

LIST OF FIGURES

LIST OF TABLES

LIST OF SYMBOLS AND ABBREVIATIONS

ATR	:	Attenuated total reflectance
BZSA	:	Benzenesulfonic acid
CPO	:	Crude palm oil
DES	:	Deep eutectic solvent
FAME	:	Fatty acid methyl ester
FFA	:	Free fatty acid
FTIR	:	Fourier transform infrared spectroscopy
IL	:	Ionic liquid
KOH	:	Potassium hydroxide
NaOH	:	Sodium hydroxide
PTSA	:	*p*-toluenesulfonic acid
SAC	:	Solid acid catalyst
SSA	:	5-sulfosalicylic acid
UCO	:	Used cooking oil

CHAPTER 1: INTRODUCTION

1.1 Research Background

The advent of increasing global energy demands has brought forward the need to develop sustainable technologies in energy production. Additionally, with the exacerbating rise of carbon emissions, the urgency to find alternative energy sources that are renewable, produces minimal or zero emissions, and environmentally sustainable is critical. In energy generation, there are pressing needs to transition away from non-renewable fossil fuels to renewable methods, and this has garnered significant research efforts into realizing energy from renewable materials and technologies that allows for the reduction of carbon emissions (Naji *et al.*, 2021). Among the various energy resources, biofuels (such as biodiesel, bioethanol and bioether) have emerged as viable source of renewable energy with high prospects in greenhouse gases emission reduction and alleviating global warming (Xie and Li, 2023). Liquid biofuels, specifically biodiesels, have gained significant prominences as a petroleum-derived diesel fuel substitute. According to Awogbemi & Kallon (2023), the global production of biodiesel increased from 38 billion litres in 2016 up to 60.7 billion litres at the end of 2022 (Figure 1.1). Correspondingly, the worldwide biodiesel market size is predicted to be valued at USD 190 billion in the year 2030, more than five-fold increase compared to the assessment year of 2021 at USD 32 billion (Awogbemi and Kallon, 2023). Hence, the demand for biodiesel has shown to be increasing across the year due to increases in demand for renewable energy. Biodiesel exhibits multitude of advantages of petroleum-based diesel fuel, such as being nontoxic, highly biodegradable in nature, being derivable from renewable sources while exhibiting similar combustion characteristics to petroleum-based diesel fuel (Changmai *et al.*, 2020). Biodiesel can be directly used as diesel fuels in conventional diesel engines and its integration does not require significant modifications to existing systems and designs. Furthermore, the combustion of biodiesel

fuel in a diesel engine is comparatively cleaner to its petroleum-derived counterpart with lower carbon monoxide, carbon dioxide, sulphur, polycyclic aromatic hydrocarbons and particulate matter emissions (Roslan *et al.*, 2022; Wang *et al.*, 2023a). According to several studies regarding the life cycle analysis of carbon dioxide emission, the production of biodiesel has been determined to reduce carbon dioxide emissions by 79 – 86 % compared to petroleum diesel fuel due to the cultivation and the catalytic conversion of the feedstocks into fuel (Esmaeili, 2022; Foteinis *et al.*, 2020; Xu *et al.*, 2022).

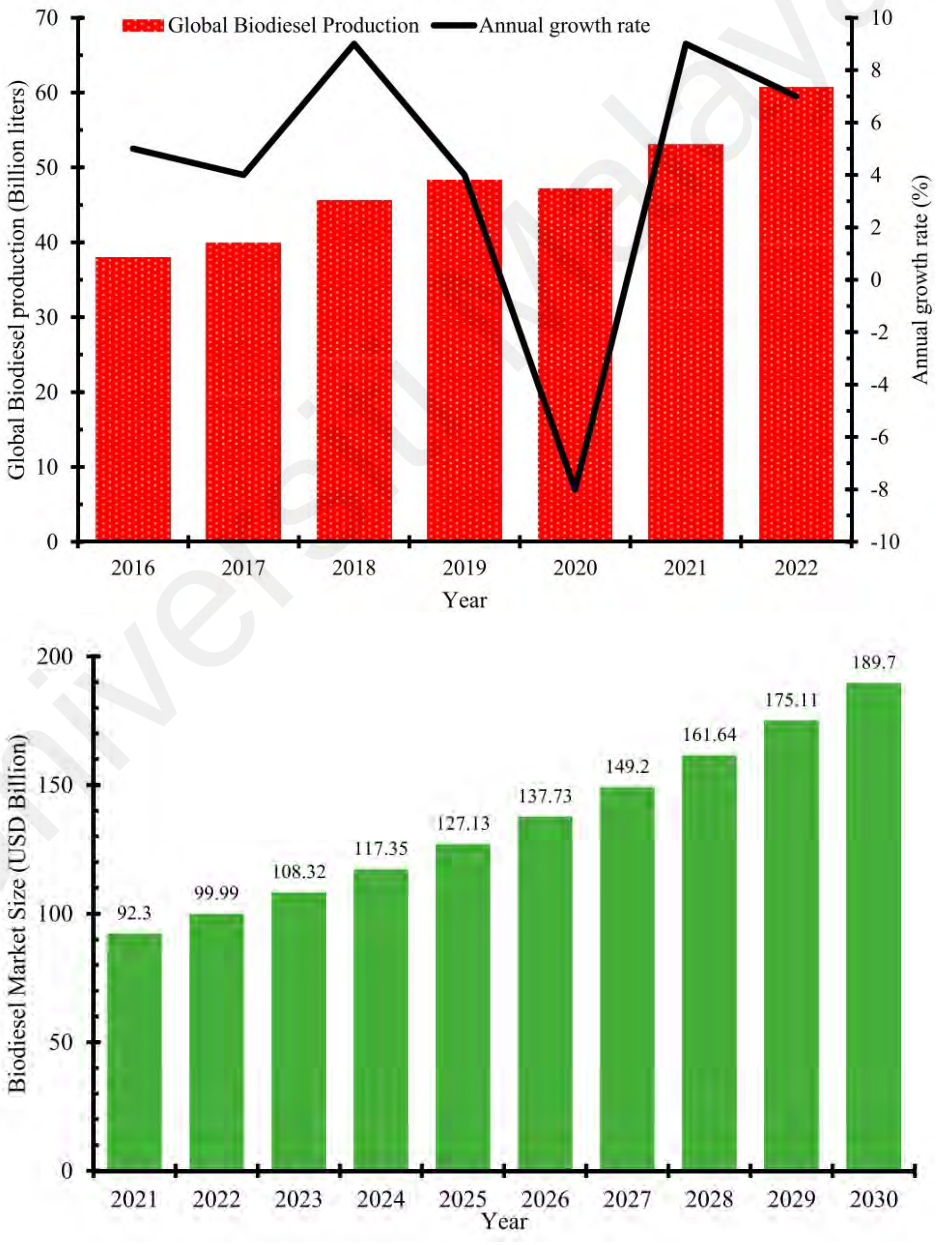

Figure 1.1: Global production of biodiesel between 2016 – 2022, and the market size of biodiesel from 2021 to 2030 (Awogbemi and Kallon, 2023).

While biodiesel fuel has evident advantages, the adoption and commercialization of biodiesel production is largely restricted based on the use of high purity virgin oil as its feedstock. This has led to uncompetitive, high costs of production due to the high costs of the pristine feedstock used, and concerns related to oil supply competition and food security (Farobie and Hartulistiyoso, 2022). Additionally, its sustainability aspects as a renewable energy resource has been questioned due to the requirements of land clearing to grow the oil crops necessary for biodiesel feedstock, resulting in significant occurrences of vast deforestation (Halimatussadiah *et al.*, 2021; Szulczyk *et al.*, 2021). These challenges are attributed to the production of first-generation biodiesel, where high purity virgin oils are used as feedstocks (Malode *et al.*, 2021). To overcome these challenges, succeeding generations (second, third and fourth) of biodiesel seek to transition away from the use of virgin oil with the use of non-conventional biodiesel feedstocks. Biodiesel production using feedstocks that are typically derived from non-food yields and waste residues, including residual biomass, waste oils and industrial effluents pertain to the production of second generation biodiesels, and this method can enhance its renewable aspect as a biofuel (Ahmed and Huddersman, 2022). Furthermore, low-value waste materials such as agro-industrial oils, brown grease, municipal sewage sludge, sludge oils, tannery waste fats, and used cooking oils (UCOs) have been explored as a biodiesel feedstock that enabled cost reduction in biodiesel manufacturing (Bai *et al.*, 2022; Booramurthy *et al.*, 2020; Liu *et al.*, 2021). As the cost of biodiesel feedstocks contribute greatly to the cost of biodiesel manufacturing with a make-up of 70 – 80 %, efforts to reduce the manufacturing costs of biodiesel can be realized by utilizing low-value, waste sources of fats (Mamtani *et al.*, 2021). The valorisation of the concerning feedstocks in efforts to reduce the production costs of biodiesel production and its reliance on high purity feedstocks can be realized with an additional pretreatment process

involving esterification reactions, and its relevant process catalysts and reaction optimization.

The use of non-food yields and waste residues as feedstocks for the production of second-generation biodiesel is not compatible with existing alkaline-catalysed transesterification processes due to the presence of high free fatty acid (FFA) content as its main impurity. Undesirable saponification reactions with the transesterification reaction process occur in the presence of high FFA content, resulting in soap formation and catalyst loss. Therefore, a prior esterification reaction step can be used to deacidify the feedstock and reduce the FFA content to a limit acceptable for transesterification to minimize soap formation and alkaline catalyst deactivation. Conventionally, esterification processes employ homogeneous acid catalysts (for example, sulphuric acid) to catalyse the esterification reaction. However, these homogeneous acid catalysts exhibit significant limitations such as being highly corrosive, non-recyclable and highly challenging to separate and purify. As such, various forms of catalysts have been developed for FFA esterification, such as ionic liquids (ILs) and deep eutectic solvents (DESs) in homogeneously catalysed system, and sulphonic acid functionalized solid acid catalysts (SACs) in heterogeneously catalysed systems.

1.2 Problem Statement

Esterification processes conventionally utilize homogeneous mineral/organic acids as catalysts to catalyse the esterification reaction of FFAs. However, these acid catalysts are highly hygroscopic in nature that possesses limitations in reaction transformation due to the promotion of hydrolysis reactions (Melero *et al.*, 2013). Homogeneous acid catalysts are prone to deactivation due to the presence of water content that induces inhibition to the catalysts (Liu *et al.*, 2006). As a result, the acid catalyst consumption in esterification

reaction processes is high due to its non-recyclability and subsequent reduction in catalytic activity, and additionally causes challenges in catalyst separation, recovery and purification. Subsequently, ILs have been developed as novel homogeneous acid catalysts, however its applications are relatively constrained by the cost of materials and synthesis, and the concerns of toxicity. Therefore, DESs were introduced as the alternative solution to overcome the challenges associated with the existing development of homogeneous acid catalysts. The formation of a deep eutectic solvent (DES) system can overcome the hygroscopicity problem of the pristine acid as it is subdued by hydrogen bonding formation and preserves the active sites of the acid catalysts. The formation of novel DES compounds can imbue the catalyst with recyclable properties, improving the practical applications of the catalyst for the esterification reactions. However, the recyclability of the DES compounds is recently known to be weaker compared to other forms of homogeneous acid catalyst (Hayyan *et al.*, 2023a). To address this observation, the suitable development of heterogeneous acid catalysts can enable improved recyclability and catalytic performances. Additionally, heterogeneous, magnetic forms of catalysts can be adapted and developed to improve the recovery of the heterogeneous acid catalysts. Therefore, the development of acid catalysts in both homogeneous and heterogeneous forms are of research interest for FFA esterification processes.

1.3 Research Objectives

The works described in this thesis aims to develop viable catalysts (homogeneous and heterogeneous catalyst materials) for the esterification of high FFA content in low-quality palm oil, that is employed as the representative feedstock for the production of biodiesel. Hence, the objectives of this research are:

1. To prepare novel DESs as homogeneous acid catalysts from API for the esterification of FFA.
2. To develop heterogeneous acid catalysts with magnetic properties as a support material for esterification of FFA and for improvement of catalyst recyclability.
3. To investigate different operating conditions such as catalyst dosage, alcohol dosage, reaction time and reaction temperature for both homogeneous and heterogeneous acid catalysts.
4. To evaluate the reaction kinetics, reaction mechanism and thermodynamic behaviour of the homogeneous and heterogeneous acid catalysts.

1.4 Research Scope

The scope of research in the works of this thesis are presented as below:

- Background studies and literature review are conducted on the study of biodiesel production methods demonstrated in industry and current research, and the relevant and recent advances in catalyst development for both homogeneous and heterogeneous catalytic systems.
- Selection of chemical components based on APIs to design novel DES catalysts, leading to the synthesis of the novel DESs.
- Design of heterogeneous catalyst support materials with magnetic properties and the investigation of the feasibility in supporting the DESs to yield a heterogeneous catalyst.
- Characterization of homogeneous DESs and heterogeneous acid catalysts using analytical methods, including spectroscopic and thermogravimetric methods.

- Validation of the optimal experimental conditions in FFA esterification and assessment of catalyst recyclability for both homogeneous DESs and heterogeneous acid catalysts.
- Calculation and determination of reaction kinetic parameters and thermodynamic factors of the homogeneous DESs and heterogeneous acid catalysts.

1.5 Outline of Thesis

This thesis is composed of five chapters, listed as below:

Chapter 1 provides a preliminary introduction into biofuels (biodiesel) production as a means to improve renewable energy generation, and the purpose for alternative, sustainable biodiesel feedstocks. The research problem statement, objectives, research methodology and thesis outline are presented.

Chapter 2 provides a comprehensive background and literature review on the biodiesel production techniques, including esterification and transesterification processes. Recent reports on the advancements of both heterogeneous and homogeneous catalyst designs are presented and discussed. The research gaps are identified and presented from the results of the literature review, and constructs the research basis of the thesis.

Chapter 3 details the research methodology on the FFA using novel DESs employed as acid catalysts comprising active pharmaceutical ingredients (APIs) as its component. Subsequently, the methodology on the design and synthesis of the DESs onto heterogeneous catalyst support is presented.

Chapter 4 describes the experimental results of the optimization study for both homogeneous DESs and heterogeneous acid catalysts, and discusses the optimum

reaction conditions determined. Furthermore, the characterization studies of the novel DESs, and the reaction kinetics and thermodynamic studies are presented.

Chapter 5 presents the conclusion of the thesis, along with several future recommendations discussed.

CHAPTER 2: LITERATURE REVIEW

2.1 Production of Biodiesel

Biodiesel is a liquid fuel mixture of fatty acid alkyl esters (FAAE) produced as a form of biofuel to be used as a direct replacement or as a blend with existing petroleum-derived diesel fuel. The quality of commercially produced biodiesel should conform to the fuel specifications of international standards, such as the EN 14214 standard published by the European Committee for Standardization (CEN) and/or the ASTM D6751 published by ASTM International. For example, the fuel specification of biodiesel includes physical properties such as its cetane number, cloud point, flash point, heating value, kinematic viscosity and sulphur content. Conventionally, commercial biodiesel is produced through the direct transesterification reaction of triglycerides from feedstocks of crop yield sources. The source of the crop feedstocks are usually endemic with respect to the location of the production facility. For example, palm oil is the dominant oil crop used as raw feedstocks in the biodiesel production and output of tropical countries including Malaysia, Nigeria and Indonesia; and soybean oil remains the primary oil crop source for biodiesel production in the United States (Parveez *et al.*, 2024; Xu *et al.*, 2022). In this context, the oil crops consumed in the transesterification reaction are required as high purity feedstocks, and thus undergo several refining stages (such as degumming, bleaching and deodorizing) prior to transesterification. The direct transesterification reaction is conducted in the presence of a short chain alcohol (methanol, ethanol) and a homogeneous basic catalyst (potassium hydroxide). Alternatively, biodiesel is also produced from the esterification reaction of fatty acids or FFAs. Conventionally, the mature industrial process of biodiesel production involves either single-step direct transesterification, or a two-step reaction process, involving esterification leading to transesterification (Thoai *et al.*, 2019). However, the selection of process in the production of biodiesel is determined by the type of oil feedstock and its qualities (edible

or non-edible oils), the choice of alcohol (as reactants and reaction solvents) and the type of catalysts chosen, as depicted in Figure 2.1.

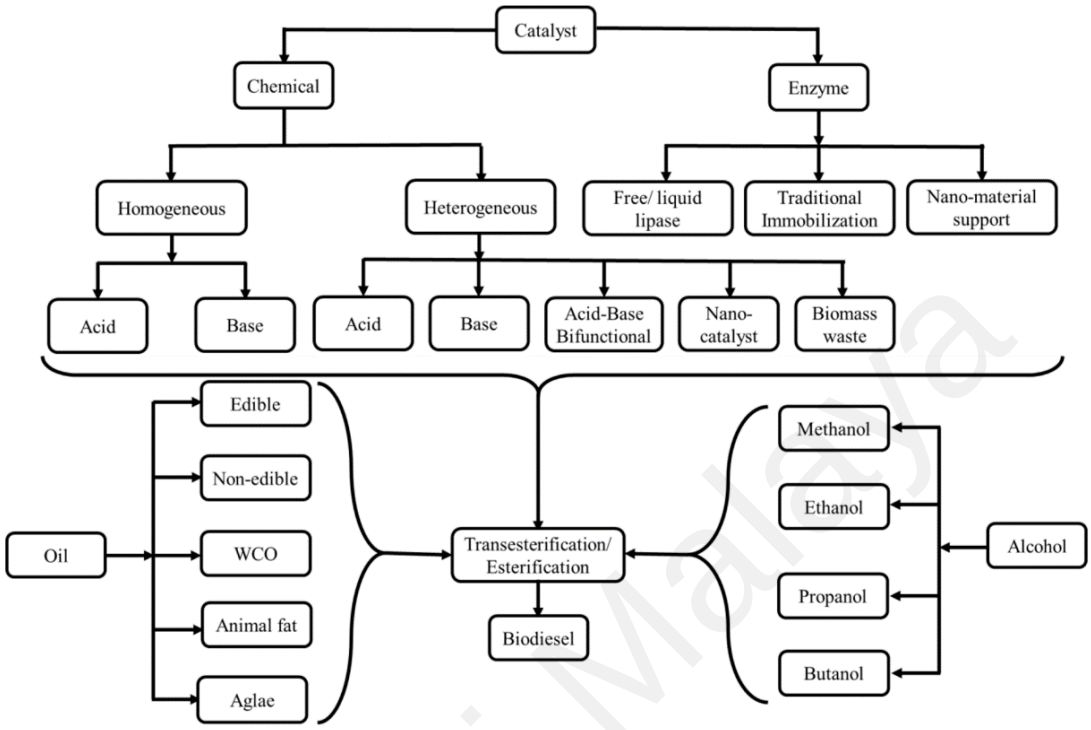

Figure 2.1: Process selection of biodiesel production process (Mandari and Devarai, 2022).

According to literature, biodiesel feedstocks are classified into generations from first to fourth to distinguish its differences in feedstock source and utilization (Camilo *et al.*, 2024). Biodiesel produced from the use of edible food crops are classified as first-generation biodiesel. This includes the consumption of oils from common crop yields such as refined canola, soybean, rapeseed and palm oil. The commercial production of biodiesels is dominated by the consumption of first-generation feedstock owing to the relative ease of feedstock conversion procedure, the ready availability of crops and its high scalability to meet fuel demands (Singh *et al.*, 2020). According to the estimations of the Organisation for Economic Cooperation and Development (2016), 81 % of the global biodiesel production was generated from refined vegetable oils, and 77 % of global

bioethanol production was obtained from maize and sugarcane processing. The disadvantages associated with first-generation biodiesel arise from the consumption of refined oil yields supplied for food production, thereby leading to economic imbalances in the pricing of foods derived from the refined oil (Mat Aron *et al.*, 2020; Singh *et al.*, 2020). Additionally, the limited availability of land area for the cultivation of oil crops to yield feedstocks for biodiesel production causes concerns for land clearing and vast deforestation. These disadvantages have spurred the exploration of alternative types of biodiesel feedstocks. A visual categorization of the biodiesel generations discussed is summarized in Figure 2.2.

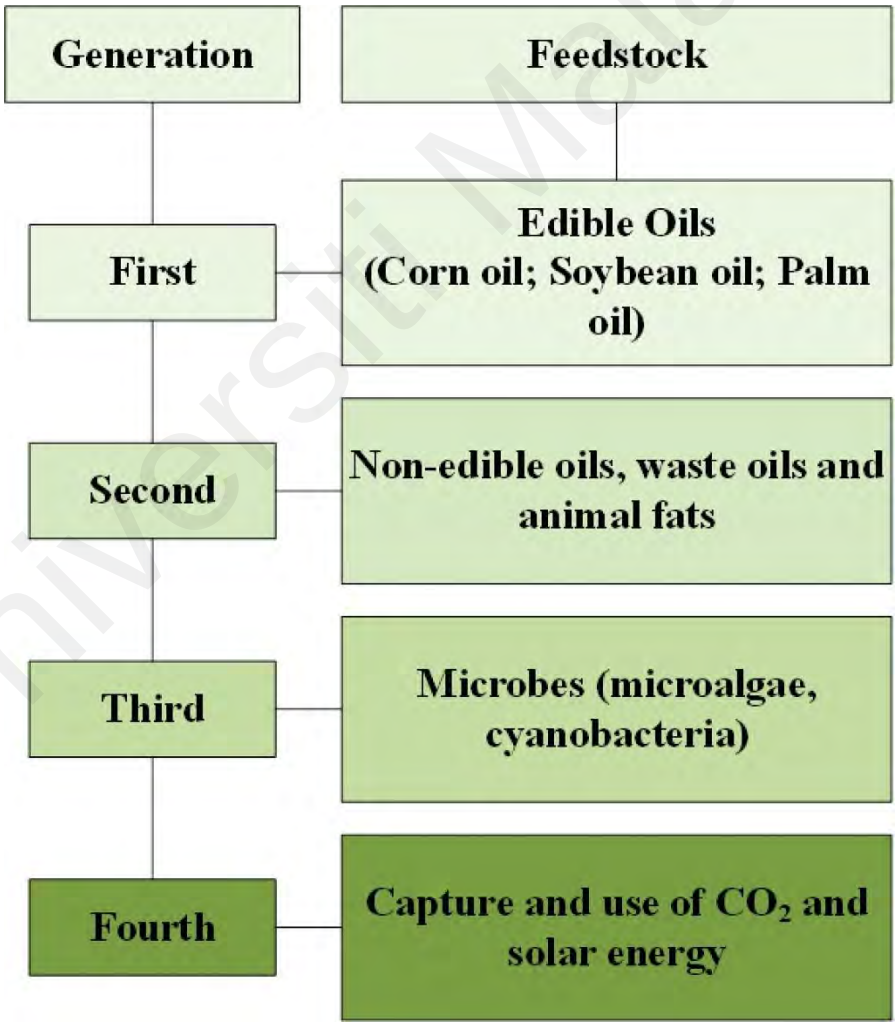

Figure 2.2: Categorization of biodiesel generations (Camilo *et al.*, 2024).

To overcome the drawbacks associated with first-generation biodiesel feedstocks, biodiesel can be viably produced from alternative, non-edible oil feedstocks, and are classified under second-generation biodiesels (Correa *et al.*, 2017). Non-edible oils such as castor, *Jatropha curcus*, rubber seed, tall oil and Mahua oil; and waste oils such as UCOs, discarded industrial oils, animal fats, industrial wastes and byproducts, sludge and grease are among the choices of sources generally classified under second-generation biodiesel feedstocks (Ahmed and Huddersman, 2022; Singh *et al.*, 2024; Zhu *et al.*, 2024). Additionally, forestry and agricultural waste that contain lignocellulosic material that can be valorised are similarly considered as second-generation biodiesel feedstocks (Saravanan *et al.*, 2022). The advantages of second-generation feedstocks are its non-competition with food supply and land use due to the inedible nature of the oils, and the low production costs associated with the utilization of low-value, waste materials. However, second-generation feedstocks are likewise faced several disadvantages, such as the low yield of non-edible crops, and the high variability of the chemical composition and impurities content of the waste feedstocks that restrict efficient scaling up of the biodiesel production process (Camilo *et al.*, 2024). Despite the disadvantages, the production of second-generation biodiesel remains attractive due to the prospects of cost reduction in utilization low-value, waste materials. For example, the production of biodiesel from waste cooking oils/ UCOs is a highly promising practice in producing sustainable and renewable energy while addressing the environmental concerns of improper disposal of excess waste cooking oils (Devaraj Naik and Udayakumar, 2021; Foteinis *et al.*, 2020).

To eliminate the reliance of plant-based feedstocks, research attention has been diverted to the production of third-generation biodiesel derived from microalgae biomass (Deshmukh *et al.*, 2019; Gaurav *et al.*, 2024). Microalgae has been touted as a highly viable source for the production of third-generation biodiesel due to its high lipid yield

and content, high productivity in microalgae cultivation, and reduction in the dependence of land cultivation while having the prospects of being cultivated in unproductive drylands. More importantly, third-generation biodiesel feedstocks enable significant reduction in greenhouse gas emissions compared to first- and second-generation biodiesel (Uslu *et al.*, 2023). However, the technology required for the production of third-generation biodiesel is comparatively niche compared to the more established first- and second-generation biodiesel production methods, and are disadvantageous due to the high initial investment costs and challenges in industrial scale implementation (Singh *et al.*, 2024). The advancement of biodiesel production in the fourth-generation is attributed to the emphasis on capturing and utilizing solar energy and carbon dioxide. Generally, fourth-generation biodiesel feedstocks encompass advances in photo-biological systems, such as the genetic modification of feedstocks and the metabolic engineering of algae feedstocks, resulting in high biomass yield (Cavelius *et al.*, 2023; Mat Aron *et al.*, 2020). The development of fourth-generation biodiesel feedstocks is relatively in its infancy and show high prospects for the sustainable production of biodiesel.

Malaysia is the second largest country in the production of palm oil, having a crude palm oil (CPO) production capacity of 19.2 million tons in the year 2020 (Srikumar *et al.*, 2024). As a result, various forms of palm oil milling and refining wastes and byproducts are produced, such as sludge palm oil (SPO), palm oil mill effluent (POME) and low-quality crude palm oil (LPO), and presents attraction opportunities in research and development to utilize the abundances of these waste materials (Parveez *et al.*, 2024). Among the selection of feedstocks available for biodiesel production, LPO, a form of agro-industrial oil byproduct from palm oil milling, is an attractive source of biodiesel feedstocks due to its high abundances and low costs (Zahan and Kano, 2018). LPO is characterized by its high acidity with high FFA content as its main impurity, and is non-edible with low commercial value, thereby posing no competition with food supply

resources due to the strict requirement in specification of refined CPO. Based on these characteristics, LPO is chosen as the representative feedstock for the research works of this thesis.

2.1.1 Transesterification of Triglycerides

Direct transesterification of crude vegetable oil is the most ubiquitous process in the industry of biodiesel production. In a typical alkali-catalysed transesterification process, lipids in the form of triglycerides are reacted with short chain alcohols (most commonly methanol) to yield fatty acid methyl esters (FAME) and glycerol, as presented in Figure 2.3. In the case of using ethanol as the reactant and solvent within the transesterification reaction, fatty acid ethyl esters (FAEE) are yielded. The transesterification of triglycerides is a reversible reaction, consisting of three consecutive reactions involving the conversion of triglycerides to diglycerides, diglycerides to monoglycerides, and terminally monoglycerides to glycerol. Methanol is chosen as the preferred short chain alcohol due to its low costs, high activity and suitable physicochemical properties for phase separation (Panchal *et al.*, 2020). The choice of alcohol is supplied in excess to drive the reaction equilibrium forward towards the formation of products.

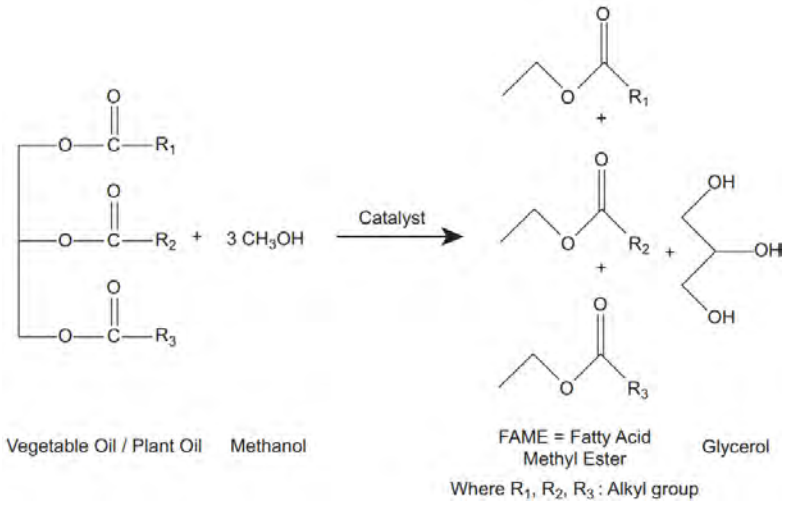

Figure 2.3: Chemical reaction of triglyceride transesterification with methanol.

The production efficiency and yield of biodiesel from alkali-catalysed transesterification processes are primarily influenced by the quality of feedstock and the performance of the catalyst. the quality of feedstock is an important measure as the presence of impurities such as FFA and moisture content in oil feedstocks supplied for direct transesterification reactions causes undesirable saponification side reactions to occur, causing catalyst deactivation and challenges in downstream biodiesel separation and purification. Due to the sensitivity of the catalyst, the process of biodiesel production involves the use of high purity, virgin vegetable oils as its feedstock (Kibar *et al.*, 2023). On the other hand, the type of catalysts influences the reaction conditions of the biodiesel transesterification process. In this context, homogeneous basic catalysts, heterogeneous basic catalysts and enzymatic catalysts can be used to produce FAME via transesterification. The involvement of alkali catalysts in transesterification reaction concerns the increased yield of the FAME product and increased rate of reaction.

The use of homogeneous alkali catalysts, such as sodium hydroxide (NaOH) or potassium hydroxide (KOH), requires lower catalyst loading and provides faster reactions, at the expense of weak catalyst recycling efficiencies and recovery. Although the alkali-catalysed reactions are comparably higher than heterogeneous catalysts, the economical aspect may be hindered due to catalyst consumption (Wang *et al.*, 2023a). An alternative approach is the utilization of heterogeneous alkali catalysts. In transesterification-based catalysis, heterogeneous alkali catalysts exhibit higher catalytic potential than homogeneous alkali catalysts based on the benefits of higher selectivity and conversion activity due to the improved availability of catalytic active sites (Basumatary *et al.*, 2023; Mahdi *et al.*, 2023). Furthermore, heterogeneous alkali catalysts exhibit greater stability and recyclability compared to homogeneous alkali catalysts. For example, alkali metal oxide catalysts derived from mixtures of calcium and aluminium oxide were synthesized through sol-gel process for the alkali-catalysed transesterification

of soybean dregs oil (Chen *et al.*, 2021). The catalyst showed remarkable recyclability performances, maintaining high FAEE yield of 76.8 % after 5 consecutive transesterification runs. In another heterogenous alkali catalyst design, cerium oxide-silica composites were alkali-modified to yield heterogeneous catalyst for the transesterification of non-edible wild olive oil feedstock (Khan *et al.*, 2021b). The heterogeneous catalyst exhibited excellent reusability, maintaining high FAME yield at > 85 % at the fifth consecutive transesterification runs with minimal catalyst deactivation. Heterogeneous alkali catalysts for the transesterification of biodiesel have been consistently developed with the emphasis on catalytic stability and reusability, however this approach is inherently limited by the higher cost of adoption of heterogeneous catalysts and the increase in response time owing to differences in mass transfer compared to homogeneous catalysts (Kosuru *et al.*, 2024).

2.1.2 Esterification of Free Fatty Acids (FFAs)

The esterification route for biodiesel production is crucial for industrial processes as it enables the pre-treatment of oils before the transesterification reaction in a two-step process to minimize occurrences of saponification. The esterification of FFA uses acidic catalysts that allows for the conversion of the high FFA contents in low value feedstocks to yield biodiesel (FAME) while enabling the remainder of the triglyceride content to subsequently undergo the conventional transesterification reaction using alkali catalysts (Naghmash *et al.*, 2022). To facilitate the esterification reaction, strong acid catalysts are used to reduce the FFA content as it is less affected by the presence of FFA and impurities when compared to alkali catalysts. As FFA esterification is reversible reaction, Le Chatelier's principle applies in shifting the reaction forward to reach the state of equilibrium. In most studies, this is done by using the methanol (or alternative short chain

alcohols such as ethanol) in excess within the reaction system. Furthermore, the presence of excess methanol acts as a solvent to reduce the overall viscosity of the system, allowing higher surface area of contact and reducing the mass transfer resistance (Marchetti, 2022). The esterification of FFA is a reversible reaction as presented in Figure 2.4.

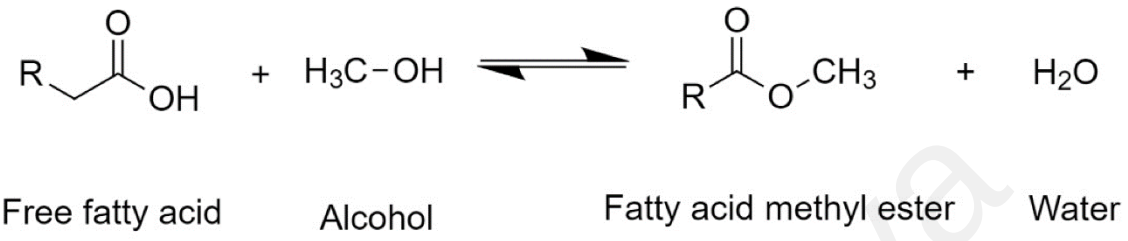

Figure 2.4: Chemical reaction of FFA esterification with methanol.

Esterification processes that are acid-catalysed are viable choices for the utilization of low quality feedstocks and valorise the materials for biodiesel production in effort to offset the demand and competition for refined, pristine oils and corroborate in reducing the production costs of biodiesel. Additionally, the adoption of the two-step process has advantages of ease of scaling up and integration with existing direct transesterification unit operations, and has been demonstrated to be more economical viable than the single-step, direct transesterification route using high purity oil feedstocks (Thoai *et al.*, 2019). In these cases, low-value waste materials that contain high FFA content such as UCO, sludge palm oil, waste animal fat, industrial sludge and grease may undergo esterification to decrease the FFA content to < 2 % using acid catalysts. For the utilisation of LPO in the works of this thesis, the acid-catalysed esterification route is chosen to effectively pretreat and valorise the oil as a viable feedstock for biodiesel production. The types of acid catalyst materials are further discussed in succeeding sections.

2.2 Catalyst Types for Biodiesel Production Through Esterification

To facilitate the esterification reaction of fatty acids/ FFAs, particular emphasis is placed on two variants of catalyst materials according to the phase with the oil and reactants: homogeneous and heterogeneous catalysts. The operating conditions of the catalysts, along with its distinct advantages and challenges are reviewed and discussed.

2.2.1 Homogeneous Acid Catalysts

Homogeneous acid catalysts are the traditional choice of catalysts employed for esterification reactions. Inorganic mineral acids such as hydrochloric acid, phosphoric acid and sulphuric acid are used to deacidify a variety of oils containing high FFA content, with sulphuric acid being the most common choice of acid used. Additionally, other types of sulfonic acids have been studied and demonstrated to enable the catalytic conversion of FFAs in oil feedstocks, such as *p*-toluenesulfonic acid (PTSA), methanesulfonic acid, 5-sulfosalicylic acid, (1R)-(-)-camphor-10-sulfonic acid and benzenesulfonic acid (BZSA) (Hayyan *et al.*, 2014a; Maquirriain *et al.*, 2021). The extensive usage of homogeneous acid catalysts are attributed to the low costs, ease of access, low catalyst loading and high reaction rates and yields (Cárdenas *et al.*, 2021). However, the disadvantages of the conventional use of homogeneous acids include causing high corrosion to equipment, being non-recyclable and requiring additional and challenging purification steps to recover the treated oil from the catalyst and methanol. Table 2.1 provides a summary on several examples of homogeneous acid catalysts and the novel choice of oil feedstock applied for pretreatment. It can be observed that the catalyst loading, methanol requirement and reaction conditions are generally low, while simultaneously being able to achieve a high conversion of FFA and treated oil yield.

Table 2.1: Types of homogeneous acid catalysts reported for FFA esterification of various feedstock types.

Homogeneous Catalyst	Feedstock	Reaction Conditions [1]	FFA Conversion/ FAME Yield	Reference
Sulphuric acid	Animal fat waste, FFA = 10.7 %	0.5 wt%, 6:1, 65 °C, 120 min	FFA Conversion = 97.2 %	(Encinar *et al.*, 2021)
5-sulfosalicylic acid dihydrate	Low grade CPO, FFA = 11.3 %	1.5 wt%, 8:1, 60 °C, 60 min	Yield of treated oil = 90%	(Hayyan *et al.*, 2021)
PTSA, methanesulfonic acid	Biodiesel-derived pure FFA, FFA > 98 %	0.35 equiv/kg, 1:1, 120 °C, 60 min	Highest FAME yield = 95 %	(Maquirriain *et al.*, 2021)
Sulphuric acid	Mealworm oil, FFA = 10.84 %	5.8 wt %, 24:1, 74 °C, 174 min	FFA Conversion = 92.74 %	(Siow *et al.*, 2021)
Sulphuric acid	Waste salmon oil, FFA = 8.37 %	1 wt%, 9:1, 59 °C, 180 min	FFA conversion = 94.9 %	(Serrano *et al.*, 2015)
(1R)-(-)-camphor-10-sulfonic acid	Acidic CPO–Sludge palm oil mixture, FFA = 8 %	1.5 wt%, 10:1, 60 °C, 30 min	FFA conversion = 87.5 %	(Hayyan *et al.*, 2014a)
BZSA	Low grade CPO, FFA = 9.3 %	0.75 wt%, 8:1, 60 °C, 30 min	FFA conversion = 90.35 % Yield of treated oil = 96 %	(Hayyan *et al.*, 2014c)

[1] Optimized reaction conditions are listed as: Catalyst loading (wt%), methanol-to-oil molar ratio, reaction temperature (°C), and reaction time (min).

2.2.2 Neoteric Designer Solvents

2.2.2.1 Ionic Liquids (ILs)

The development of ionic liquids (ILs) as homogeneous acidic catalysts for esterification reactions in biodiesel production stem from its unique characteristics and prospects as a designer solvent (Muhammad *et al.*, 2015). ILs are generally classified as designer solvents that have high potentials in replacing conventional organic solvents to overcome certain limitations with its use, such as the high flammability and volatility (Nejrotti *et al.*, 2022). Additionally, ILs can be applied to other task specific applications

such as catalysis and extraction. On this basis, ILs can be designed to substitute and replace conventional homogeneous mineral acids used in esterification processes, and address challenges related to the catalyst recycling and product separation associated with the use of homogeneous acids (Andreani and Rocha, 2012; Zhao and Baker, 2013). More significantly, ILs exhibit exemplary recyclability and stability compared to homogeneous acid catalysts based on its distinct molecular structure (He *et al.*, 2013; Ullah *et al.*, 2015). Specifically, ILs are organic salts comprising discrete ionic compounds, and typically exists as a liquid in room temperature as a result of its < 100 °C melting temperature (also known as room temperature ionic liquids, RTILs). Several examples of the anions and cations involved in the formation of ILs are presented in Figure 2.5. ILs are known as designer solvents owing to their tuneable characteristics, and by changing the involved anions and cations can in turn influence its physicochemical properties and its task specific applications (Feng *et al.*, 2020). Additionally, ILs exhibit notable advantages over conventional solvents and organic acids, such as having low to negligible vapour pressure, wide electrochemical window, high thermal stability and strong chemical dissolution (Zhuo *et al.*, 2024).

ILs have gained increased prominence in applications as a viable substitute in reaction solvents, electrolytes and catalysts (Gomes *et al.*, 2019; Ullah *et al.*, 2019). ILs can be applied for the purpose of biodiesel production, and has been extensively studied for esterification and transesterification reactions as both a catalyst and reaction solvent (Mohammad Fauzi and Amin, 2012; Troter *et al.*, 2016). More relevantly, ILs have been investigated as effective Bronsted acid catalysts for the esterification of fatty acids/ FFAs in various feedstocks. Particularly, ILs with the relevant sulphonic acid functional groups are the most common and studied for the esterification reaction of fatty acids/ FFAs. Some of the earlier reports on the use of ILs for FFA esterification was conducted by Elsheikh *et al.* (2011). Herein, the authors investigated imidazolium-based ILs with increase side

chain lengths, namely 1-butyl-3-methylimidazolium hydrogensulphate ([BMIM]HSO_4), 1-butylimidazolium hydrogensulphate ([BIM]HSO_4) and 1-methylimidazolium hydrogensulphate ([MIM]HSO_4), for the FFA esterification of CPO. In the conclusion of the study, the [BMIM]HSO_4 was determined to be the highest performing catalyst for FFA esterification owing to its increased chain length compared to other ILs in this study. The esterification reaction condition was optimally conducted at 4.5 wt% IL dosage and 12:1 methanol-to-oil molar ratio at a reaction temperature of 160 °C for 2 h, thereby enabling a final biodiesel yield of 98.4 % through transesterification. Successively, the [BMIM]HSO_4 IL was applied for the esterification of UCO with high FFA content of 4.03 mg KOH/g acid value (Ullah *et al.*, 2015). Via the two-step process, the esterification of UCO using [BMIM]HSO_4 IL enabled the high biodiesel yield of 95.65 % from the successive second step of transesterification. The [BMIM]HSO_4 IL demonstrated high catalyst reusability, maintaining a high FAME yield of 83 % even after six recycling runs. Similarly, the [MIM]HSO_4 IL was synthesized and applied for the FAME production from oleic acid (Roman *et al.*, 2019). The maximum FFA conversion of 95 % was achieved with a high, optimized reaction conditions of 15 wt% catalyst dosage, 15:1 methanol-to-oil molar ratio and 8 h reaction time at 110 °C. In another study, the 3-(N,N-dimethyldodecylammonium) propane sulfonic acid p-toluenesulfonate ([DDPA][Tos]) IL was synthesized for the FFA esterification in oleic acid (He *et al.*, 2013). Under the optimum conditions of 10 mol% IL dosage, 1.5:1 methanol-to-FFA molar ratio a reaction temperature of 60 °C for 180 min, the IL catalyst achieved a high conversion yield of 96.5 %. The [DDPA][Tos] IL exhibited exceptional catalyst reusability and maintained > 90 % conversion after nine reuse runs, demonstrating its effective recyclability properties as a potential catalyst for FFA esterification.

Various configurations and advancements of ILs have since been synthesized and successfully applied to the esterification reaction of fatty acids/ FFAs. For example,

dicationic/ multicationic ILs that are functionalized with relevant sulfonic acid groups are of great research interests due to its binuclear/ multinuclear characteristics that enable higher catalytic efficiencies and tuneability (El-Nagar, 2023; Masri *et al.*, 2020). For example, acidic, dicationic ILs derived from N,N,N′,N′-tetramethyl ethylenediamine and 1,4-diazabicyclo[2,2,2]octane were synthesized for the esterification of FFA in oleic acid (Masri *et al.*, 2018). With the integration and assistances of ultrasonication at 30 W of 20 kHz ultrasonic frequency, the high FAME yield of 89 % was achieved with 1 wt% IL catalyst dosage, 9:1 methanol-to-oil molar ratio, 60 °C reaction temperature for 1 h. Acidic ILs composed of ethylenediamine, 1,3-propanesulfonate and sulfonic acid moieties were reported for the synthesis of biodiesel by esterification of oleic acid (Li *et al.*, 2021b). This synthesis strategy yielded acidic ILs functionalized with multiple $–SO_3H$ functional groups that enabled ultrahigh oleic acid conversion at 97.58 % at low catalyst dosages of 3 wt% and 13:1 alcohol-to-oil molar ratio. Likewise, Han *et al.* (2022) reported on the synthesis of several ILs composed of 1,2-bis(diphenylphosphino)ethane, 1,3-propanesulfonate and sulphuric/ phosphotungstic acid moieties, yielding novel double-site acidic ILs for the esterification of FFAs in oleic acid. The highlight of this study is the self-solidifying mechanism observed during the esterification reactions, whereby the ILs was soluble and exhibited homogeneity with the esterification reaction medium, and can be precipitated post-reaction as a heterogeneous solid. The IL catalyst achieved a high biodiesel yield of 98.65 % using the optimized reaction conditions of 6 wt% IL dosage, 10:1 methanol molar ratio requirement, 60 °C reaction temperature for 4 h, and kept exceptional FFA conversion after nine recycling runs. In another study, a series of tuneable aryl imidazolium-based ILs were synthesized for the esterification of FFAs to biodiesel fuel (Thul *et al.*, 2021). The novel synthesized ILs did not exhibit noticeable vapours as opposed to the dissolution of acids in conventional ILs, and showed results of FAME yield as high as 98 %. In summary, ILs are highly tailorable and exhibit high

tunability for the application of fatty acid/ FFA esterification for the production of biodiesel as reviewed in literature.

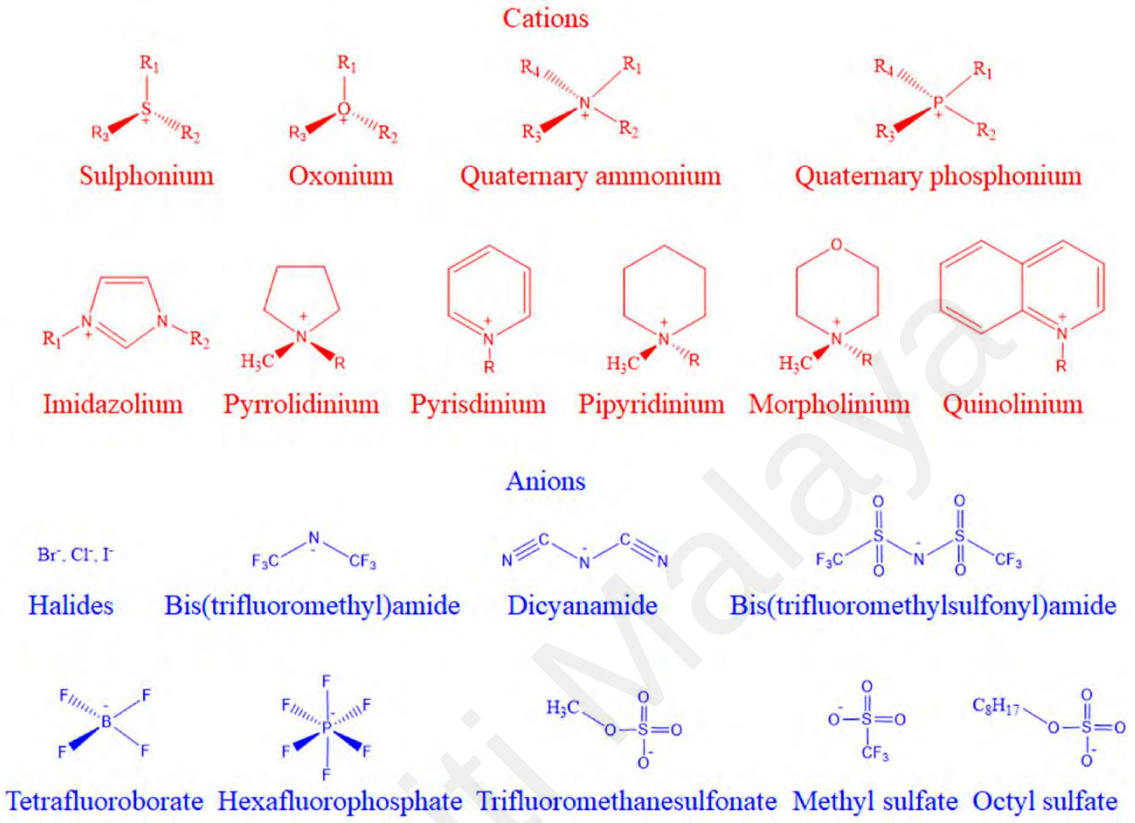

Figure 2.5: Examples of discrete anions and cations for ILs (Zhuo *et al.*, 2024).

Despite its merits as a multifunctional, designer solvent, ILs have reported downside as documented in literature, that are the high cost of synthesis of the ILs, and the prevalence of its substantial toxicity and poor/partial biodegradability (Qiu and Wang, 2022; Xia *et al.*, 2018). In a review conducted by de Jesus & Maciel Filho (2022), the biodegradability of most imidazolium-based ILs were identified to be not readily biodegradable, showing persistency and toxicity as a results of the anions and cations involved in ILs. In light of this observation, research attention has been shifted to analogues of ILs known as deep eutectic solvents (DESs), with hopes to overcome the drawbacks of conventional ILs and improve its green and sustainability aspect as the

future green designer solvent. Hence, research into the application of DESs have similar aspirations to ILs as green substitutes for materials.

2.2.2.2 Deep Eutectic Solvents (DESs)

DESs are a class of emerging designer solvents with molecular interactions based on the concept of melting point depression as shown in Figure 2.6. In a typical binary DES system, the DES consists of a hydrogen bond donor (HBD) and hydrogen bond acceptor (HBA) component, and when physically combined at a certain molar ratio, results in the formation of a DES supramolecular structure through complex, intrinsic hydrogen bonding (Martínez *et al.*, 2022). DESs can subsequently be formed with more than two components and are categorized as ternary DESs. DESs are analogues of ILs and exhibit similar physicochemical properties to it, such as having low to negligible volatility, being highly tuneable and tailored to certain task specific applications, and having wide electrochemical window (Jha *et al.*, 2020). As a results, DESs have seen increased applications in various fields, including electrochemistry, organic synthesis and solvent extraction (Abranches and Coutinho, 2022; Omar and Sadeghi, 2023). Recently, DESs have seen various catalytic applications and uses, particularly in the field of biomass treatment, conversion and upgrading (Kalhor and Ghandi, 2021).

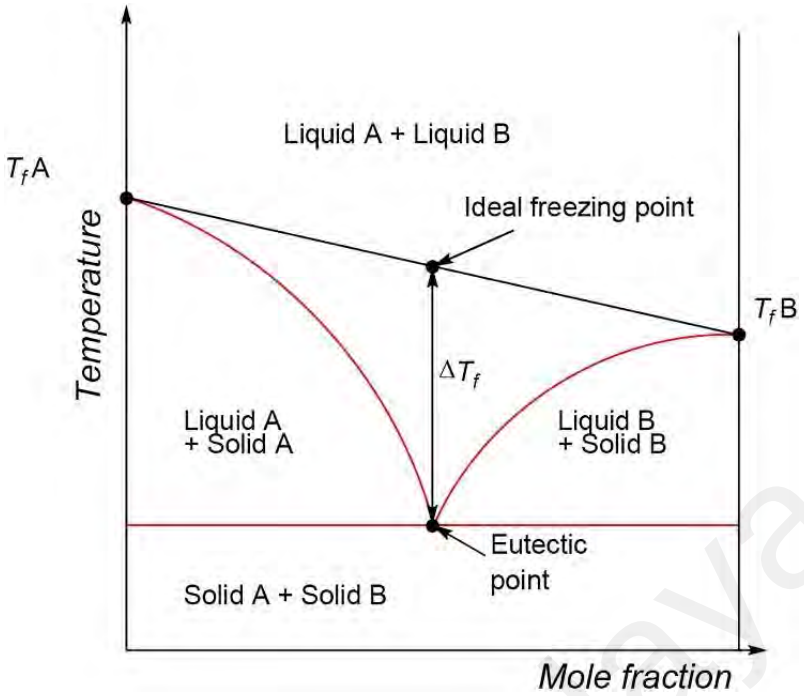

Figure 2.6: Schematic diagram representing the formation of a eutectic mixture (Martínez *et al.*, 2022).

Although DESs are often touted as the next generation of designer solvents, recent investigations reveal several inherent limitations pertaining to DESs and its applications. Firstly, most prior literature has generalized DESs as being benign and innocuous. While this generalization is acceptable for the earlier known reports of DESs, recent reports have revealed higher cytotoxicity when combined as a DES mixture compared to its individual components (Hayyan *et al.*, 2013c; Hayyan *et al.*, 2016). The effect of cytotoxicity is inherent when hazardous and toxic HBD constituents are used in the DES system (Martínez *et al.*, 2022). For example, the formation of amino acid-based DESs revealed high toxicity than choline chloride-based DESs and its individual constituents (Li *et al.*, 2023b). Cao *et al.* (2023) compared the toxicity of DESs synthesised from 1,8-diazabicyclo[5.4.0]-undec-7-ene and compared its toxicity (IC_{50}) with other common DESs, revealing exceedingly high toxicity (266 times) than that of choline chloride: glycerol DESs. In summary, the design of a DES system should be focused on selecting constituents that pose minimal harm towards humans and the environment, as the choice

of constituents holistically influence the resultant DESs in various aspects such as the physicochemical properties, cytotoxicity, ecotoxicity and its task specific applications (Omar and Sadeghi, 2023).

Some examples of low toxicity DESs are Natural DESs (NADESs). NADESs are a relatively emerging class of biomaterials-derived DESs primarily focused on the formulation of DESs using natural, bio-available components that possesses environmentally friendly properties such as high biodegradability, high biocompatibility and low- to non-toxicity in nature (Picchio *et al.*, 2022; Usmani *et al.*, 2023). NADESs can be composed of plant-based primary metabolites such as alcohols, amino acids, carboxylic acids and simple sugars (Marchel *et al.*, 2022). Examples of DES and NADES constituents are presented in Figure 2.7. Notable chemical constituents in common DESs include quaternary ammonium salts such as choline chloride, polyol compounds such as ethylene glycol and glycerol, amides and thioamides, metal salts and polyols. NADESs are highly effective in flavonoid and bioactive compounds extraction as a solvent, and has shown prominence in enhancing green extraction techniques (Gómez *et al.*, 2019). On the other hand, therapeutic DESs (THEDESs) are a novel category of DESs that utilize APIs as its constituent in the formation of a eutectic mixture/ DES compound (Rahman *et al.*, 2021). Given the unique properties endowed by the formation of DES, THEDESs have been greatly demonstrated of applications in drug delivery, drug stabilisation and drug bioavailability (Silva *et al.*, 2020). The discovery of THEDESs has revealed another class of compounds that shows viability in the formation of DESs. Given its infancy of assessing the extent of THEDESs with regards to its toxicity and physicochemical properties, the research gap to investigate APIs as a DES constituent for other application is present.

Due to its similarities with ILs in terms of tunability and multifunctional properties, and embodying improvements in reducing toxicity and hazard, increased research attention has been paid to the development of DESs and NADESs. In recent years, DESs have been demonstrated in applicable fields of organic syntheses, catalysis, electrochemistry, and carbon capture and utilization (Murshid *et al.*, 2019; Zhang *et al.*, 2022). In these applications, DESs are used as reaction solvents, catalysts, electrolytes and substrates. Furthermore, the tailorable properties of DESs and NADESs can be exploited for the use in solubilizing specific bioactive compounds based on its polarity, making it ideal to be used as a green solvent for the efficient extraction of compounds from plant origins. DESs have been demonstrated for the green extraction of various polar and non-polar molecules such as alkaloids, flavonoids and phenolic acids (Cao *et al.*, 2020; Lanjekar and Rathod, 2021; Wang *et al.*, 2023c). On the other hand, DESs exhibit good interfacial compatibility with electrode materials based on its non-corrosive, non-flammable and tuneable properties, making it a highly ideal and functional material as electrolytes in electrochemical energy storage devices such as metal batteries and electrochemical capacitors (Azmi *et al.*, 2022; Hu *et al.*, 2020). On the scope of biomass valorisation and upgrading, DESs have shown particular usefulness in applications of lignocellulosic biomass pretreatment (Li *et al.*, 2023a; Wang and Lee, 2021). Additionally, DESs can used as catalyst materials for the catalytic conversion of biomass, including the production of biofuels for renewable energy generation (Li *et al.*, 2022; Liu *et al.*, 2020c).

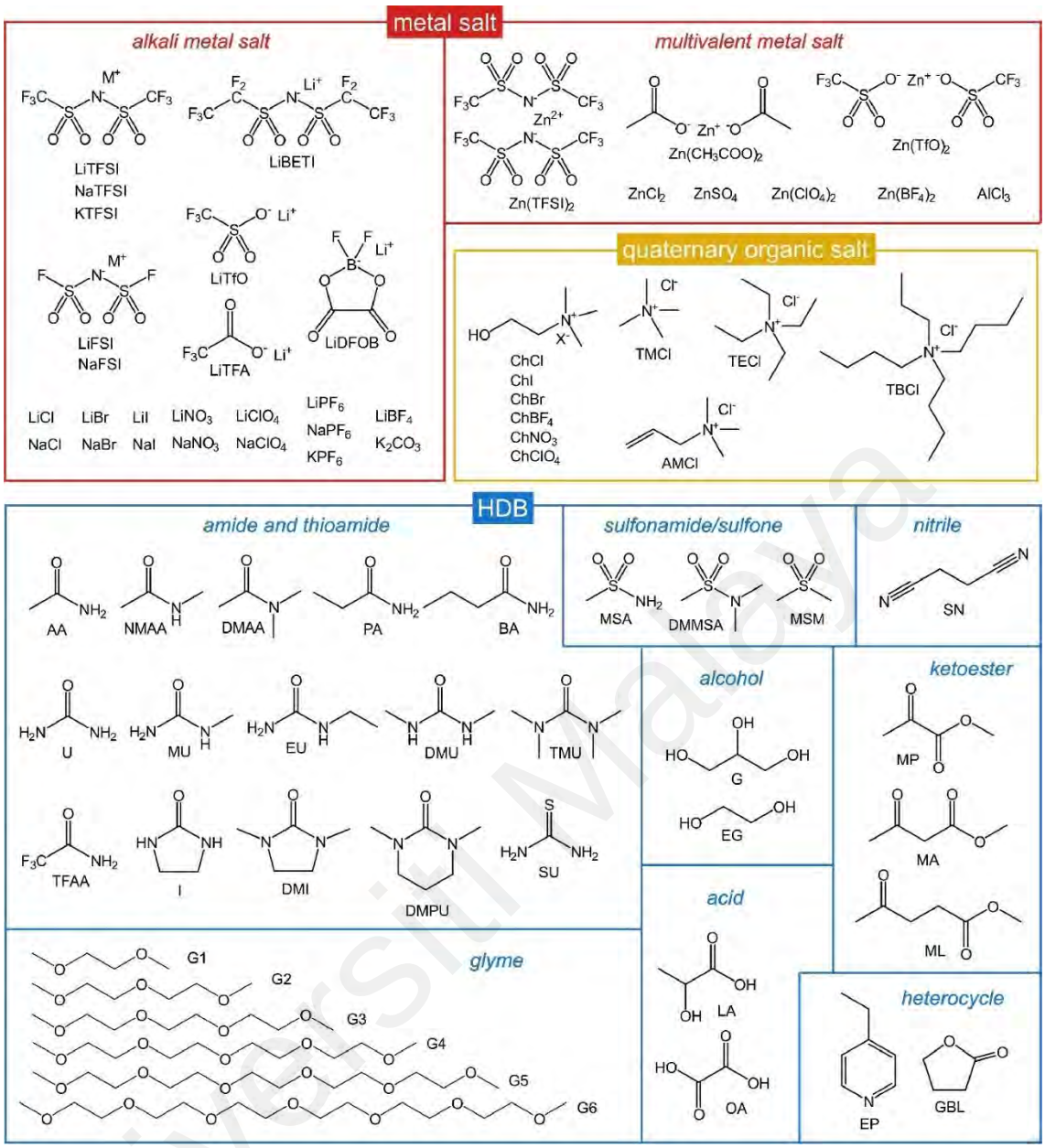

Figure 2.7: Examples of DES constituents divided into HBD and HBA components (Azmi *et al.*, 2023).

2.2.2.3 Physicochemical Properties of DESs

The plethora of compounds and chemical moieties that are known and yet to be known to form DES compounds gives rise to the tailorable characteristics of DESs. The physicochemical properties of DESs are a function of the compositions of HBA and HBD components within the DES system. In theory, the variety of components and its respective component ratios within a DES system means that the formulation of DES

compounds are virtually unlimited, each with its respective characteristics and physicochemical properties (Triolo *et al.*, 2023). As increasing number of studies emerge on the application of DESs, fundamental studies on understanding the physicochemical properties of the DESs are essential to ensure the rational design of solvent that are intended to replace conventional organic solvents and materials. Additionally, the knowledge of the physicochemical properties of DESs contribute to the design of equipment and vessels in operating the DES system. According to a search in the Web of Science database as shown in Figure 2.8, publications concerning DESs were shown to increase across the last twenty years (Figure 2.8 (a)), with an increasing number of reports on the physicochemical properties of DESs as shown in Figure 2.8 (b). This may be due to the need to investigate the fundamental properties of DESs to understand how different DES systems behave, and support its potential application into chemical processes.

Currently, the physicochemical properties of DESs are measured empirically, where each system of DESs are reported in literature on a case by case basis (Omar and Sadeghi, 2023). Herein, fundamental physicochemical properties of the DESs, such as its density, viscosity, electrical and thermal conductivity, surface tension, refractive index, heat capacity, speed of sound in solvent medium and ionicity are reported for each composition of DESs that are empirically measured and analysed. The physicochemical properties of the DESs are often reported for properties with temperature dependence relationships, and are correlated using relevant fitting models (for example, linear, quadratic or Arrhenius models). For instance, increasing carbon lengths of polyol-based (ethylene-, diethylene-, triethylene- and tetraethylene glycol as HBD compounds) DESs were reported for its physicochemical properties (Hayyan *et al.*, 2020; Hayyan *et al.*, 2015; Ibrahim *et al.*, 2017, 2019). From the same research group, phosphonium-based DESs were reported for its physicochemical properties, with particular emphasis placed on studying the electrochemical properties with the purpose of utilizing its as zinc air

battery electrolytes (Hayyan *et al.*, 2023b). Recently, an extensive study on the physicochemical properties of benzyl triethylammonium chloride-based DESs was published (Singh *et al.*, 2023). The study reports on the combination of benzyl triethylammonium chloride with choices of organic acids (acetic acid, levulinic acid and others) or polyols (ethylene glycol, 1,4-butanediol and 1,2-propanediol) to yield DESs with varying physical, chemical and thermal properties. In another study, sugar-based DESs composed of fructose, sorbitol or xylitol combined with glycerol and water were studied for its physicochemical properties (Lomba *et al.*, 2023). Additionally, its thermodynamic properties, such as the isentropic compressibility and the isobaric heat capacity were calculated and reported.

In line with the development of DESs, systematic reviews on the physicochemical properties of DESs should be regularly conducted to compile the discovery and application of known and novel DESs. For example, the physicochemical properties of DESs have been reviewed by several active research groups (El Achkar *et al.*, 2021; Ijardar *et al.*, 2022; Omar and Sadeghi, 2022). By evaluating the physicochemical properties of DESs, the empirical results enable the development of rapid and accurate models that can be used to predict and screen for potential DESs that enables time and resource savings in the development of DESs (Aroso *et al.*, 2017). The compilation of physiochemical properties of DESs enable the cross verification of existing literature data and identify gaps in the synthesis of novel DES compounds.

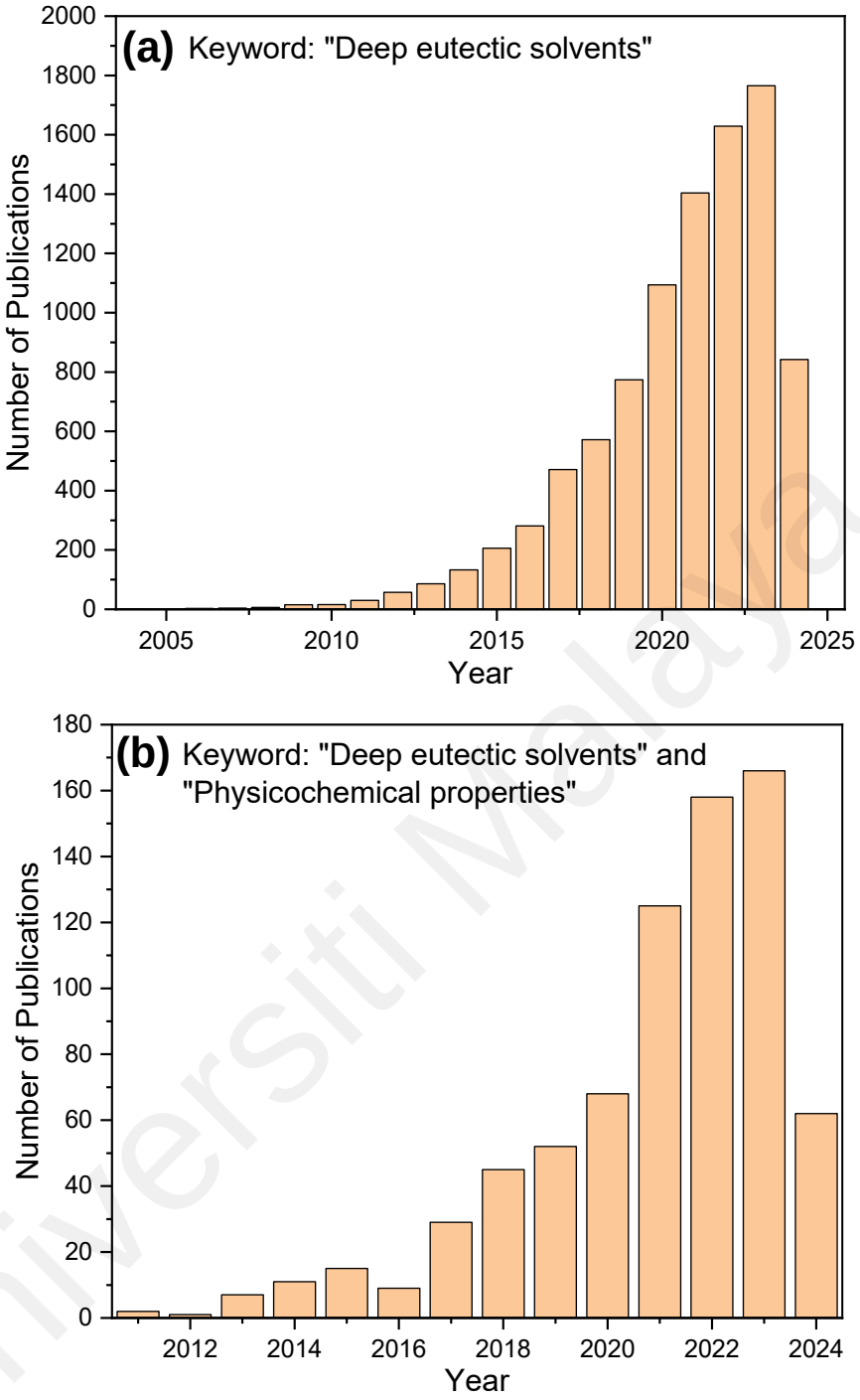

Figure 2.8: Number of publications concerning DESs and its physicochemical properties from the Web of Science database (Date accessed: 2nd July 2024).

2.3 Application of DESs in Biodiesel Production

In the application of DESs for biomass valorisation and energy production, DESs have shown a multitude of functional use and properties pertaining to the synthesis of biodiesel. Generally, DESs have been applied to biodiesel production as a substitute or a co-product, a purifying agent or as catalysts (Amesho *et al.*, 2023; Huang *et al.*, 2024). The use of DESs as a co-product (co-solvent) and as a purifying agent is discussed in this section. Triethanolamine-based DESs with various HBD compounds including amides, polyols, organic acids and ammonium salts were studied as co-solvents for the transesterification reaction of black mustard seed oil catalysed by conventional calcium oxide catalysts (Đorđević *et al.*, 2023). At 20 wt% of DES loading, the addition of triethanolamine:ChCl DES resulted in the highest FAEE content yield of 98.5 % by ethanolysis, with other DESs achieving relatively high FAEE content yield between 89.1 – 98 %. In another study, a series of amide-, polyol- and acetamide-based DESs were studied for the activation of sodium-loaded ZSM-5/calcium oxide nanocatalysts in the transesterification of extracted halophytic oils (ShenavaeiZare *et al.*, 2021). The use of the ChCl:ethylene glycol DESs resulted in high biodiesel yields of up to 95 %, while negating the need for catalyst reactivation by calcination. ChCl-based DESs consisting of various amide- and polyol-based HBD components were similarly studied as co-solvents for the transesterification reaction of sunflower oil by ethanolysis using calcium oxide catalysts (Troter *et al.*, 2018). The study concluded that polyol-based DESs yielded higher FAEE content at shorter reaction times compared to amide-based DESs owing to the activation of the calcium oxide catalysts in both its calcined and uncalcined forms. DESs comprising ChCl and glycerol (1:2 molar ratio) was employed as a novel co-solvent for biodiesel production with the objectives of minimizing volatile organic solvents use (Gu *et al.*, 2015). Specifically, 10 wt% of ChCl:glycerol DES was added as a co-solvent into the transesterification reaction system of rapeseed oil, with 1 wt% of NaOH as the alkali

catalyst and 1:5 methanol-to-oil molar ratio as the reactant and solvent. The addition of ChCl:glycerol DES as a co-solvent resulted in an improved FAME yield up to 95 %. The authors attributed the improvements in FAME yield to the unique solvation ability of the DES that was inferred to change the phase distributions with the reaction system.

In other applications, DESs have been studied as novel biodiesel purification solutions to replace the conventional process of wet washing to purify crude biodiesel. The works of Shahbaz *et al*. pioneered the study on using polyol-based DESs for the purification process of biodiesel by the removal of glycerol and residual KOH catalyst from crude biodiesel synthesised from the transesterification of CPO (Shahbaz *et al.*, 2010; Shahbaz *et al.*, 2011a, 2011b). The use of another polyol type DES (ChCl:glycerol:triethylene glycol) was similarly demonstrated for the purification of biodiesel produced from the transesterification of commercial soybean oil, and showed better removal performances than hot water washing (dos Santos *et al.*, 2022). In another study, ChCl:ethylene glycol DESs were used as liquid-liquid extractor solvent for the high performance extraction of glycerides and glycerol from crude biodiesel in a laboratory-scale column (Sander *et al.*, 2024). In conclusion, DESs exhibit multifunctional uses for the application of biodiesel production in the context of process intensification and downstream processing. The improvements are attributed to the rational screening and selection of the HBA and HBD components that contribute to the process enhancements. In the following sections, DESs deployed as catalysts for the esterification of biodiesel feedstocks are reviewed and discussed.

2.4 DESs as Homogeneous Acid Catalysts in FFA Esterification

Sulfonic acids are highly hygroscopic due to the presence of the sulfonic acid functional group (–SO_3H) (Liu *et al.*, 2006). Recently, certain sulfonic acid compounds

such as PTSA have been reported to be able to form DES compounds with common DES constituents such as ChCl. Hence, the conversion of pristine hygroscopic sulfonic acids into DESs can be a viable synthesis strategy to improve the hygroscopicity of the sulfonic acid (Hayyan *et al.*, 2013a). Additionally, the use of DESs in applications of catalysis enable unique advantage based on its tuneable properties (Álvarez *et al.*, 2024). In the FFA esterification process, homogeneous acidic DESs are primarily used the active catalyst in the reaction. Acidic DESs have been studied for the novel FFA esterification process through glycerolysis, that is the reaction of FFAs with glycerol as opposed to the conventional use of alcohols. This method enables the circular use of glycerol as the byproduct of transesterification, thereby reducing the overall costs of biodiesel production (Williamson *et al.*, 2017). A novel quaternary ammonium salt-based DESs was reported as an acidic catalyst for the esterification of FFA through glycerolysis (Mamtani *et al.*, 2023). Herein, the DES synthesized based on PTSA and tetrabutylammonium hydrogen sulphate at a molar ratio of 2:1. The study was conducted for the esterification of oleic acid, palm fatty acid distillate and brown grease. At the optimum reaction conditions of 10 wt% catalyst dosage, 6:1 glycerol-to-oil molar ratio, 130 °C reaction temperature for 10 min and 600 rpm stirring speed, the highest FFA conversion of 94 % was achieved. Previously, phosphonium-based DESs have been studied for the esterification of FFA by glycerolysis (Zhang *et al.*, 2020). The DES was composed of allyl triphenylphosphonium bromide and PTSA at a molar ratio of 1:3, and yielded high FFA conversion of 90 % in the valorisation of vegetable oil deodorizer distillate as the non-edible feedstock for biodiesel production. In a preceding study, the same phosphonium-based DES was studied for the esterification of oleic acid with glycerol (Williamson *et al.*, 2017). Herein, the authors reported high FFA conversion and mono- and di-glyceride yield of 95 % and 85 % respectively, at the optimized reaction

conditions of 5 wt% catalyst dosage, 6:1 glycerol-to-oil molar ratio, 150 °C reaction temperature for 30 min.

Homogeneous acidic DESs are established as the active catalyst in the FFA esterification reaction process by methanolysis (Qin *et al.*, 2020). Several novel acidic DESs based on PTSA and quaternary ammonium salts were synthesized as novel catalysts and reaction media for biodiesel production (Table 2.3, Entry 3) (Liu *et al.*, 2020d). The authors reported on the use of several HBAs with increasing carbon chain lengths, which are tetraethyl ammonium bromide, tetrabutyl ammonium bromide, tetrahexyl ammonium bromide, tetraoctyl ammonium bromide and ChCl in the formation of DES compounds with PTSA. With RSM optimization, a maximum FAME yield of 99.2 % was obtained with the reaction conditions of 24.6 wt% catalyst dosage, methanol-to-oil molar ratio of 12.5 and 70.5 °C reaction temperature for 5 h. Noteworthily, in the catalyst optimization stage, the increase in the carbon chain length of the quaternary ammonium salts (from tetraethyl ammonium bromide to tetraoctyl ammonium bromide) was observed to increase the FAME yield and conversion from 38.0 % to 67.9 %, and this was attributed to the increased lipophilicity of the DESs as a result of the higher carbon chain length. In another study, DESs based on PTSA and methyltriphenylphosphonium bromide (3:1 molar ratio) were synthesized for the FFA esterification of acidic CPO with high FFA content at 9.6 % (Table 2.3, Entry 2) (Hayyan *et al.*, 2022). At the optimized reaction conditions of 3 wt% catalyst dosage, 10:1 methanol-to-oil molar ratio, 30 min reaction time at 60 °C, high FFA conversion was achieved at 96 %. From the Hayyan *et al*. group, various novel DESs have been reportedly synthesized and optimized for the FFA esterification of varying low-value feedstock as a pretreatment step, and the reported DESs along with the optimized reaction conditions are tabulated in Table 2.3. Given the similarities in equipment setup, the reported catalyst and methanol requirements range between 1 – 3 wt% and 8:1 – 10:1 respectively (Hayyan *et al.*, 2013a; Hayyan *et al.*,

2014b; Hayyan *et al.*, 2017). The development of DESs as catalysts for the FFA esterification to yield FAME is supported by preceding studies on the synthesis of novel DESs with unique tuneable properties, such as exhibiting switchable acidity and basicity (Qin *et al.*, 2019). A summary of DESs utilized as acidic catalysts for methanolysis and glycerolysis reactions in biodiesel production is presented in Table 2.3.

Table 2.2: DESs for FFA esterification through methanolysis and glycerolysis.

Selection of DES catalyst	Feedstock	Reaction Conditions [2]	FFA Conversion/ FAME Yield	Reference
PTSA: Tetrabutylammonium hydrogen sulphate 2:1	Oleic acid	10 wt%, 6:1, 130 °C, 10 min	FFA conversion = 94 %	(Mamtani *et al.*, 2023)
PTSA: Methyltriphenylphosphonium bromide 3:1	Acidic CPO, FFA = 9.61 %	3 wt%, 10:1, 60 °C, 30 min	FFA conversion = 96 % Yield of treated oil = 97 %	(Hayyan *et al.*, 2022)
PTSA: Tetraoctyl ammonium bromide 2:1	Olive oil	24.6 wt%, 12.5:1, 70.5 °C, 5 h	FAME yield = 99.2 %	(Liu *et al.*, 2020d)
PTSA: Allyl triphenylphosphonium bromide 3:1	Vegetable oil deodorizer distillate	5 wt%, 6:1, 160 °C, 10 min	FFA conversion = 90 %	(Zhang *et al.*, 2020)
PTSA: Allyltriphenylphosphonium bromide 3:1	Oleic acid	5 wt%, 6:1, 150 °C, 30 min	FFA conversion = 95 % Mono-, di-glyceride yield = 85 %	(Williamson *et al.*, 2017)
(1R)-(-)-10-Camphorsulphonic acid: Choline chloride 1:1	Acidic CPO–Sludge palm oil mixture, FFA = 8.1 %	2.5 wt% 10:1 60 °C 40 min	FFA conversion = 90 %	(Hayyan *et al.*, 2017)
PTSA: Benzyltrimethylammonium chloride 3:1	Low grade CPO, FFA = 9.2 %	2 wt% 10:1 60 °C 30 min	Not reported	(Rashid *et al.*, 2017)

PTSA: Benzyltrimethylammonium chloride 1:1	Acetic acid	10 wt%, 10:1, 90 °C, 180 min	Acetic acid conversion = 68.4 %	(Taysun *et al.*, 2016)
PTSA: Choline chloride 3:1	Acidic CPO, FFA = 9 %	0.75 wt%, 10:1, 60 °C, 30 min	FFA conversion = 96 % Yield of treated oil = 97 %	(Hayyan *et al.*, 2014b)
PTSA: Allyltriphenylphosphonium bromide 3:1	Low grade CPO, FFA = 9.3 %	1 wt%, 10:1, 60 °C, 30 min	FFA conversion = 90.53 % Yield of treated oil = 96 %	(Hayyan *et al.*, 2013a)
PTSA: N,N-diethylenethanol ammonium chloride 3:1	Low grade CPO, FFA = 9.5 %	0.75 wt%, 8:1, 60 °C, 30 min	FFA conversion = 92.6 % Yield of treated oil = 97 %	(Hayyan *et al.*, 2013b)

[2] Optimized reaction conditions are reported as: Catalyst loading (wt%), methanol-/ glycerol-to-oil molar ratio, reaction temperature (°C), and reaction time (min).

2.5 Heterogeneous Solid Acid Catalysts (SACs) in FFA Esterification

Various heterogeneous solid acid catalysts (SACs) have been reported for the successful catalysis of FFA esterification for biodiesel production (Figure 2.9). SACs have garnered significant development as a heterogeneous catalyst material for the biodiesel esterification process owing to its advantages over homogeneous catalysts, such as being highly recyclable, having lower corrosiveness, and enabling sustainable catalyst design particularly when derived from biomass (Zhou *et al.*, 2023). Additionally, homogeneous acid components such as organic acids, ILs and DESs can be supported onto the heterogeneous SACs, essentially converting the catalysis phase from homogeneous to heterogeneous. When applying SACs in esterification reactions, certain challenges may arise, such as the high mass transfer in the use of zeolites, or the loss of acid sites due to acid solubilisation in reaction medium that is observed in some

impregnated SACs. Water content generated from the hydrolysis reaction in esterification can similarly diminish catalytic behaviour due to its hygroscopicity, causing undesirable catalyst deactivation (Dabbawala *et al.*, 2015). Hence, the rational design of SACs for the esterification reaction in biodiesel production should encompass high catalytic conversion while maintaining high stability and satisfactory reusability performances.

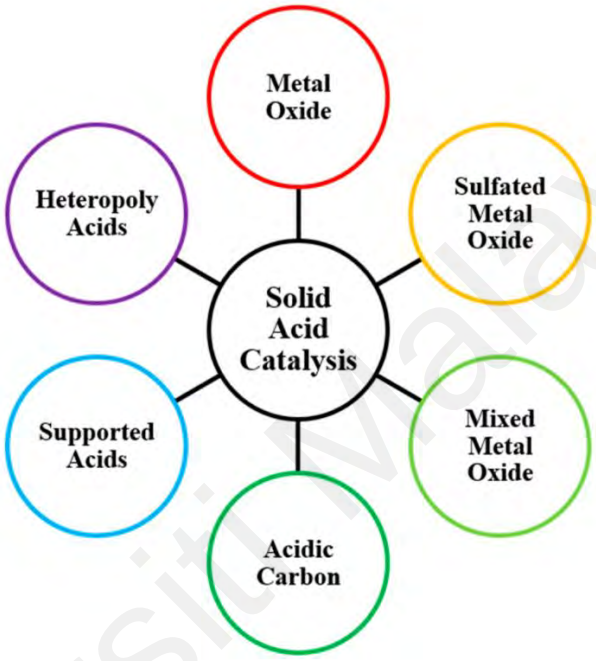

Figure 2.9: Diversity of sulphonated SACs for biodiesel production (Lowe *et al.*, 2022).

2.5.1 Porous-based Support Materials as SACs in FFA Esterification

As shown in Figure 2.9, a relevant catalyst design protocol is through the functionalization of homogeneous sulfonic acids onto various types of heterogeneous materials (Lowe *et al.*, 2022). Herein, catalyst materials exhibit different types of internal structures, such as bulk materials and metal–supported catalytic materials. Generally, porous and non-porous materials that form the basis of supported catalysts combine the functions of the bulk materials and the relevant functional groups contributing to the catalytic reaction (Figure 2.10) (Melián-Cabrera, 2021). Various catalyst materials have

been studied for the application of catalysis in biodiesel production. Relevant examples include materials such as porous/ mesoporous silicas, hydroxyapatites, metal organic frameworks (MOFs), carbon-based materials yielding supported heterogeneous SACs in the catalytic reactions to produce biodiesel (Chen *et al.*, 2022; Mandari and Devarai, 2022). Additionally, other types of catalytic materials have been studied for catalytic applications, such as organic ion-exchange resins, metal oxides and polymers (Tan *et al.*, 2021).

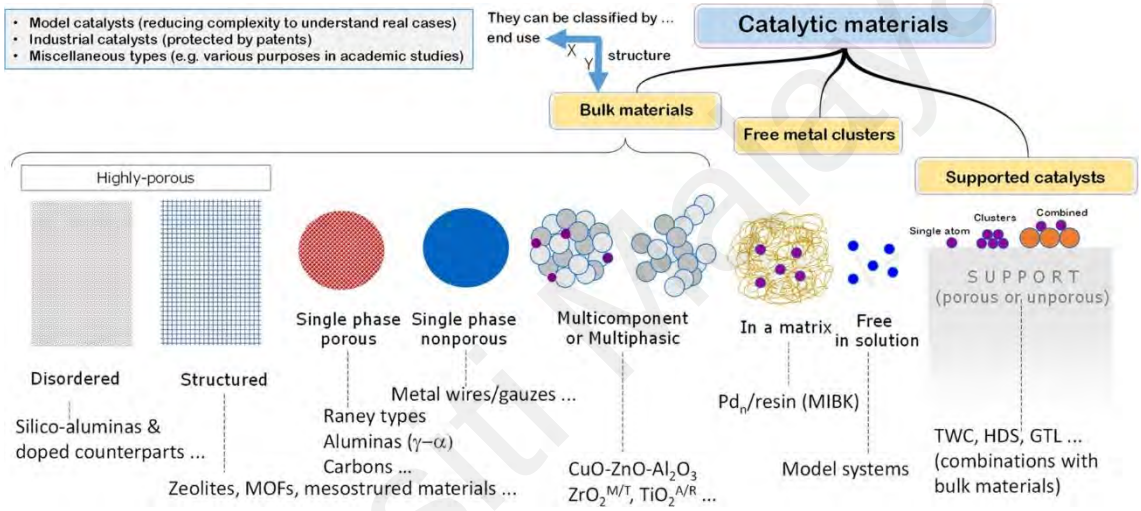

Figure 2.10: Categories of catalytic materials according to bulk materials, free metal clusters and supported catalysts (Melián-Cabrera, 2021).

Ordered porous, inorganic materials are among one of the most widely studied catalytic support materials for the production of biodiesel, owing to its unique properties of having uniform pore sizes, high thermal stability and chemical inertness, and adequate development of surface area for functional group attachment (Testa and La Parola, 2021). Hence, sulphonic acid functional groups can be functionalized onto such inorganic materials, where the inorganic material acts as the carrier of the sulphonic acids. Examples of porous, inorganic materials include silica materials (zeolites, SBA-15 molecular sieves, MCM-41 and MCM-48 mesoporous silica) and MOFs (examples

include MIL-101, UiO-66 and ZIF-8 MOFs) (Gouda *et al.*, 2022; Tan *et al.*, 2021). Yusuf *et al.* (2023) reported on the synthesis of sulphonated zinc oxide catalysts supported on β-zeolite for the esterification of UCO. The catalyst was reported with high surface area (250.26 m^2/g) and high pore volume (0.17 cm^3/g), enabling high oil conversion of up to 96.9 % at optimum reaction conditions. In another study, PTSA and methanesulfonic acid were supported onto UiO-66 MOFs and the prepared SACs were applied for the catalytic esterification of palmitic and oleic acid (Liu *et al.*, 2020b). PTSA and methanesulfonic acid showed good compatibility with the UiO-66 MOF by simple impregnation method in synthesis, resulting in a heterogeneous SAC with high catalytic surface area of 959 - 1059 m^2/g. As a result, high FFA conversions of 97 – 97.1 % was achieved using both types of supported SACs at relatively mild conditions of 4 h reaction time at 100 °C, with 10 wt% of catalyst dosage. Similarly, PTSA was likewise supported onto UiO-66 MOFs through defect coordination to form SACs for oleic acid esterification (Li *et al.*, 2021a). The integration of PTSA into the porous structure of UiO-66 causes increase of the average pore diameter compared to pristine UiO-66, thereby improving the catalyst pore size to the mesoporous scale and improving the accessibility of oleic acid to the catalyst active site. As a result, high oleic acid conversion to biodiesel was achieved at 91.3 %. Bismuth-based MOFs (Bi-BDC, Bi-BTC) were hydrothermally synthesized as a support for phosphomolybdic acid, and applied for the fatty acid esterification (Zhang *et al.*, 2023). At optimal reaction conditions of 5 wt% catalyst dosage, 20:1 alcohol-to-FFA molar ratio, 160 °C reaction temperature for 3 h, the conversion of oleic acid as the model oil was high at 92.5 %. Moreover, the SAC was demonstrated for the esterification of two actual samples of high acidity non-edible crude oils (Jatropha curcas and Euphorbia lathyris oils) with high fatty acid conversion of 70.6 - 78.5 % at slightly higher reaction times (4 h), further emphasizing its feasibility as SAC in treating low-value oils.

2.5.2 Carbon-based Support Materials as SACs for FFA Esterification

In efforts to valorise biomaterials and address the abundance of agricultural waste and biomass, varies studies have been devoted to the development of catalyst support materials from biomass-based carbon sources (Changmai *et al.*, 2020; Gupta and Paul, 2014; Mahajan and Gupta, 2020). Carbon-based SACs with $–SO_3H$ functional groups are highly viable catalysts for fatty acid/ FFA conversion (Rechnia-Gorący *et al.*, 2018). For example, the carbonization of cacao shells and subsequent sulphonation with sulphuric acid was conducted to yield SACs for the esterification of oleic acid (Mendaros *et al.*, 2020). The optimal synthesis parameters yielded SACs that exhibit high acid site densities at 0.85 mmol SO_3H/g, in turn resulting in high catalytic conversion of 78 % after three recycling runs. Subsequently, açaí seed-derived sulphonated activated carbon was deployed for the FFA esterification of waste frying oil with high FFA content at 2.90 mg of KOH/g (Zavarize *et al.*, 2023). The seed-derived carbon catalyst was facilely prepared with direct sulphonation using sulphuric acid, enabling high FFA conversion at 97.1% at optimal conditions. In a similar synthesis procedure of carbonization and direct sulphonation, carbon SACs derived from bamboo charcoal were developed for biodiesel production from non-edible soybean saponin acid oil via esterification reaction of its FFA content (Tang *et al.*, 2023). The direct sulphonation of the carbonized bamboo charcoal yielded SACs with high acid densities of up to 1.476 mmol SO_3H/g, contributing to the high FFA conversion in the acidic oil at 98.26 %. In conclusion, carbon-based SACs enable the valorisation of carbon-rich waste biomass materials that are relatively simple in preparation for the synthesis of catalysts for biodiesel production.

2.5.3 Polymer-based Support Materials as SACs for FFA Esterification

Another relevant class of support materials for SAC synthesis is through the use of polymer type supports that have desirable properties such as having high chemical and thermal stability (Zhang *et al.*, 2016). For example, polyvinyl alcohol (PVA) was used as the supporting polymer for the synthesis of sulfonated SACs in the synthesis of 5-hydroxymethylfurfural, an important biofuel derivative (Perez and Dumont, 2021). Herein, sulfosuccinic acid was used as the polymer crosslinker, yielding -SO_3H functionalized PVA and resulting in high conversion of fructose to 5-hydroxymethylfurfural at 94.3 %. In another study, polystyrene was composited with activated carbon and sewage sludge to yield SACs for the acid-catalysed transesterification of sludge lipids (Hatami *et al.*, 2022). The sulphonation of the SAC composite was conducted with the arylation of 4-aminobenzenesulfonic acid, of which the highest acid density were obtained at optimized synthesis parameters as 1.36 mmol SO_3H/g. Additionally, the coating of the SAC with polystyrene was claimed to improve its SAC recoverability, maintaining stable biodiesel yield even after nine recycling runs. The use of polystyrene as polymer-type SACs have been extensively studied (Andrijanto *et al.*, 2012). Kalla *et al.* (2018) developed novel SACs based on the hyper crosslinking of phenol and bisphenol A using dimethoxymethane and functionalized using chlorosulfonic acid, yielding highly acidic polymeric-based SACs for the esterification of FFAs. As a result, the SAC was able to achieve high yields of 95 % at room temperature and 6 h contact time reaction conditions. A mesoporous, polymeric SAC was developed from the copolymerization of divinyl-benzene with 1-vinylimidazole (Pan *et al.*, 2016). The high surface acidity (2.6 mmol g^{-1}) and mesoporous structure of the novel polymeric SAC enables high attainment of FAME content at 94 % from the conversion of crude *Jatropha curcas* oil.

2.5.4 Magnetic-based Support Materials as SACs for FFA Esterification

Furthermore, catalyst recovery and recyclability of SACs can be enhanced with the integration of a magnetic component such as ferromagnetic magnetite nanoparticles (Fe_3O_4), yielding magnetic responsive composite-type SACs that can be easily separated from the reaction mixture via magnetic forces introduced externally (Krishnan *et al.*, 2021). The schematic diagram on the use of magnetic SACs for biodiesel production via esterification is presented in Figure 2.11. To endow a heterogeneous catalyst with magnetic properties, a composite structure comprising elements of cobalt, iron or nickel oxides can be synthesized. For example, magnetic catalysts and nanocatalysts can be synthesized with the composition of magnetite (Fe_3O_4) nanoparticles that can be easily synthesised by co-precipitation method (Kumar *et al.*, 2021). Magnetic catalysts are relatively easier to separate and recover from a reaction system compared to non-magnetic catalysts that are commonly recovered by centrifugation and filtration (Vasić *et al.*, 2020). Hence, various magnetic composite/nanocomposite catalyst materials have been reportedly synthesized and investigated for catalytic applications in biodiesel production, particularly for the esterification reaction by acid catalysis (Xie and Li, 2023). Ali *et al.* (2020) reported on the synthesis of cuprospinel ($CuFe_2O_4$)-based magnetic nanocatalyst for waste frying oil transesterification that exhibited exceptional biodiesel yield (90.24 %) and ease of separation and recovery magnetically. 1-butyl-3-methylimidazolium hydrogen sulphate acidic IL was synthesised and supported on a Fe_3O_4/SiO_2 composite for the methyl esterification reaction of waste seed oils (Yu *et al.*, 2021). The authors reported high catalytic efficiency and stability (87.6 % conversion after four reaction cycles) while exhibiting ease of separation due to its magnetic properties. In another study, magnetically recyclable SACs composed of dual acidic ILs were synthesized for the esterification of a model low-quality oil derived from commercial soybean oil (Xie and Wang, 2021). The synthesis procedure involves the

copolymerization of the 1-vinyl-3-(3-sulfopropyl)imidazolium hydrogen sulfate IL, effectively grafting the polymerized ILs onto the magnetic silica composite material. The novel SAC resulted in high oil conversion of 94.2 % as contributed by the increased Bronsted acidic functionality of the polymeric IL, and exhibited high catalytic activity at 86 % after five reuse runs. Esterification of oleic acid using novel magnetic $CoFe_2O_4$@MoS_2 SACs was demonstrated by Ibrahim *et al.* (2024). The magnetic catalyst composition was revealed to have high acid density at (2.1 mmol H^+/g), enabling high oleic acid conversion at 98.2 %. Carbon-based SACs can be viably composited with magnetic nanocomponents to yield magnetic catalysts that exhibit improved functionality in terms of recyclability and recovery. For example, nanosized, magnetically separable SACs have been developed using a composite design of Fe_3O_4, biochar and direct sulphonation for the esterification of high FFA jatropha, soybean and *mesua assamica* oil (Chutia and Phukan, 2024). The SACs produced high biodiesel yields between 95.3 - 96.8 % under optimum reaction parameters and are attributed to the high acidity and acid density of the SACs (3.9 and 1.8 mmol/g respectively). Rice husk-derived biochar was sulphonated and magnetized using zinc and iron chloride, yielding magnetic SACs for the esterification of oleic acids (Saidi *et al.*, 2023). The rice husk biochar was used as a solid support material for the magnetic components and sulphonic acid functional group, of which the components were synthesized onto the biochar by facile impregnation methods. As a result, a high biodiesel yield of 98.11 % was achieved, and the novel SAC maintained high catalytic conversion after six runs at 80.64 %. In conclusion, examples of heterogeneous SACs developed for the esterification of fatty acids/ FFAs are summarized in Table 2.4. It can be deduced that various approaches in heterogeneous SACs are applied and conducted to yield highly effective Bronsted acidic SACs for the esterification reaction of biodiesel production.

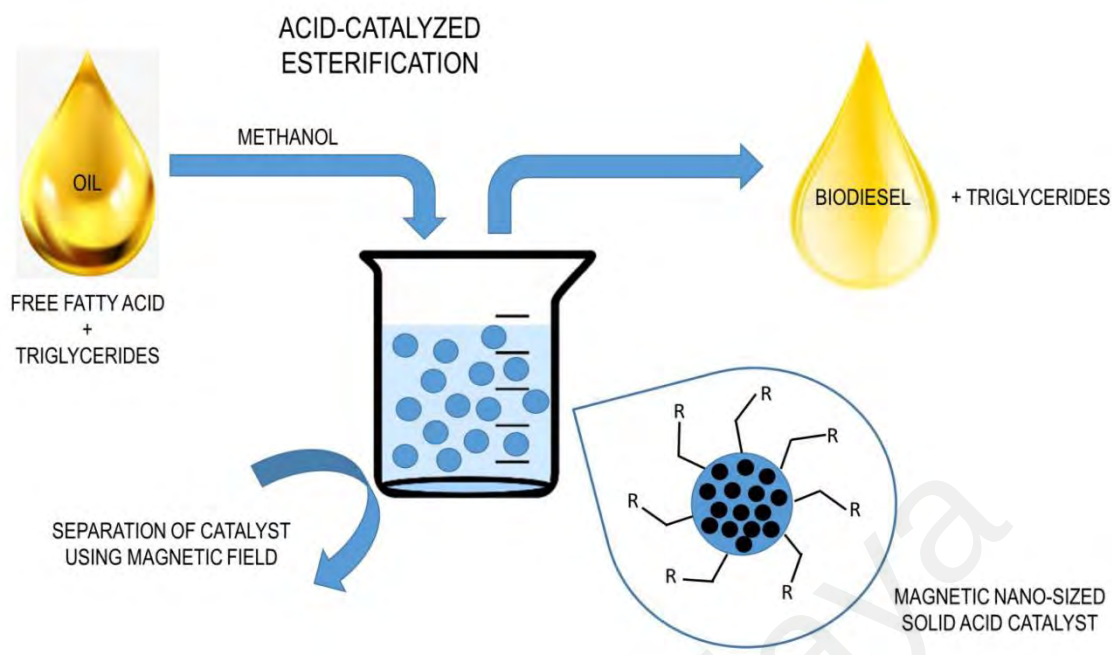

Figure 2.11: Schematic diagram of magnetic SACs for biodiesel production via esterification (Vasić *et al.*, 2020).

Table 2.3: Summary of heterogeneous SACs for biodiesel production by esterification.

Heterogeneous Catalyst Material	Oil Feedstock	Reaction Conditions [3]	FFA Conversion/ FAME Yield	Reference
Activated bentonite-based SACs	Distilled deodorized palm oil, FFA = 84 %	5 wt%, 6:1, 160 °C, 120 min	Highest FFA conversion = 93 %	(Luz *et al.*, 2024)
$CoFe_2O_4$@MoS_2	Oleic acid	7.5 wt%, 15:1, 140 °C, 120 min	Oleic acid conversion = 98.2 %	(Ibrahim *et al.*, 2024)
Açaí seed-derived sulphonated activated carbon	Waste frying oil, FFA = 2.90 mg of KOH/g	8 wt%, 60:1, 60 °C, 150 min	FFA conversion = 97.1%	(Zavarize *et al.*, 2023)
$CoFe_2O_4$@GO	Waste edible oil, FFA = 2.21 %	5.22 wt%, 16:1, 64.75 °C, 55.75 min	Highest biodiesel yield = 98.17 %	(Tamjidi *et al.*, 2022)
1-vinyl-3-(3-sulfopropyl)imidazolium hydrogen sulfate IL grafted onto Fe_3O_4/SiO_2	Soybean oil, FFA = 20 wt%	8 wt%, 30:1, 130 °C, 8 h	Oil conversion = 94.2 % FFA conversion = 100 %	(Xie and Wang, 2021)

Titanium oxysulphate sulphuric acid complex hydrate	Low grade crude palm oil, FFA = 11.3 %	7 wt%, 10:1, 60 °C, 120 min	Yield of treated oil = 90%	(Hayyan *et al.*, 2021)
Cement Kiln Dust	Waste Cooking Oil	2 wt%, 18:1, 65 °C, 6 h	FFA to FAME Conversion = 98.8 %	(Al-Sakkari *et al.*, 2020)
Sulphonated cacao shell	Oleic acid	7 wt%, 7:1, 65 °C, 24 h	Oleic acid conversion = 77 %	(Mendaros *et al.*, 2020)
$HSiW/Al_2O_3$ solid heteropolyacid catalyst	Yellow grease, FFA = 12.26 %	3 wt%, 27:1, 190 °C, 23 h	-	(Gaurav *et al.*, 2019)
Sulfonated D-glucose acid catalyst	Palm fatty acid distillate, FFA = 90.04 %	4 wt%, 10:1, 65 °C, 4 h	FFA conversion = 93.30 % FAME yield = 91.87 %	(Kefas *et al.*, 2018)

[3] Optimized reaction conditions are reported as: Catalyst loading (wt%), methanol-/ glycerol-to-oil molar ratio, reaction temperature (°C), and reaction time (min).

2.6 Identified Research Gaps

It is recently reported that DESs can be formed with the inclusion of certain APIs, such as paracetamol and ibuprofen. This enables the design and synthesis of novel class of DESs for use as an emerging material for green chemistry and engineering. As established in previous studies, the formation of DESs for the acid-catalysed esterification of high FFA feedstock enables improvements in the use of the homogeneous acids (Hayyan *et al.*, 2022; Hayyan *et al.*, 2017). In the application of API-based DESs for the FFA esterification reaction as a catalyst material, it is unknown whether the formation of APIs may enhance or inhibit the catalytic performances of the DES. In a recent study, the PTSA sulphonic acid was reported to be able to form DES compounds with paracetamol, an API, and was applied to the esterification of mixed oils with high FFA content (Hayyan *et al.*, 2023a). On the other hand, the sulphonic acids of 5-sulfosalicylic acid (SSA) and benzenesulfonic acid (BZSA) are not often studied for the FFA esterification reaction of

low-value feedstocks. The formation of DES compounds using these sulphonic acid are not known nor documented, according to reviews of published DES catalysts.

The PTSA:paracetamol DES reported appreciable catalytic activity in the esterification of FFAs in microalgae-palm oil mixtures. However, the DES and its pristine acid counterparts exhibited weak recyclability. The weak recyclability of the DESs in esterification reaction are documented in literature, and usually have a catalytic reaction decay of more than 50 % after several recycling runs (Hayyan *et al.*, 2017; Rashid *et al.*, 2017). Therefore, the weak recyclability of the DESs and its pristine acid components can be addressed and researched. Based on the recent literature on supported heterogeneous SACs, the potential of the DESs and its acids as heterogeneous catalysts in esterification reactions remains unexplored. Based on the list of heterogeneous supports, the use of Fe_3O_4/Polyvinyl alcohol (PVA) magnetic composite materials are not often studied for the application of FFA esterification. PVA is a synthetic biopolymer that has desirable properties of having high thermal and chemical stability, and has shown potential in applications in functional materials and composites, such as hydrogels in biomedical applications and catalyst support materials (Zhang *et al.*, 2016). The use of PVA as a composite material with Fe_3O_4 has been recently reported as shown in Figure 2.12, which is highly prospective in the synthesis of support materials for heterogeneous SACs due to its magnetic properties (Maleki *et al.*, 2019; Rahimi *et al.*, 2020). Moreover, the feasibility of supporting sulphonic acids and DESs onto the Fe_3O_4/PVA composite material is not known, and presents as a potential solution in improving the recyclability performance of DESs for FFA esterification in LPO.

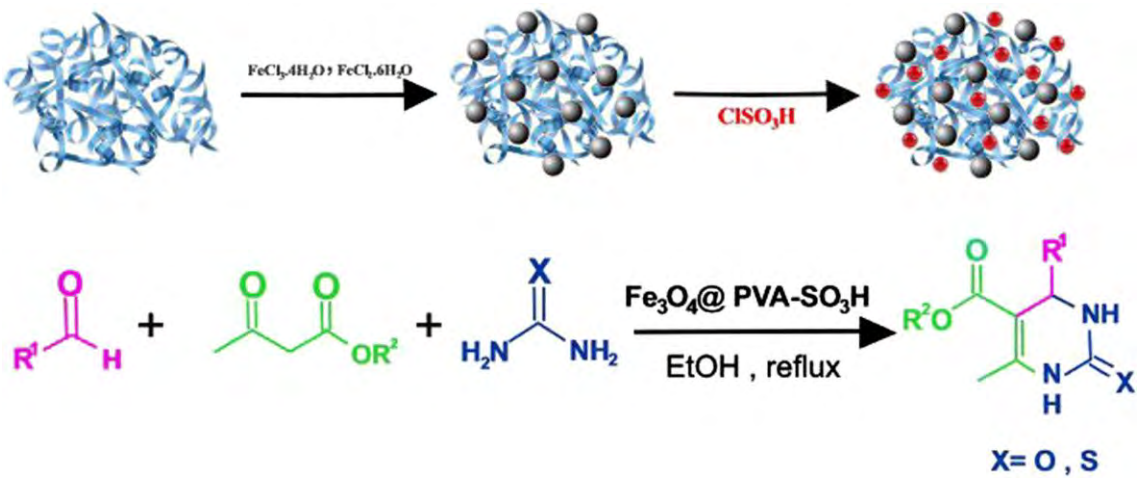

Figure 2.12: Process flow diagram of the synthesis of Fe_3O_4@PVA-SO_3H for the chemical synthesis of dihydropyrimidine (Maleki *et al.*, 2019).

CHAPTER 3: EXPERIMENTAL METHODOLOGY

3.1 Materials and Chemicals

Low-quality palm oil (LPO) was provided by a local palm oil mill in Selangor, Malaysia, and was used as the non-edible oil feedstock. The initial FFA content of the LPO studied for the esterification reaction using acid DES catalysts was recorded as 12.43 %. On the other hand, the initial FFA content of the LPO studied for the esterification reaction using heterogeneous SACs was recorded as 9.66 %. Table 3.1 reports the physicochemical properties of the LPO along with the test methods used to provide the measurements. Subsequently, Table 3.2 presents the fatty acid profile and composition of the LPO used in these studies. Hexadecenoic acid and 9-cis-Octadecenoic acid (palmitic acid and oleic acid respectively) was determined as the primary composition of unsaturated fatty acids of the LPO.

Table 3.1: Physicochemical properties of LPO.

Parameters	Test Method	Values
Peroxide value (ml mol/kg)	ISO 3960:2007	1.43 ± 0.66
Moisture content (%)	ISO 662:1998	1.1 ± 0.40
Iodine value, IV	ISO 3961:1996	52.3 ± 0.68
Impurities (%)	ISO 663:2007	0.052 ± 0.06
Saponification value (mg KOH/g oil)	ISO 3657:2002	191 ± 1.40
Unsaponification matter (%)	ISO 3596:2000	1.48 ± 1.25
Phosphorus (mg/kg)	ISO 10540-2:2003	10.8 ± 0.1
Ash (%)	ISO 6884:1985	0.012 ± 0.01
DOBI (Index)	MPOB Test Method p2.9: 2004	0.54 ± 1.12

Table 3.2: Fatty acid composition profile of LPO as analysed by gas chromatography.

Systematic name of fatty acid	Number of Carbon and Double Bonds	Fatty acid composition (%)
Hexanoic acid	C6:0	0.02
Octanoic acid	C8:0	0.13
Decanoic acid	C10:0	0.12
Dodecanoic acid	C12:0	1.79
Tetradecanoic acid	C14:0	1.55
Hexadecanoic acid	C16:0	39.5
cis-9-Hexadecenoic acid	C16:1	0.14
Octadecanoic acid	C18:0	4.06
9-cis-Octadecenoic acid	C18:1	41.22
9,12-cis-Octadecadienoic acid	C18:2	10.95
9,12,15-cis-Octadecatrienoic acid	C18:3	0.38
Eicosanoic acid	C20:0	0.14

The chemicals used for the synthesis of the novel DESs are as follows: 5-sulfosalicylic acid dihydrate (SSA, CAS Number: 5965-83-3, purity ⩾ 99.0 %) was procured from Merck Malaysia. Benzenesulfonic acid (BZSA, CAS Number: 98-11-3, purity ⩾ 90 %) and paracetamol (PCM, CAS Number: 103-90-2, purity ⩾ 99.0 %, BioXtra) were both purchased from Sigma-Aldrich Malaysia. The chemicals were used as supplied without further purification.

In the synthesis of the heterogeneous catalyst support, anhydrous iron (III) chloride ($FeCl_3$ ≥ 98 %) was obtained from HmbG Chemicals Malaysia, and iron (II) sulphate heptahydrate ($FeSO_4 \cdot 7H_2O$, ≥ 99.5 %) was obtained from R&M Chemicals Malaysia. Polyvinyl alcohol (PVA, molecular weight ~ 60,000, ≥ 98.0 % degree of hydrolysis) and maleic acid (≥ 99 %, Analytical reagent) was purchased from Merck Malaysia. Ammonium hydroxide solution ($NH_3.H_2O$, 25 % w/v solution) was purchased from R&M Chemicals Malaysia. Methanol (anhydrous, 99.8 % purity) and propan-2-ol (ACS

reagent) was purchased from Sigma-Aldrich Malaysia. Potassium hydroxide pellets (KOH, ≥85 % purity) were procured from HmbG Chemicals Malaysia.

3.2 Synthesis of Catalyst

3.2.1 Synthesis of API-based DESs

The API-based DESs were synthesized according to the formulation as follows: Brønsted acids (SSA or BZSA) were mixed with paracetamol at a molar ratio of 3:1. Prior to synthesis, the chemicals involved in DES synthesis were dried in a vacuum oven at 50 °C for 24 h to remove any moisture adsorbed during chemical storage. The dried chemicals were transferred to a sealed vial, and underwent vigorous mechanical stirring of 350 rpm for 1 – 3 h, or until a homogeneous solution is obtained (Ma and Row, 2021; Russo *et al.*, 2022). The stirring was conducted at 80 °C using a hot plate stirrer to enable the components to effectively mix and form a eutectic mixture. Upon completion, the synthesized DESs were collected in a sealed vial and stored in a desiccator. All DESs were liquid in phase at elevated temperatures and no precipitation was observed after 24 h of storage. The average molecular weight of the DES was computed using Equation 3.1 (AlOmar *et al.*, 2016):

$$\boldsymbol{MW_{DES} = x_{HBA} MW_{HBA} + x_{HBD} MW_{HBD}} \quad \text{(Equation 3.1)}$$

where MW_{DES} is the resultant average molecular weight of the novel DES, x_{HBA} and x_{HBD} are the molar fraction of the HBA and HBD component respectively, MW_{HBA} is the average molecular weight of the HBA component, and MW_{HBD} is the average molecular weight of the HBD component.

3.2.2 Synthesis of Fe_3O_4/PVA Magnetic Composite

Fe_3O_4/PVA magnetic composites were synthesised based on the in situ co-precipitation method (Fazelinia *et al.*, 2023; Kamalzare *et al.*, 2021). A 5 w/v % PVA solution was produced by dissolving PVA in distilled water under vigorous stirring for 4 h at 80 °C. Subsequently, 12 mL of $NH_3.H_2O$ was added to the PVA solution to adjust the pH to 11. At the same time, 0.02 mol of $FeCl_3$ and 0.01 mol of $FeSO_4 \cdot 7H_2O$ were dissolved in 10 mL of distilled water to form a 2:1 Fe^{3+}:Fe^{2+} ratio mixture, serving as the Fe^{3+} and Fe^{2+} precursors for the synthesis of Fe_3O_4 magnetic nanoparticles by co-precipitation. This mixture was added dropwise using a micropipette into the $NH_3.H_2O$–PVA solution under stirring at 350 rpm. The solution gradually turned black and was continuously stirred for 2 h at 60 °C under N_2 atmosphere. The black particles precipitate (denoted as Fe_3O_4/PVA) was recovered using an external magnet and washed several times with distilled water and dried at 60 °C overnight.

3.2.3 Synthesis of Acids and DESs Supported on Fe_3O_4/PVA

The synthesis protocol was adapted from the proposed method described by (Kamalzare *et al.*, 2021). with slight modification. To synthesise the acid-supported Fe_3O_4/PVA, a 1:1 by mass ratio of Fe_3O_4/PVA and acid/DES was taken (Swami *et al.*, 2023). 1 g of Fe_3O_4/PVA was dispersed in 15 mL of distilled water, and simultaneously 1 g of acid (BZSA, PTSA or SSA) or DES compound ([3BZSA:PCM], [3PTSA:PCM] or [3SSA:PCM]) was dissolved in 10 mL of distilled water. The acid solution was added to the Fe_3O_4/PVA solution and continuously stirred for 15 min at ambient temperature. Subsequently, 30 wt% of maleic acid was added as the crosslinker for the composite according to a previous optimization study (Mok *et al.*, 2020) and then,1 mL of 37 % HCl was added to catalyse the crosslinking process. Finally, the mixture of synthesised

composite (denoted as Fe_3O_4/PVA/Acid) was stirred for 30 min at room temperature, and subsequently collected using an external magnet. To remove any residuals remaining with composite, the Fe_3O_4/PVA/Acid was washed by several times using distilled water and dried at 60 °C overnight.

3.3 Characterization of Catalysts

3.3.1 Characterization Studies of API-based DESs

To observe the formation of the DES and discern the functional groups present, attenuated total reflectance Fourier transform infrared (ATR-FTIR) spectroscopy was used to obtain the FTIR spectra of the synthesised DESs. ATR-FTIR spectrophotometer (Perkin Elmer Spectrum 100) was used to record the FTIR spectra of DESs from wave number ranges of 650 to 4000 cm^{-1} at a scan resolution of 4 cm^{-1} for sixteen repeated, averaged scans. As novel acidic catalysts are formed, the acidity of the DESs were revealed through the Hammett acidity function using UV-vis spectroscopy (Hao *et al.*, 2017; Yu *et al.*, 2022). 4-nitroaniline (CAS No.: 100-01-6, Merck, ≥99 %) was employed as the basic indicator and distilled water was used as the solvent (Cui *et al.*, 2017). Unprotonated form of 4-nitroaniline shows the highest absorbance at a wavelength of 380 nm in water, and the Hammett acidity function (H_0) for the reference and acids were measured at this wavelength (Sun *et al.*, 2015).

3.3.2 Characterization Studies of Fe_3O_4/PVA/Acid Magnetic Composite

The synthesised Fe_3O_4/PVA/Acid was characterized for its morphology and elemental composition using field emission scanning electron microscopy (FESEM) imaging and energy dispersive X-ray spectroscopy (EDX) analysis (FEI Quanta FEG 650 S scanning

electron microscope). The structural phase of the synthesised Fe_3O_4/PVA and Fe_3O_4/PVA/Acid were revealed using x-ray diffraction (XRD) analysis, that was conducted on the Malvern PANalytical EMPYREAN diffractometer system using CuKα radiation (λ = 1.5406 Å) at two theta (2θ) angle range of 10 – 80 (0.01 step size), and operated at 45 kV volts and 40 mA current. The thermogravimetric analyses (TGA) was conducted using a PerkinElmer Pyris 6 TGA analyser and the thermal behaviour was observed from 30 – 800 °C at a 10 °C/min heating rate under nitrogen gas flow. The energy binding and oxidation states of the Fe_3O_4/PVA/Acid composite were determined through x-ray photoelectron spectroscopy (XPS) conducted on the Axis Ultra DLD (KRATOS model) x-ray photoelectron spectrometer using a monochromated Al Kα radiation (1486.6 eV) as excitation source (15 kV). The elemental peaks from the XPS analysis were analysed and deconvoluted using the XPSPEAK41 software with mixed Gaussian Lorentzian functions after subtraction of the linear-type background.

3.4 Esterification Experimental Setup

The LPO was preheated at 70 °C for 1 h until a homogeneous phase was observed, as the LPO existed as a thick semisolid when stored in room temperature. 20 g of LPO was added to a closed, jacketed reactor equipped with an overhead condenser. The FFA limit post-esterification reaction was pre-determined at below 2 %. The initial and final FFA content was calculated as wt% of palmitic acid as shown in Equation 3.2 according to AOCS Official Method Ca 5a-40 (AOCS, 2017; Teh and Lau, 2023):

$$\boldsymbol{FFA}\ (\%) = \frac{\mathbf{25.6}\times \boldsymbol{N}\times \boldsymbol{V}}{\boldsymbol{m_{oil}}} \qquad \text{(Equation 3.2)}$$

where N is the normality of the alkali (KOH) used, V is the volume of alkali (mL) and m_{oil} is the oil sample mass (g). To determine the FFA content by titrimetric method, 1.0 g of oil sample was diluted and fully dissolved in 50 mL of isopropanol neutralized with

0.1% phenolphthalein solution. The solution was subsequently titrated with 0.1 N potassium hydroxide until a persistent, faint pink colour was observed. Furthermore, the product yield, referring to the conversion of FFA into FAME, was determined according to Equation 3.3:

$$\boldsymbol{Conversion} = \frac{\boldsymbol{FFA_i - FFA_0}}{\boldsymbol{FFA_i}} \times \mathbf{100}\% \qquad \text{(Equation 3.3)}$$

where FFA_i and FFA_0 are the initial and final FFA values before and after esterification, respectively.

3.4.1 Experimental Setup for Esterification Reaction using API-based DESs

The acidic catalysts (DES) and methanol were subsequently charged into the reactor. The esterification reaction was conducted at a fixed stirring speed of 350 rpm (magnetic stirring), and other experimental parameters, namely the DES catalyst dosage (0.25 – 3.0 wt%), methanol ratio (2:1 – 18:1 to oil), reaction time (10 – 100 min), and temperature (40 – 80 °C) were procedurally optimized by the single factor optimization method. The reaction results were triplicated to validate the esterification conditions and the standard errors were presented.

To further assess the performance of the DES catalysts, a catalyst recyclability test was conducted, involving the recovery of the DES catalyst by centrifugation from the esterified products at the end of reaction. At the end of every esterification run, the mixture was transferred to a centrifuge tube and subjected to centrifugation at 3000 rpm for 15 min. Based on the density and viscosity differences between the treated oil and the methanol phase, the methanol phase was separated and recovered from the top layer of the centrifuge tube. The retrieved methanol was evaporated by heat, whereby the DES was recovered and subsequently added to fresh LPO without regeneration. The

esterification reaction runs were carried out and repeated according to the fixed optimum conditions to observe the extent of the DES catalytic activity when recycled.

3.4.2 Experimental Setup for Esterification Reaction using Fe_3O_4/PVA/Acid Magnetic Composite

The Fe_3O_4/PVA/Acid catalyst was added to the reactants of 20 g of LPO and methanol in a sealed, jacketed reactor equipped with an overhead condenser, where the mixture was stirred at 350 rpm constantly throughout the experiment. A screening stage was conducted to preliminarily evaluate the catalytic performance of the FFA esterification reaction and determine the most suitable catalyst including either the sulphonic acids or DES compounds supported on the Fe_3O_4/PVA magnetic composite. Subsequently, the preferred catalyst material was determined from the screening procedure for further characterization and optimization (by single factor optimization). The optimization parameters including: catalyst loading within the range of 5 – 20 wt %, methanol requirement within 10:1 – 25:1 methanol-to-oil molar ratio, contact time within 1 – 6 h, and reaction temperatures 30 – 70 °C. The esterification experiments were triplicated and the average FFA content is presented along with the standard deviation. The recyclability performance of the heterogeneous magnetic catalyst was also conducted. At the end of reaction, the catalyst was easily recovered using an external magnet and regenerated by washing repeatedly up to three times with distilled water, and subjected to oven drying at 60 °C overnight. The recovered catalyst was added to fresh LPO and the extent of the esterification reaction was evaluated.

CHAPTER 4: RESULTS AND DISCUSSION

4.1 Spectroscopic Characterisation of API-based DESs

4.1.1 FTIR Spectra of API-based DESs

The FTIR spectra lines were obtained for the novel API-based DESs synthesised to ascertain and tag the functional groups involved within the DES formation. The spectral lines of the Brønsted acids (BZSA and SSA), PCM and the synthesised DESs of [3SSA:PCM] and [3BZSA:PCM] are shown in Figure 4.1. The O–H stretching spectra bands at around 3000 – 3410 cm^{-1} that are characteristic of DES hydrogen bonding interactions were observed for all DESs constituents and DESs except for the [3BZSA:PCM] spectra. This can be attributed to the weaker hydrogen bond formation between DES constituents that result in weak, broad bands typically observed in DESs consisting of phenol sulfonic acids such as PTSA (Rodriguez Rodriguez *et al.*, 2019). In the FTIR spectra of the [3SSA:PCM] and [3BZSA:PCM] DESs, C=O stretching of the secondary amide found in the PCM compound can be assigned to the peak at 1677 cm^{-1}. Additionally, the peak at 1507 cm^{-1} is assigned to the C=C stretching vibration of the benzene ring of the PCM, suggesting that the PCM compound is incorporated in the formation of the DES with the Brønsted acids. These peaks may also suggest hydrogen bond donating interactions between the aromatic rings of the PCM and Brønsted acids in the formation of the DES compounds. Asymmetric C–H bending of the methyl group (–CH_3) can be ascribed to the strong peaks detected at 1447 – 1449 cm^{-1} describing the DES constituents. O–H bending of the phenol functional groups contributed by SSA and PCM moieties can be assigned to the medium peak at 1342 cm^{-1} (Zapata *et al.*, 2021). Several peaks revealed the presence of sulphur group interactions. The symmetric stretching of O=S=O within the sulfonic acid (–SO_3H) functional group can be assigned to the vibration peak at 1126 cm^{-1} (Jiang *et al.*, 2020; Liu *et al.*, 2020a). The peak at 1027 cm^{-1} can be assigned to the bending motion of C–S bonds. The peak detected at 837 cm^{-1} can

be ascribed to the hydrogen-oxygen bonding between –OH and the sulfonic acid group, suggesting the formation of a eutectic mixture through hydrogen bonding (Hazmi *et al.*, 2022).

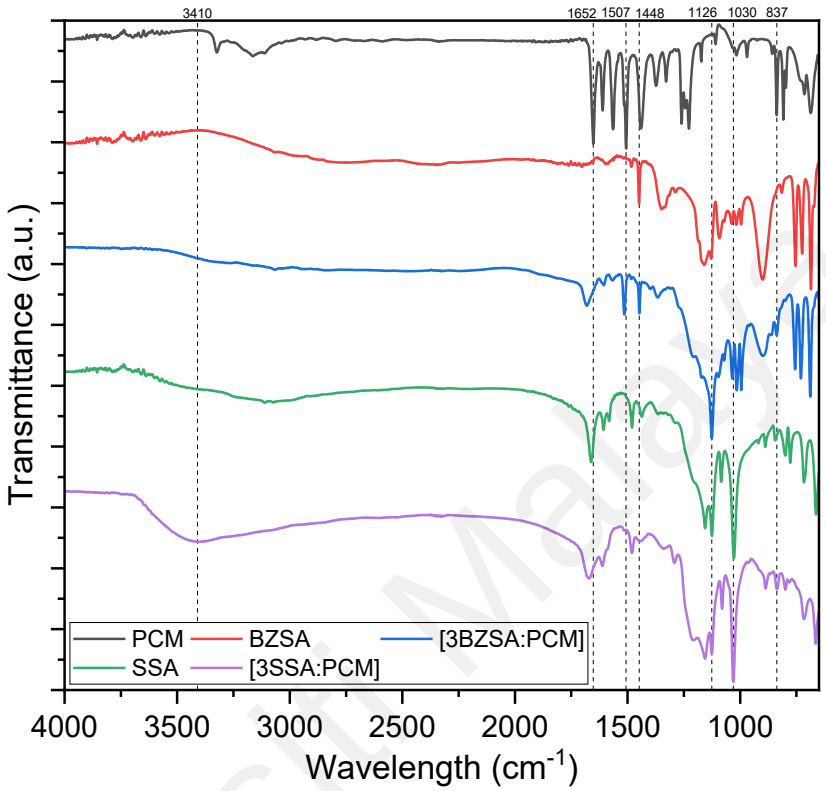

Figure 4.1: FTIR spectra of PCM, Bronsted acids (BZSA and SSA) and synthesized DESs.

4.1.2 Hammett Acidity Function of Acidic DESs

To provide further insights into the properties of the novel DESs, the acidity of the investigated DESs were studied using the Hammett acid function. The acidities of API-based DESs were quantified using 4-nitroaniline (pK_a of 4-nitroaniline = 0.99) as the indicator through UV-vis spectroscopy. According to the procedures detailed by Cui *et al.* (2017), the DESs and 4-nitroaniline were dissolved in water at concentrations of 4.0×10^{-2} mol/L and 7.24×10^{-5} mol/L (0.01 g/L), respectively. Furthermore, the Brønsted acid constituents of the DESs were also involved (dissolved at 4.0×10^{-2} mol/L) to study the effects of DES formation on the acidity of the mixture. In its unprotonated

form, 4-nitroaniline showed maximal absorbance of 380 nm in water. The DES/ Brønsted acids and 4-nitroaniline mixture was stirred overnight and the UV-vis spectra was measured at 298.15 K. The Hammett acidity function (H_0) of the DESs/ Brønsted acids were calculated using Equation 4.1:

$$H_0 = pK(I)_{aq} + \log\left(\frac{[I]}{[IH^+]}\right) \quad \text{(Equation 4.1)}$$

where $pK(I)_{aq}$ is the indicator (I) pK_a value, $[I]$ is the molar concentration of the indicator's unprotonated form, and $[IH^+]$ is the molar concentration of the indicator's protonated form.

The UV-vis absorbance spectra of the DESs/ Brønsted acids and 4-nitroaniline are presented in Figure 4.2. The maximal absorbance of the 4-nitroaniline indicator was observed to decreased with the addition of DESs/ Bronsted acids, and the H_0 values were calculated and are presented in Table 4.1. The acidity of the samples measured are ranked as SSA (1.21) > BZSA (1.26) > [3SSA:PCM] (1.27) > [3BZSA:PCM] (1.32). Based on the H_0 values, the acidity of the DESs were recorded to be lower than its Bronsted acid constituent. This may be attributed to the addition of PCM as a weak organic acid (pKa = 9.5) to form a eutectic mixture based on hydrogen bonding interactions, that contributes to the weaker acidity of the DES compared to its neat Bronsted acid form (Ayoub, 2021; Chen *et al.*, 2023). SSA and its derived DESs are more acidic than those based off of BZSA owing to the presence of an electron withdrawing group (carboxylic acid, −COOH) at the meta position of the arenesulfonic acid group (Gandhi *et al.*, 2011).

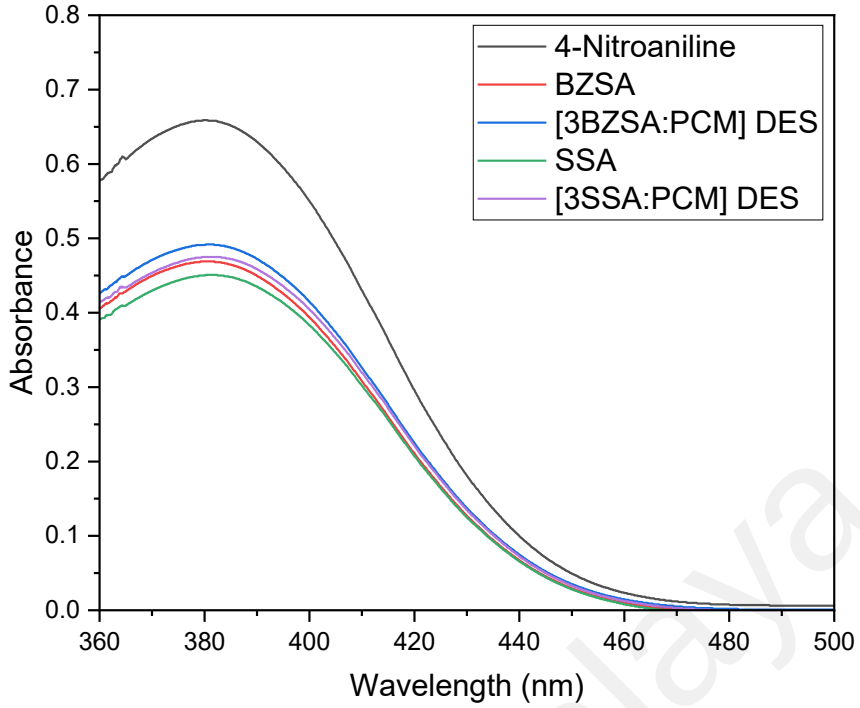

Figure 4.2: UV-Vis absorbance spectra of 4-nitroaniline, Bronsted acids and API-based DESs dissolved in water at 298.15 K.

Table 4.1: UV–Vis absorbance spectra of 4-nitroaniline in the presence of different DESs in water at the concentration of 40.0 mmol/l and 298.15 K.

Sample	A_{max}	[I] (%)	[IH] (%)	H_0
4-Nitroaniline	0.659	100	0	-
BZSA	0.469	65.23	34.77	1.263
[3BZSA:PCM]	0.491	68.29	31.71	1.323
SSA	0.450	62.59	37.41	1.213
[3SSA:PCM]	0.475	66.06	33.94	1.279

4.2 Computational Evaluation of DESs and its Interaction with Methanol

4.2.1 Sigma Profile Analysis for DES Formation

The combination mechanism of the API-based DESs was studied and represented using the COSMO-RS computational model by means of the HBD and HBA interaction mechanism. Firstly, the chemical structures of the molecules involved in this study were drawn, and their geometry optimisation was conducted at the Hartree–Fock level and 6–31G* basis set. To generate the .cosmo file, the single-point calculation was conducted through DFT calculations with Becke–Perdew and the Triple-ζ Zeta Valence Potential (TZVP) basis set (Salleh *et al.*, 2018). The created cosmo files were exported to COSMOthermX for mixture properties calculation and the electroneutral approach was used to represent the DES in COSMO-RS. The σ-profile diagrams of the DES constituents (BZSA and SSA as HBD, and PCM as HBA) were generated and presented in Figure 4.3. The σ-profiles can be interpreted as a bifurcated diagram consisting of the non-polar and polar (hydrogen bond donor and hydrogen bond acceptor) region. Additionally, the sigma surfaces of the parent molecules involved in the DES formation are included in Figure 4.3, whereby regions of red, green and blue indicate gradients of higher electronegative, non-polar and higher electropositive surfaces respectively. Here, the major peaks in the non-polar region (-0.001 – 0.004 e/Å^2) can be attributed to the presence of the aromatic ring in all three DES constituents, describing the non-polar nature of the molecules (Khan *et al.*, 2021a). In the positive σ region, the significant peak at +0.01 e/Å^2 is ascribed to the oxygen (O) atoms present in the acid functional groups of BZSA and SSA, whereas the peak at +0.014 e/Å^2 is ascribed to the O atoms contributed by the phenolic hydroxyl group and the amide group of PCM. These peaks present in the positive region (σ > +0.008 e/Å^2) reflect the ability of the molecule to act as an HBA. In contrast, the negative region (σ < -0.008 e/Å^2) represents the ability of the molecule to act as a HBD, and all three molecules show small peaks (-0.019 e/Å^2 for BZSA and SSA,

and -0.016 e/Å^2 for PCM) within this region, attributed to the presence of hydrogen (H) atoms. The σ-profile of all three DES constituents reveal that the individual components may exhibit high compatibility amongst each other to form DESs, where peaks contributing to hydrogen bond donating and accepting mechanisms were evident and significant on both positive and negative regions (Hizaddin *et al.*, 2022). In conclusion, the interpretation of the COSMO-RS computational model qualitatively indicated hydrogen bonding donating and accepting abilities of BZSA, PCM and SSA molecules, which can explain the possible and viable formation of a DES compound using these constituents (Aissaoui *et al.*, 2017).

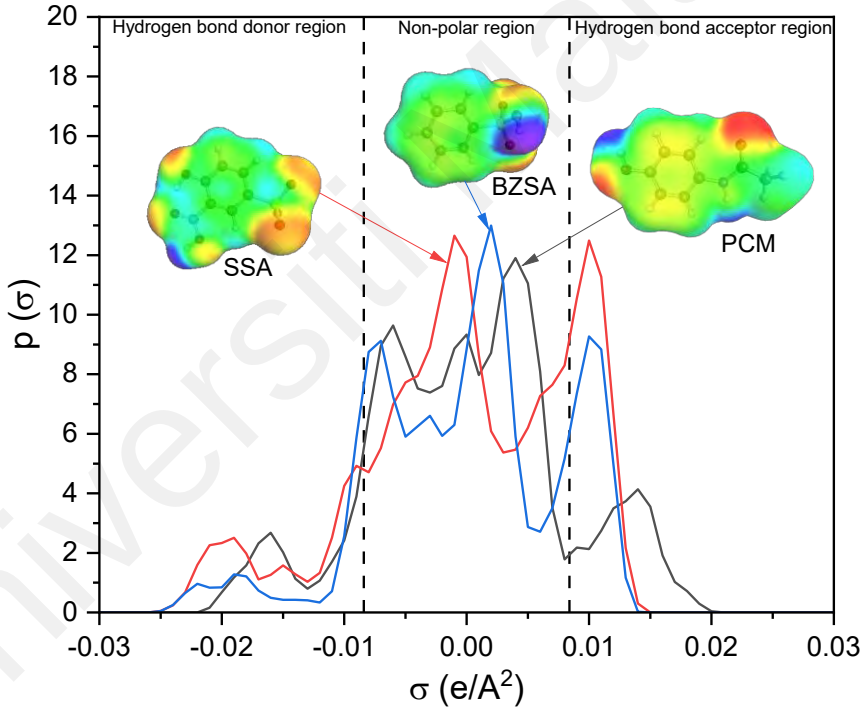

Figure 4.3: Screening charge density (σ) and molecular surfaces of DES constituents generated by COSMO-RS computational prediction process.

4.2.2 Computational Evaluation of DES Interaction with Methanol

As a homogeneous catalyst for esterification, it is insightful to study the solubility of the API-based DESs in the reaction solvent, i.e., methanol. To support the experimental

findings, COSMO-RS was used to study the interactions of the DESs with methanol. Firstly, the relative solubility of the API-based DESs were screened by means of a qualitative solubility comparison, i.e., complete miscibility approaching unity value, between solutes in a selected solvent (in methanol for the application of FFA esterification). The API-based DESs were screened for relative solubility in methanol in comparison with common organic solvents, in which the result is depicted in Figure 4.4. The API-based DESs were determined to be as highly miscible in methanol as dimethylsulfoxide (DMSO), and showed higher solubility in methanol than other conventional polar solvents such as ethanol and propanol. When compared to the solubility of pure paracetamol component in methanol, the API-based DESs showed relatively greater solubility, and may be attributed to complex hydrogen bond formations between DES constituents that interacts with methanol.

Furthermore, the molecular interactions between DESs and solvents were investigated through the σ-profile and σ-potential, as illustrated in Figure 4.5. To provide adequate comparison, four solute categories, that are the API-based DESs, DMSO, acetonitrile and *n*-nonane were evaluated for its σ-profile and σ-potential diagrams based on the decreasing solubility sequence. The sigma profiles of the DESs and selected organic solvents were generated by COSMO-RS (Figure 4.5). The σ-profile of methanol exhibited charge density peaks in both non-polar and polar regions. Subsequently, the screening charge density for [3SSA:PCM] and [3BZSA:PCM] DESs revealed significant peaks in all three regions aligning with methanol, suggesting that these molecules can interact strongly and promote solubility. Thus, the DESs can be deduced from the σ-profile to behave both as an HBD and a HBA component when interacting with methanol. The positive σ-profile peaks at 0.008 – 0.02 e/Å^2 illustrate the high electronegativity of the O, S and N atoms in attracting H atoms at the hydrogen-bond acceptor region, whereas the peaks at -0.008 – -0.02 e/Å^2 illustrates the high electropositivity of the H atoms (Alioui

et al., 2020). These are attributed to the sulfonic acid functional groups within the SSA and BZSA moiety of the API-based DESs that enable and promote hydrogen bonding with the hydroxyl group present within the methanol.

The σ-potential analysis presented in Figure 4.5 reveals the intermolecular affinity within a mixture. Increased intermolecular interactions is indicated by a higher negative value of μ (σ), whereas higher repulsion tendencies are indicated by a higher positive μ (σ) value. For both [3SSA:PCM] and [3BZSA:PCM] DESs, its *σ*-potential plot revealed high negative values in the hydrogen-bond acceptor regions, suggesting strong affinity for HBD molecules. Additionally, both DESs showed higher negative values in the HBA region than the Para:PTSA (1:3) DES reported by Hayyan *et al.* (2023a), which may induce stronger interaction and enhanced solubility in methanol compared to the API-based DES derived from PTSA. Attractive forces are also evident when observing the curves of the acetonitrile, DMSO and methanol solvents at the hydrogen-bond donor region, indicating participation in polar interactions. As the hydrocarbon model, *n*-nonane revealed a parabolic *σ*-potential curve that shows positive values in both polar regions, suggesting their non-participation in polar interactions and their nonpolar nature (Mohan *et al.*, 2022). In conclusion, the results of computational prediction processes through σ-profile, σ-potential diagram and relative solubility screening supports the formation of the novel DESs, and the good solubility of the API-based DESs as a homogeneous acid esterification catalyst in methanol.

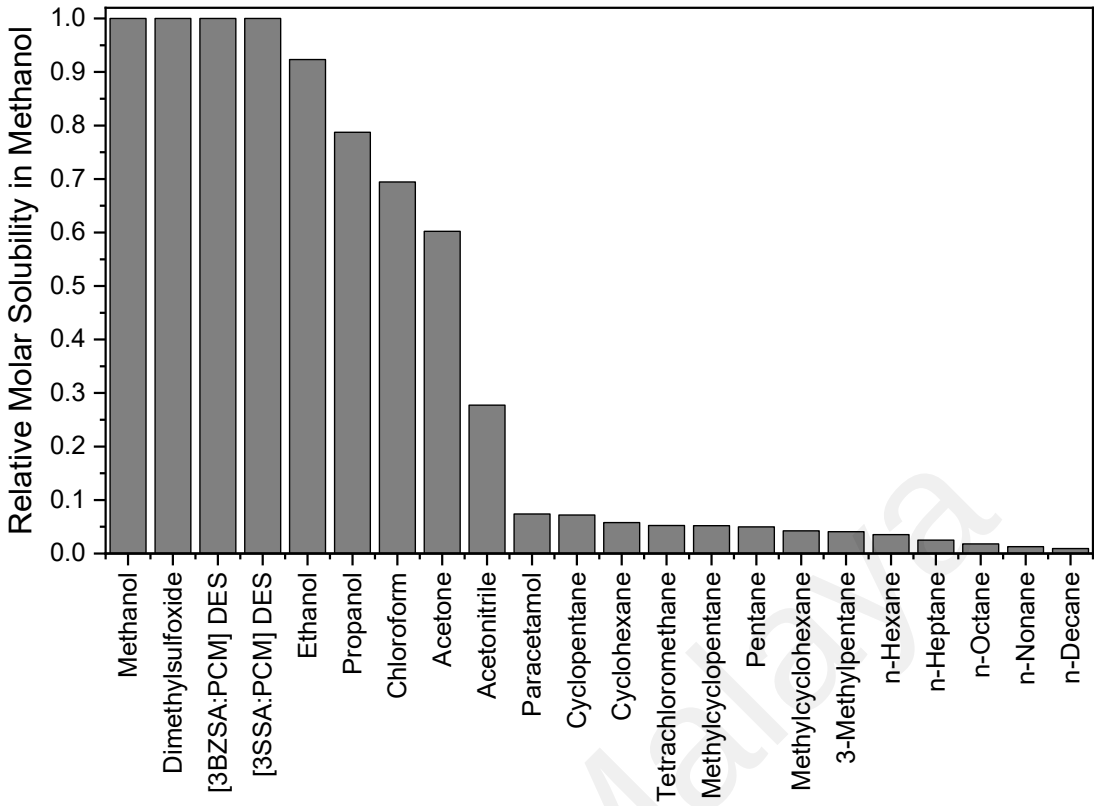

Figure 4.4: Relative molar solubility of API-based DESs with various organic compounds in methanol.

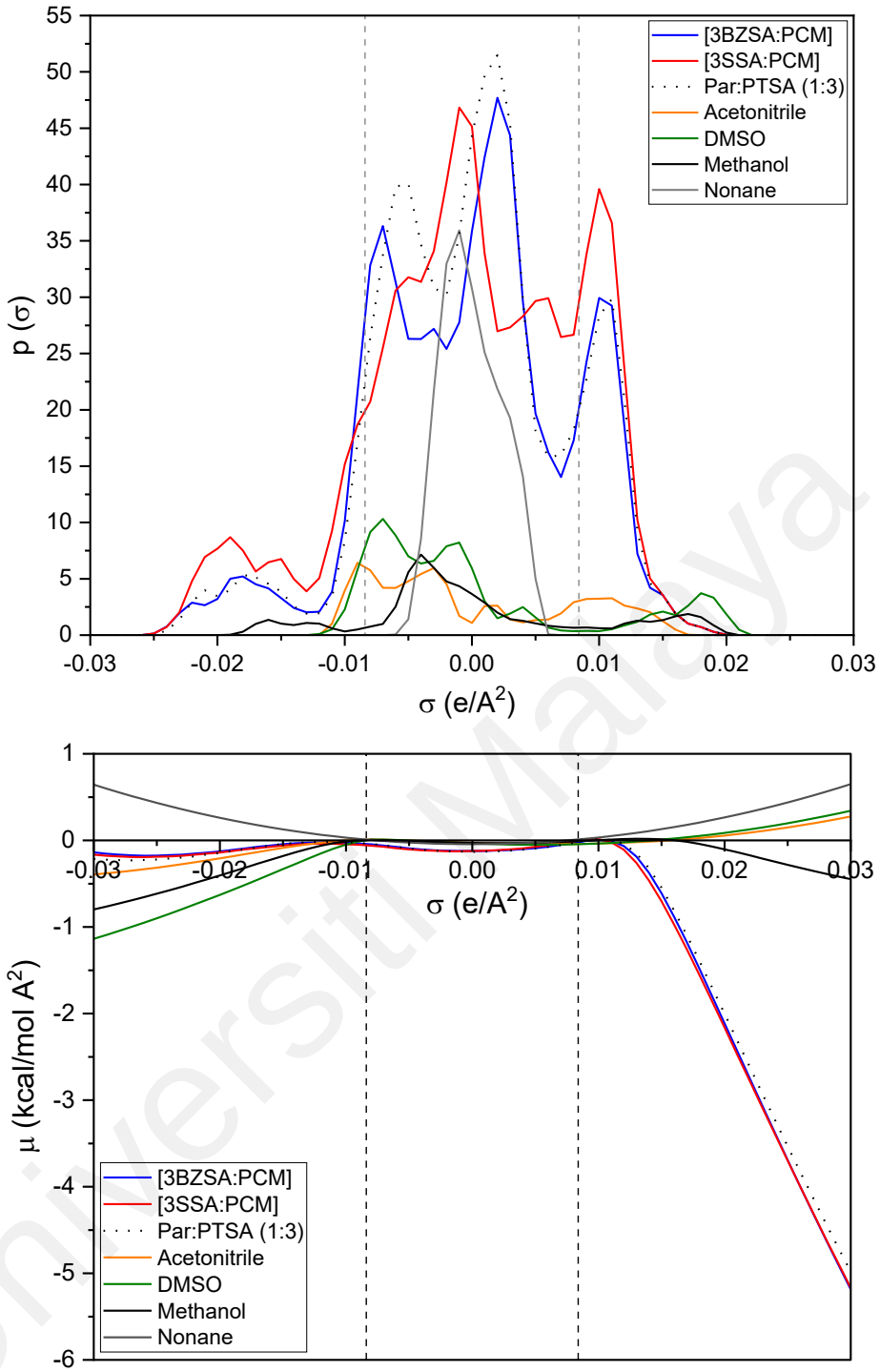

Figure 4.5: σ-profile and σ-potential diagrams of the API-based DESs and selected organic solvents.

4.3 Optimization of Esterification Reaction Catalysed by DESs

4.3.1 Effect of DES Catalyst Dosage

The effect of DES catalyst dosage (from 0.25 – 3.00 wt%) on the reduction of FFA content, and the trend of FFA to FAME conversion in LPO is presented in Figure 4.6. As the DES catalyst dosage is investigated as the manipulated variable, other reaction variables, such as reaction temperature (60 °C), reaction time (90 min), mixing speed (350 rpm) and methanol molar ratio (20:1) were kept constant. The [3BZSA:PCM] DES exhibited high FFA reduction at the low dosage of 0.25 wt% to oil compared to the [3SSA:PCM] DES, yielding a FFA to FAME conversion rate of 80.13 %. Furthermore, the conversion rate was observed to increase with increasing DES catalyst dosage for all trends, which can be attributed to the increased number of sulphonic acid functional groups available throughout the reaction that provided greater proton donation and increased reaction rates (Lu *et al.*, 2022). The FFA limit of < 2 % was achieved at 1.5 and 2.5 wt% using [3BZSA:PCM] and [3SSA:PCM] DESs respectively, and the recorded catalyst dosage was taken as the optimal dosage parameter.

Compared to other homogeneous acid catalysts employed for the deacidification of oil feedstocks, the optimal DES catalyst dosage determined in this study is in line with previous studies (1 – 10 wt%) (Chai *et al.*, 2014). In another study on the esterification of FFA in oleic acid, Williamson et al. reported on the use of a novel phosphonium-based DES comprising allyl triphenylphosphonium bromide and p-toluenesulfonic acid (1:3 component molar ratio in DES). 95 % FFA conversion from direct glycerolysis reaction was achieved at 5 wt% of DES loading, while subsequently achieving the lowest activation energy of 54.64 kJ/mol (Williamson *et al.*, 2017). A quaternary ammonium-based DES comprising tetrabutyl ammonium hydrogensulphate and p-toluenesulfonic acid (1:2 molar ratio composition in DES) was reported as a catalyst for FFA reduction and conversion in PFAD and brown grease through glycerolysis (Mamtani *et al.*, 2023).

Upon determining the optimum reaction conditions using oleic acid as a model (10 wt% catalyst dosage, 6:1 glycerol to oil molar ratio, reaction temperature of 130 °C and 10 min reaction time), the novel DES showed similar conversion performances in treating PFAD and brown grease, achieving up to 94 % equilibrium conversion.

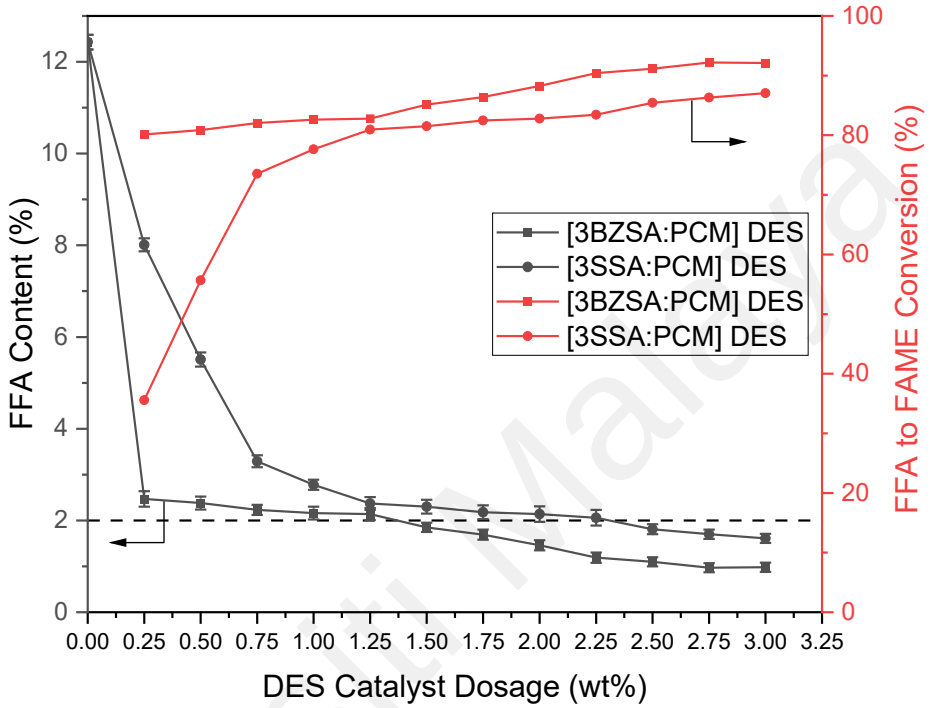

Figure 4.6: Effect of DES acid catalyst dosage on the reduction of FFA content and the conversion of FFA to FAME.

4.3.2 Effect of Alcohol Molar Ratio

FFA esterification is a reversible reaction, and the use of excess methanol as a reactant component is crucial to enable forward reaction according to Le Chatelier's principle (Ganesan *et al.*, 2020). The extent of excess methanol molar ratio to oil required was investigated and presented in Figure 4.7. A gradual reduction of FFA was observed in both API-based DES catalysed systems, where the [3BZSA:PCM] and [3SSA:PCM] DES catalysts attained the FFA percentage target of below 2 % at 8:1 and 16:1 methanol-to-oil molar ratio respectively. The higher methanol requirement of the [3SSA:PCM] DES catalyst may be due to its high viscosity and delay in solvation within the methanol phase.

In literature, various studies involving methanol volume optimization reported using optimal methanol in excess ratios from 10:1 – 20:1 (Ahmed and Huddersman, 2022; Devaraj Naik and Udayakumar, 2021; Soontarapa *et al.*, 2023). The optimization of methanol volume enables lower consumption of reaction materials, milder reaction conditions and short reaction times (Ofoefule *et al.*, 2019). In other study-specific optimization experiments, the methanol molar ratio is investigated in high molar ratios, between 25:1 to 75:1 (Jisieike *et al.*, 2023; Kushwaha *et al.*, 2023). Excessive amounts of methanol may lead to undesirable ester (biodiesel) hydrolysis as a result of backwards reaction, and reduces the area of contact between reactants by diluting the reaction system (da Luz Corrêa *et al.*, 2020; Ibrahim *et al.*, 2020b). Increasing the methanol loading beyond 16:1 molar ratio was not observed to yield significant improvements to the FFA reduction and conversion, and the optimal methanol molar ratio for each DESs were taken when the FFA content is reduced to the set limit.

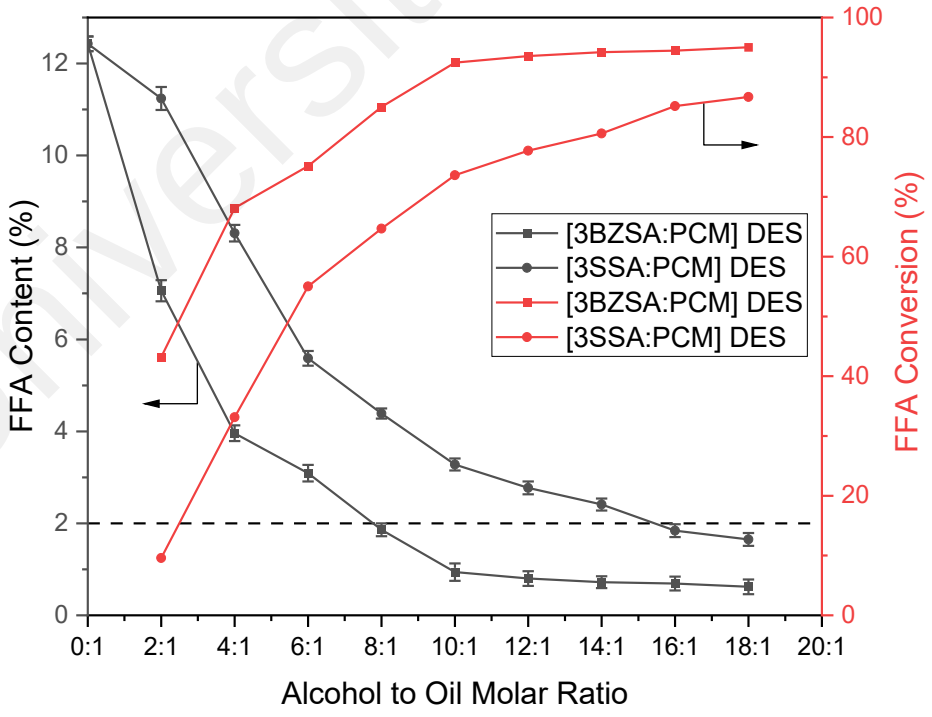

Figure 4.7: Effect of alcohol (methanol) to oil molar ratio on the reduction of FFA content and the conversion of FFA to FAME.

4.3.3 Effect of Reaction Time

Acid catalyst contact time should be sufficient to enable the FFA esterification reaction to be shifted forward and achieve an optimal equilibrium of state in reaction. However, with a similar basis to excess methanol volume in a reversible reaction, excessive reaction time is not necessary once a state of equilibrium is reached (da Luz Corrêa *et al.*, 2020). The effect of reaction time on the efficacy of FFA reduction is presented in Figure 4.8. Following a gradual reduction of FFA content across time, the [3BZSA:PCM] DES achieved the FFA limit at 50 min of reaction time, yielding a treated oil sample with 1.76 % of FFA content. Contrastingly, the [3SSA:PCM] DES required almost double the reaction time at 90 min compared to [3BZSA:PCM], achieving an FFA value of 1.77 %. The optimum reaction time taken for both DESs were comparable to previously reported acidic DESs applied for FFA esterification reactions. Furthermore, as a homogeneous phase catalyst to the oil feed, the reaction time required to achieve equilibrium in this study is comparatively lower than some heterogeneous acidic catalysts. For example, oleic acid esterification using a novel glucose substrate-derived carbon-based catalyst was reported to require 120 min of reaction time as the optimum condition, resulting in ≥ 97.5 % conversion of FFA to methyl oleate (Rokhum *et al.*, 2022). In a similar study utilizing biomass materials, waste angle wing shells were used as the sulphated catalyst support for palm fatty acid distillate (PFAD) esterification. High FAME conversion of 98 % was reported using 5 wt% of catalyst loading at 180 min reaction time (Syazwani *et al.*, 2019).. Hence, the development of homogeneous catalysts may enable lower reaction times owing to the lower mass transfer resistance when compared to heterogeneous catalysts.

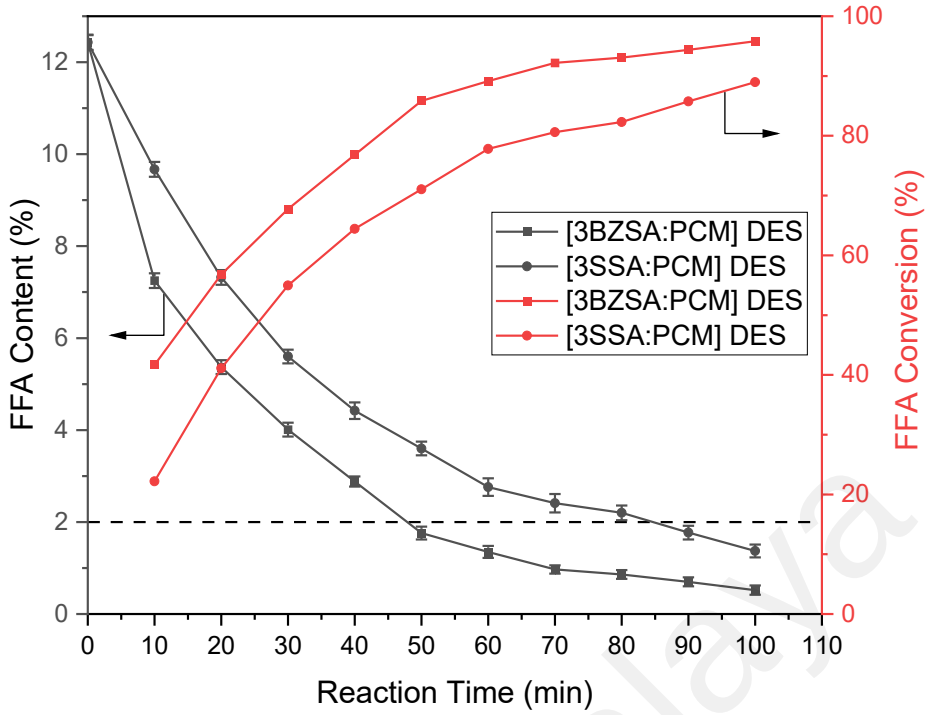

Figure 4.8: Effect of catalyst reaction time on the reduction of FFA content and the conversion of FFA to FAME.

4.3.4 Effect of Reaction Temperature

The reaction temperature was investigated for temperatures between 40 – 80 °C to ascertain the optimal temperature. As esterification reactions are endothermic, reactions conducted in room temperature involving acidic catalysts are unfeasible, and 40 °C is chosen as the mildest starting temperature. As presented in Figure 4.9, the increase in temperature enabled FFA reduction to below the 2 % limit feasibly at 60 °C for both DESs, although [3BZSA:PCM] DES achieved the FFA limit (1.62 %) at 50 °C, which was accepted as its optimal reaction temperature. At reaction temperatures of 70 and 80 °C, the FFA content reduction was lower, and subsequently had a weaker effect on the FAME conversion. Based on previous studies involving similar laboratory setups, this observation may be attributed to the loss of methanol through evaporation and boiling at elevated temperatures (Hayyan *et al.*, 2023a). The esterification reaction conducted at 60

°C provided sufficient reaction conditions for the highest equilibrium conversion to be achieved and was accepted as the optimum reaction temperature.

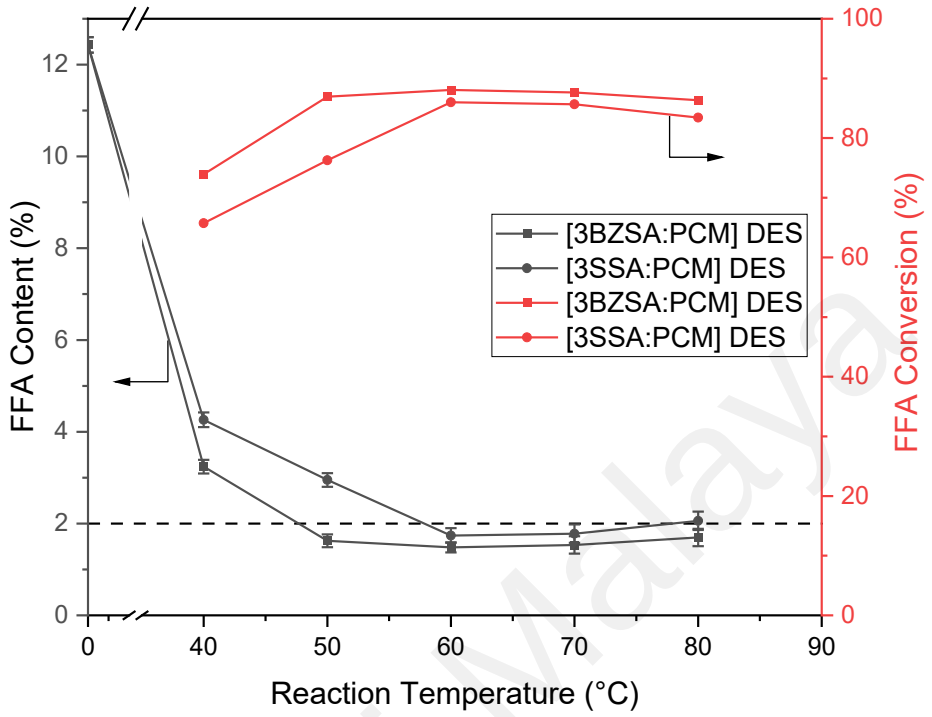

Figure 4.9: Effect of reaction temperature on the reduction of FFA content and the conversion of FFA to FAME.

4.3.5 Validation of Optimized Reaction Conditions and Recyclability Study

To validate the optimum parameters for each reaction condition specific to each DES, the experiment was repeated using the reaction conditions determined from the OVAT optimization. The optimum reaction conditions using the [3BZSA:PCM] DES catalyst were determined as follows: 1.5 wt% DES catalyst dosage, 8:1 methanol-to-oil molar ratio, for 50 min reaction time at 50 °C reaction temperature, resulting in a final FFA value of 1.69 %. On the other hand, the [3SSA:PCM] DES catalyst system was determined to be optimized at the following conditions: 2.5 wt% DES catalyst dosage, 16:1 methanol-to-oil molar ratio, for 90 min reaction time at 60 °C reaction temperature, resulting in a final FFA value of 1.74 %. The resulting FFA values were reported to be

satisfactory in achieving the predetermined FFA limit of < 2 %. Evidently, the novel [3SSA:PCM] DES required higher reaction conditions across all reaction parameters (DES catalyst dosage, methanol volume, reaction time and temperature) compared to the [3BZSA:PCM] DES. This suggests that the [3BZSA:PCM] DES exhibits a higher catalytic activity than the [3SSA:PCM] DES by requiring lower reaction parameters to achieve the same FFA limit.

Subsequently, the recyclability study of the FFA esterification reaction was conducted based on the optimized reaction conditions and the results are presented in Figure 4.10. The conversion rate of FFA into FAME recorded for the first run was reflective of the optimized results, achieving high percentages of 86.77 % and 95.37 % using [3SSA:PCM] and [3BZSA:PCM] respectively. The DESs were recovered without any intermediate purification steps and were directed charged into a fresh batch of LPO oil feed. As the recycling runs progress, the [3BZSA:PCM] DES was able to maintain 50 % FFA conversion at the 3rd run (FFA conversion of 67.91 %), however the [3SSA:PCM] DES was only able to maintain the conversion up to the 2nd run (FFA conversion of 55.09 %). Beyond the 4th recycle run, the DESs have been deactivated as the highest FFA conversion achieved was 41.70 %. The catalyst deactivation may be attributed to the accumulation of water generated as a result of the esterification reaction byproduct, as only the methanol was evaporated during the DES catalyst recovery process. Compared to the previous study in using [3PTSA:PCM] as the DES catalyst, the [3SSA:PCM] DES achieved similar recyclability performances, whereas the [3BZSA:PCM] DES performed better by one additional recycling run. However, when compared to existing literature, the DESs reported here exhibit weak recyclability performances than most ILs and DESs, and reveals its limitation in as a material in biomass valorisation (Kalhor and Ghandi, 2021). Particularly for the [3SSA:PCM] DES, the weak performances in recyclability may be due to its high viscosities and high melting point compared to [3BZSA:PCM].

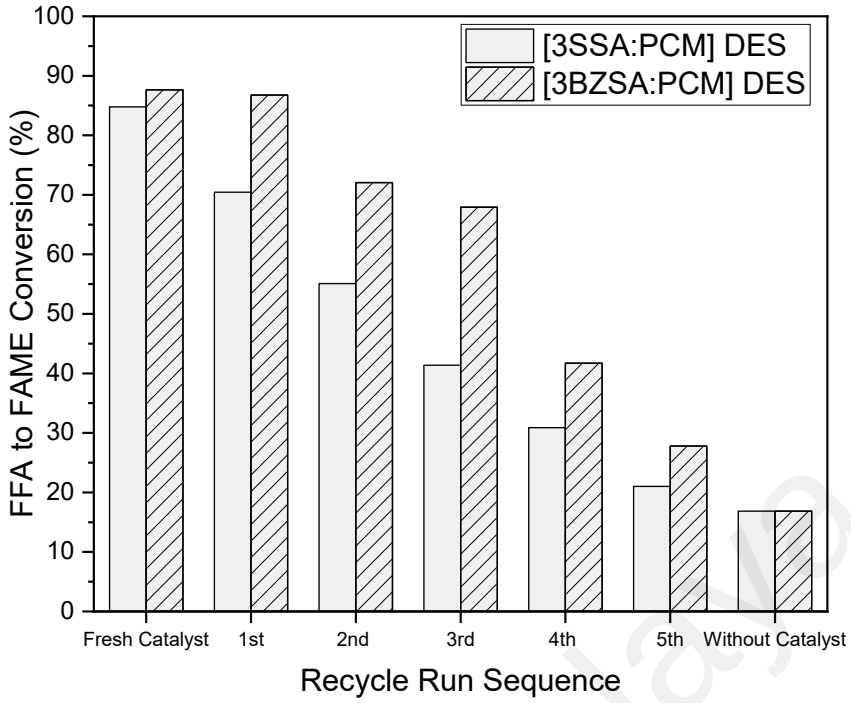

Figure 4.10: Recyclability study on novel API-based DESs in the conversion of FFA to FAME.

4.3.6 Reaction Kinetics and Thermodynamic Study of API-based DESs for FFA Esterification

The deacidification of LPO is carried out by reversible, acid-catalysed esterification reaction of its high FFA content with methanol as a reactant, yielding FAME and water. In order to increase the rate of forward reaction, two strategies can be employed: either remove one of the undesired products (in the present system, water), or use one of the reactants in excess (in the present system, methanol). Given the impracticality of water removal from the system, excess methanol is used to shift the reaction rate forward (Encinar *et al.*, 2021). To further evaluate the catalytic activity of the four novel API-based DESs, the reaction kinetics of FFA esterification at temperatures of 40 °C, 50 °C and 60 °C were investigated. FFA esterification reaction is expressed in Equation 4.2, where one molecule of FFA reacts with methanol to yield one molecule of FAME and one molecule of water.

$$FFA + Methanol \rightleftharpoons FAME + H_2O \quad \text{(Equation 4.2)}$$

The rate of reaction for Equation 4.2 is expressed as Equation 4.3;

$$r_{FFA} = -\frac{d[FFA]_t}{dt} = k_1[FFA][Methanol] + k_2[FAME][H_2O] \quad \text{(Equation 4.3)}$$

where k_1 and k_2 represent the forward and reverse reaction rate constants, respectively. According to generalized tendencies in literature, the rate expression of the kinetic model will be simplified without considering intermediate steps according to several assumptions (Berrios *et al.*, 2007; Saimon *et al.*, 2020):

(i) The esterification follows a pseudo first order rate of reaction.

(ii) The reverse reaction (hydrolysis of FAME) can be neglected when an excess of methanol to oil ratio is utilized (10:1).

(iii) The presence of excess methanol concentration can be taken as a constant, where the $k_1[Methanol]$ is simplified to k. Thus, the experimental data is simplified to a first-order rate law, as expressed by Equation 4.4.

$$r_{FFA} = -\frac{d[FFA]_t}{dt} = k[FFA] \quad \text{(Equation 4.4)}$$

By integrating and rearranging Equation 4.4, a linearized equation is obtained as shown by Equation 4.5.

$$ln[FFA]_t = (-k)(t) + ln[FFA]_0 \quad \text{(Equation 4.5)}$$

The rate constant (k) was evaluated using the regression fitting (R^2) at the optimum reaction conditions. Subsequently, the activation energy (E_a) and frequency factor (A) can be determined by the linearized form of the Arrhenius equation (Equation 4.6 and Equation 4.7) using different reaction temperatures.

$$k = Ae^{\frac{-E_a}{RT}} \quad \text{(Equation 4.6)}$$

$$\ln k = -\frac{E_a}{RT} + \ln A \quad \text{(Equation 4.7)}$$

Satisfactory coefficients of determination values ($R^2 > 0.9$) were obtained through the fitting of the empirical esterification reaction data into the linearized Arrhenius plot as shown in Figure 4.11 (a), and the reaction kinetic factors of E_a and A values were calculated and presented in Table 4.2. The [3BZSA:PCM] DES exhibited the lowest activation energy value of 40.91 kJ/mol, whereas the [3BZSA:PCM] DES required an activation energy of 50.89 kJ/mol according to the pseudo first order rate of reaction. The lower activation energy of this DES catalyst enabled lower reaction conditions as validated in the optimized reaction conditions, indicative by the high FFA reduction and catalytic activity of the API-based DES. Hence, the reaction kinetics study supports the optimum reaction conditions and the FFA reduction performances using the novel API-based DESs.

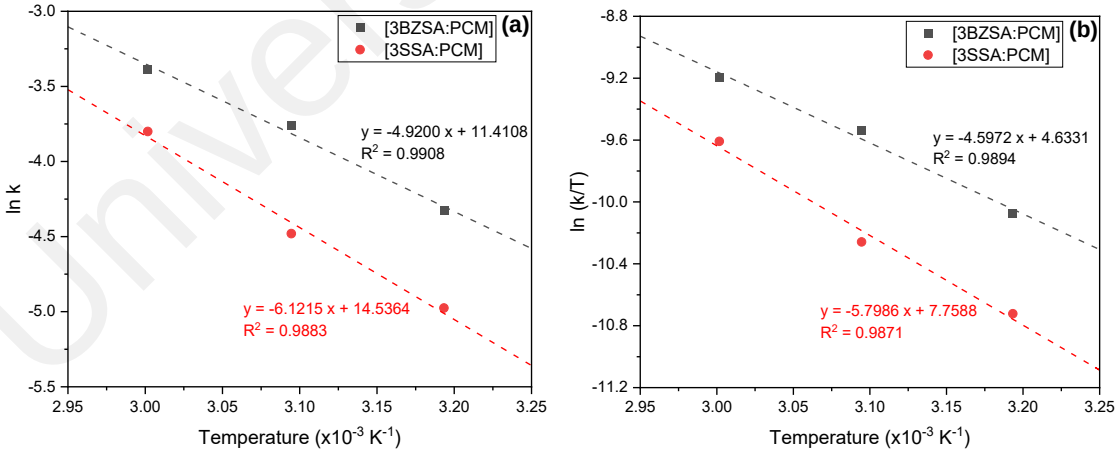

Figure 4.11: (a) Arrhenius plot and (b) Eyring–Polanyi plot of reaction rate constants in investigating the temperature dependency of FFA esterification using novel API-based DES catalysts.

Table 4.2: Tabulation of reaction kinetic factors for the FFA esterification reactions using novel API-based DESs.

DES Catalyst	Activation energy, E_a (kJ/mol)	Frequency factor, A (min^{-1})	Coefficient of Determination (R^2)
[3BZSA:PCM]	40.91	9.028×10^4	0.9908
[3SSA:PCM]	50.89	2.056×10^6	0.9883

The values of the reaction rate constants, k, determined from Equation 4.5 were used to further investigate the thermodynamic factors of the esterification reaction. The Eyring-Polanyi model was used to describe the relationship of the parameters as presented in Equation 4.8 – 4.9, and the linearized form of equation is derived to be Equation 4.10 (Encinar *et al.*, 2016; Tamjidi *et al.*, 2022):

$$k = K\frac{k_B T}{h}e^{\left(-\frac{\Delta G^\circ}{RT}\right)} \quad \text{(Equation 4.8)}$$

$$\Delta G^\circ = \Delta H^\circ - T\Delta S^\circ \quad \text{(Equation 4.9)}$$

$$ln\left(\frac{k}{T}\right) = -\frac{\Delta H^\circ}{RT} + ln\left(\frac{\kappa_B}{h}\right) + \frac{\Delta S^\circ}{R} + lnK \quad \text{(Equation 4.10)}$$

Where ΔH° is the standard enthalpy of the reaction system, ΔS° is the entropy of activation of the reaction system, ΔG° is the Gibbs free energy, determined from Equation 4.8, k is the rate constant at temperature T, κ_B is the Boltzmann constant, h is the Planck constant, K is the transmission coefficient ($K = 1$), and R is the universal gas constant taken as 8.314 J mol^{-1} K^{-1}.

The thermodynamic analysis was defined from the slope and intercept of the Eyring-Polanyi plot as illustrated in Figure 4.11 (b). Based on the satisfactory coefficients of determination values (R^2 > 0.9), the thermodynamic parameters were calculated and presented in Table 4.3. According to the calculated parameters, the FFA esterification reaction using API-based DESs were determined to be endothermic (ΔH° > 0), non-

spontaneous ($\Delta S° < 0$ and $\Delta G° > 0$), and consequently endergonic across all three temperatures (313.15 – 333.15 K) analysed (Ridwan *et al.*, 2021). Positive values of enthalpy indicate that product generation is required by external heat input to shift the reactants to the transition state, which is represented physically by factoring reaction temperatures in FFA esterification and biodiesel yield. Negative values of entropy indicates that most of the energy inputs were directed to the reaction as opposed to outward dispersion (Ahmad Farid *et al.*, 2018). Positive values of Gibbs free energy shows that the FFA esterification with methanol was determined to be non-spontaneous and endergonic in nature. The thermodynamic parameters of the various participating reactants in esterification reaction were in agreement with experimental trends and catalyst behaviour of prior studies on acid-catalysed esterification of FFA (Ketzer and de Castilhos, 2021; Nayak *et al.*, 2021). The results of these previous studies agreed that the FFA esterification reaction for biodiesel production were endothermic and endergonic reactions.

Table 4.3: Values of thermodynamic factors for the FFA esterification reactions using novel API-based DESs.

DES Catalyst	Standard enthalpy, $\Delta H°$ (kJ/mol)	Entropy of activation, $\Delta S°$ (kJ/mol)	Gibbs Free Energy, $\Delta G°$ (kJ/mol)			R^2
			313.15 K	323.15 K	333.15 K	
[3SSA:PCM]	48.20	-0.133	89.89	91.20	92.53	0.9871
[3BZSA:PCM]	38.22	-0.159	88.02	89.61	91.20	0.9894

4.4 Supporting of DESs onto Fe_3O_4/PVA Magnetic Composites for FFA Esterification

4.4.1 Screening Results of Catalyst Performance in FFA Esterification

The screening results of the catalysts supporting the DESs and sulfonic acids were presented in Figure 4.12. The screening of the catalyst performance was conducted at excess operating conditions (10 wt% catalyst loading, 20:1 methanol-to-oil molar ratio, 6 h contact time and reaction temperature at 60 °C) to enable the reaction to achieve equilibrium. From the screening results presented in Figure 4.12, PTSA supported on Fe_3O_4/PVA (denoted as Fe_3O_4/PVA/PTSA) exhibited the highest catalytic performance, reducing the FFA value down to 1.98 % below the predetermined limit, equivalent to 79.53 % conversion; followed by Fe_3O_4/PVA/SSA at 66.51 % FFA conversion. Among the list of catalysts supported on Fe_3O_4/PVA, the pristine acid components exhibited greater FFA conversion than their counterpart composed within the DES system. A plausible explanation to this may be that the DES system exhibited stronger molecular bonding with the water solvent while it was solvated, leading to the formation of an aqueous DES system (Picciolini *et al.*, 2023; Wang *et al.*, 2021). Hence, the DESs may be inferred to be incompatible with the Fe_3O_4/PVA composite based on the low FFA conversion results as the support was unable to exhibit catalytic effect. BZSA and [3BZSA:PCM] DES exhibited the weakest FFA esterification performance at 31.29 % and 29.70 % FFA conversion when supported on Fe_3O_4/PVA, which may be attributed to the weak attachment of the molecules and functional groups to the Fe_3O_4/PVA support material. Hence, Fe_3O_4/PVA/PTSA was determined as the best performing catalyst from the screening stage and further optimization studies were conducted.

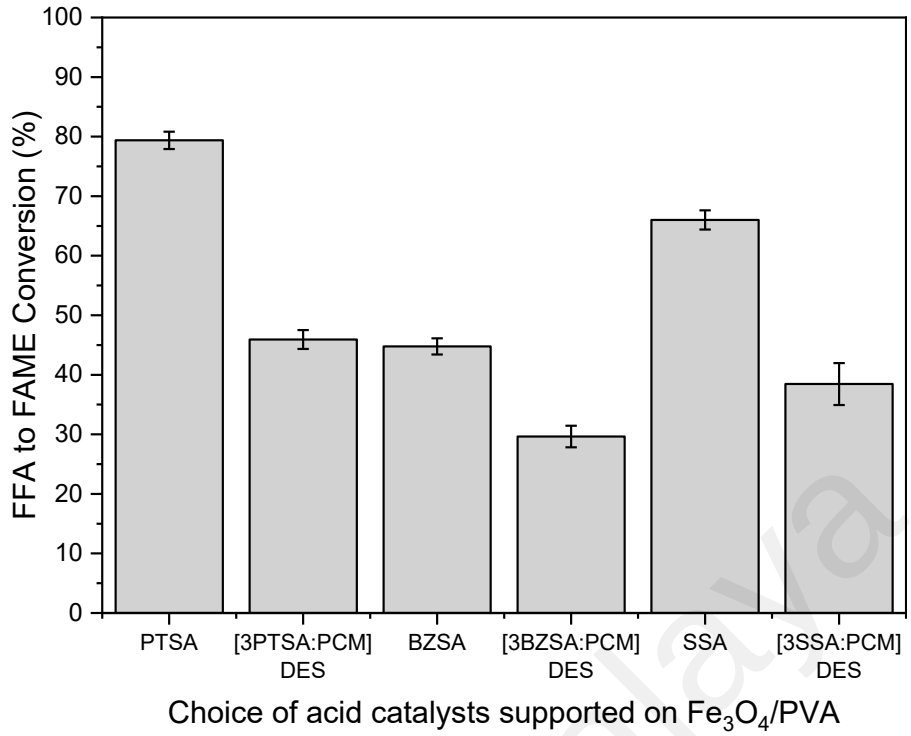

Figure 4.12: Screening of FFA esterification catalytic performance using sulphonic acids and DESs supported on Fe_3O_4/PVA magnetic composite.

4.4.2 FESEM and EDX Results

FESEM imaging and EDX analysis was used to provide topographical and elemental information of the synthesised Fe_3O_4/PVA/PTSA composite as presented in Figure 4.13, accompanied with the photographic images of the magnetic response of the Fe_3O_4/PVA/PTSA composite in water. The spherical shape of the Fe_3O_4/PVA/PTSA composite (Figure 4.13 (a) – (c)) was observed from the FESEM image that is in agreement with previously reported studies on modified Fe_3O_4/PVA (Maleki *et al.*, 2019). Furthermore, the elemental distribution of C (23.21 %), Fe (46.11 %), O (27.83 %) and S (2.85 %) was determined from the EDX analysis (Figure 4.13 (f)), suggesting that the PTSA is synthesised onto the Fe_3O_4/PVA matrix. The presence of the S element is contributed by the sulphonic acid functional group of the PTSA molecule, whereas the Fe and O element peaks in the EDX spectra plot affirms the presence of Fe_3O_4 (Ba-Abbad *et al.*, 2022). Additionally, the high carbon (C) element is attributed to the maleic acid-

crosslinked PVA polymer chains and the benzene ring of the PTSA molecules. In summary, the EDX spectra plot elucidates the presence of Fe_3O_4, PVA and PTSA, thus supporting the screening results on the presence of catalytic activity for FFA esterification.

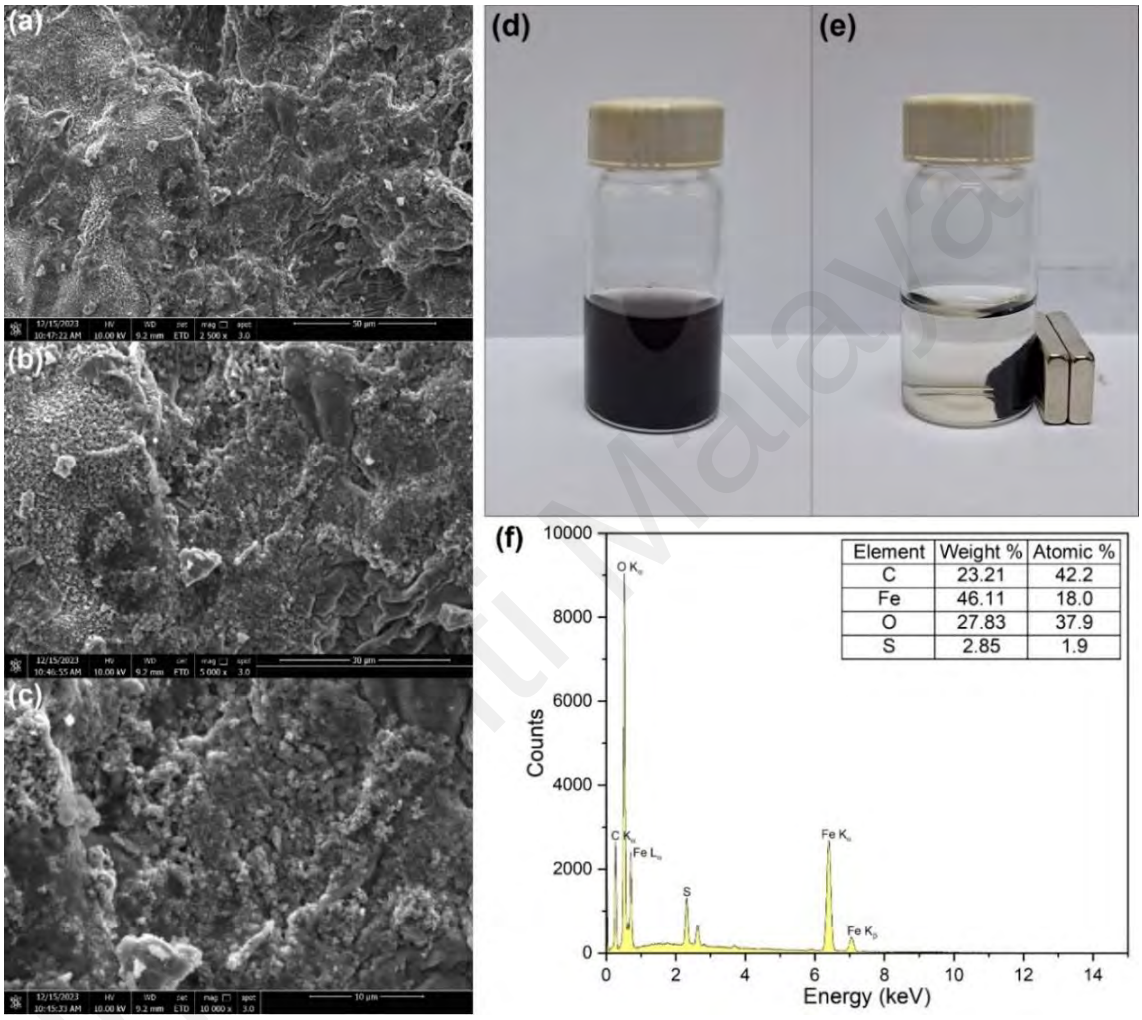

Figure 4.13: FESEM imaging of the Fe_3O_4/PVA/PTSA composite at (a) 2,500×, (b) 5,000×, and (c) 10,000× magnification; photographic image of (d) dispersion of Fe_3O_4/PVA/PTSA composite in water and (e) magnetic response of the Fe_3O_4/PVA/PTSA composite; and (f) EDX spectra plot of the Fe_3O_4/PVA/PTSA composite.

4.4.3 Thermogravimetric and Derivative Thermogravimetric Results

The TGA and derivative thermogravimetry (DTG) curves of the Fe_3O_4/PVA and Fe_3O_4/PVA/PTSA composite is presented in Figure 4.14. According to the DTG curves

derived from the TGA data, two peaks were observed at 246.2 – 246.8 °C and 441.4 – 460.2 °C, which correspond to the breaking down of the polymer network of PVA and the dehydration of –OH groups among the PVA chains respectively (Kurchania *et al.*, 2014). Furthermore, the calculated peak at 86.17 °C observed for the Fe_3O_4/PVA/PTSA curve may be attributed to the release of physically adsorbed water molecules arising from the acid modification step conducted extensively in the distilled water medium. The trends of the TGA curves were in good agreement with previously reported results in literature pertaining to the synthesis of Fe_3O_4/PVA (Maleki *et al.*, 2019).

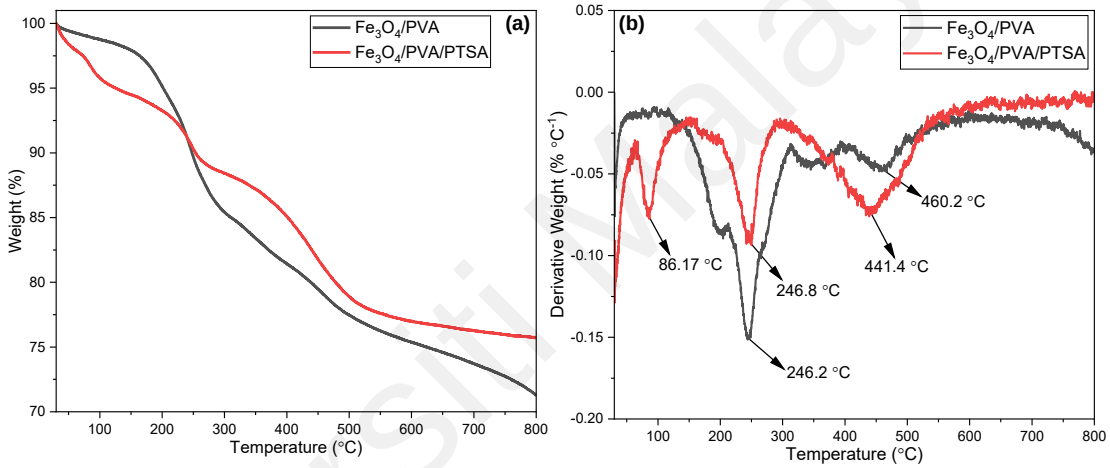

Figure 4.14: TGA and DTG curves of the Fe_3O_4/PVA and Fe_3O_4/PVA/PTSA composite.

4.4.4 X-Ray Diffraction Data

XRD data of Fe_3O_4/PVA and Fe_3O_4/PVA/PTSA is presented in Figure 4.15. The peaks appearing at 2θ = 30.15 °, 35.54 °, 43.33 °, 53.58 °, 57.32 ° and 62.78 ° is in good correlation with the standard JCPDS Card No. 88-0315 for Fe_3O_4 and affirms the synthesis. Furthermore, the broad peak centred at around 22 ° is assigned to the diffraction pattern of amorphous PVA (Maleki *et al.*, 2019). The XRD pattern for Fe_3O_4/PVA/PTSA revealed a fringe peak at 2θ = 32.69 °, which may be attributed to the coating interaction between the PVA chains and the Fe_3O_4 particle (Rahimi *et al.*, 2020).

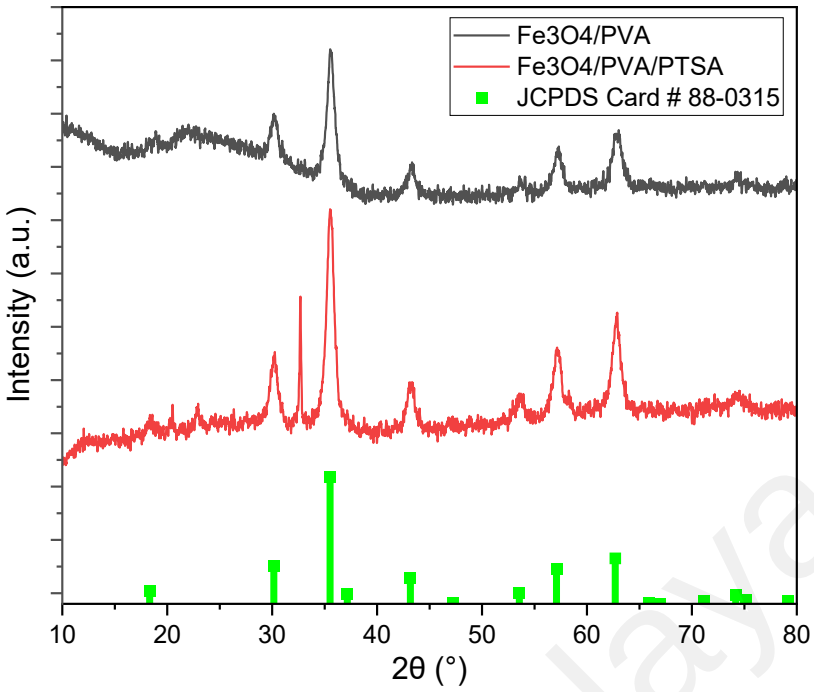

Figure 4.15: XRD patterns for Fe_3O_4/PVA and Fe_3O_4/PVA/PTSA composite.

4.4.5 XPS Analysis

The surface chemistry of the Fe_3O_4/PVA/PTSA catalyst was analysed using XPS analysis. Figure 4.16 presents the survey spectra of the Fe_3O_4/PVA/PTSA composite, indicating the peak detections of sulphur (S 2p), oxygen (O 1s), iron (Fe 2p) and carbon (C 1s) elements. The high resolution spectra of S 2p can be deconvoluted into two peaks at 168.3 and 169.6 eV that is assigned to the $-SO_3H$ groups of the PTSA molecule synthesised onto the surface of Fe_3O_4/PVA (Wang *et al.*, 2015; Zheng *et al.*, 2024). The three peaks determined in the deconvoluted O 1s spectra at 529.9, 531.2 and 532.4 eV may be assigned to oxygen in the form of Fe–O, H–O, and C–O respectively (Luo *et al.*, 2019). In the Fe 2p spectrum, the detection of asymmetric peaks at 710.5 and 724.1 eV (corresponding to the Fe $2p_{3/2}$ and Fe $2p_{1/2}$ phase) and the absence of a satellite peak at 719.0 eV verified the synthesis of Fe_3O_4-based composites (Ali *et al.*, 2018). The C 1s spectra was deconvoluted into three peaks at binding energies of 284.8, 286.3 and 288.6 eV that could be assigned to the functional groups of C–C, C–O and C═O respectively

(Luo *et al.*, 2019). The XPS spectra did not reveal other peaks contributed by magnetic compounds such as FeO, FeOOH or Fe_2O_3. In summary, the XPS analysis confirms the successful synthesis of Fe_3O_4/PVA/PTSA composite, supported by the analytical results of XRD and TGA analysis.

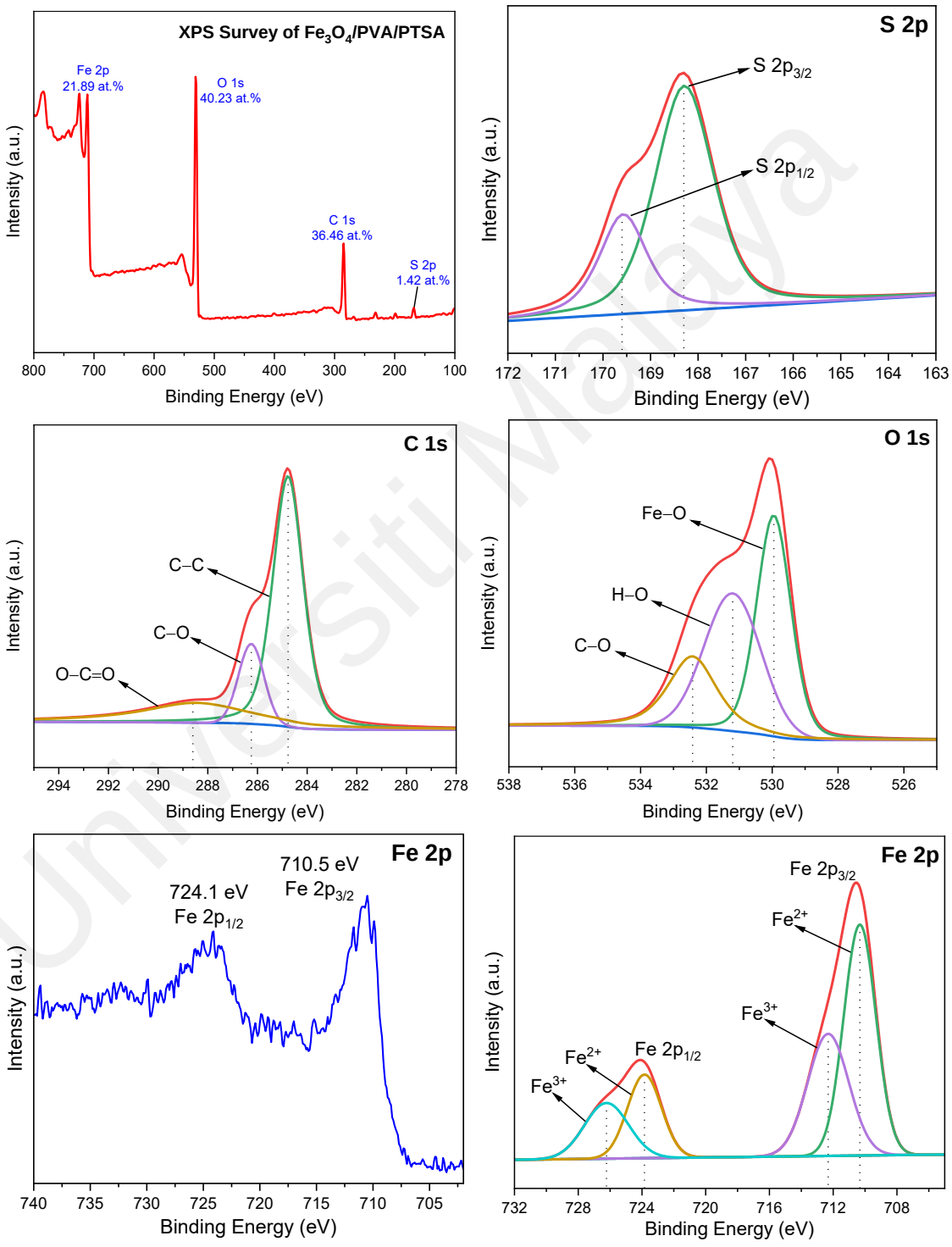

Figure 4.16: XPS survey spectrum and high-resolution XPS scan spectra over (e) S 2p, (f) O 1s, (g – h) Fe 2p, and (i) C 1s for the Fe_3O_4/PVA/PTSA composite.

4.4.6 Optimization of FFA Esterification

4.4.6.1 Effect of Catalyst Loading

The effect of catalyst loading is presented in Figure 4.17. The catalyst loading of the Fe_3O_4/PVA/PTSA composite was manipulated from 5 - 20 wt% on FFA esterification. At 10 wt% catalyst loading, the FFA value below 2 % limit was achieved, equating to a FFA to FAME conversion percentage of 79.33 %. At double of catalyst loading as 20 wt%, the FFA conversion rate of 84.38 % was achieved. By increasing of catalyst loading, the FFA conversion rate was increased due to the increase of contact and density of the active sites to accelerate the reaction. Additionally, Wang *et al.* (2019) reported that novel synthesis of a magnetic sulphonated SAC based on zirconium and iron chelated using sodium alginate or sodium carboxymethylcellulose. The loading of the magnetic catalyst was studied from 3 – 11 wt%, where 9 wt% of catalyst loading achieved the highest biodiesel yield of 94.3 % from the esterification of oleic acid. In another study, PTSA and methanesulphonic acid supported on UiO-66 MOFs were studied for the esterification of palmitic acids with methanol, n-butanol and n-decanol at 25 g/mol (10 wt% of palmitic acid) of catalyst content (Liu *et al.*, 2020b). Hence, the catalyst loading of 10 wt% was reported in this study as optimum loading for highest FFA conversion.

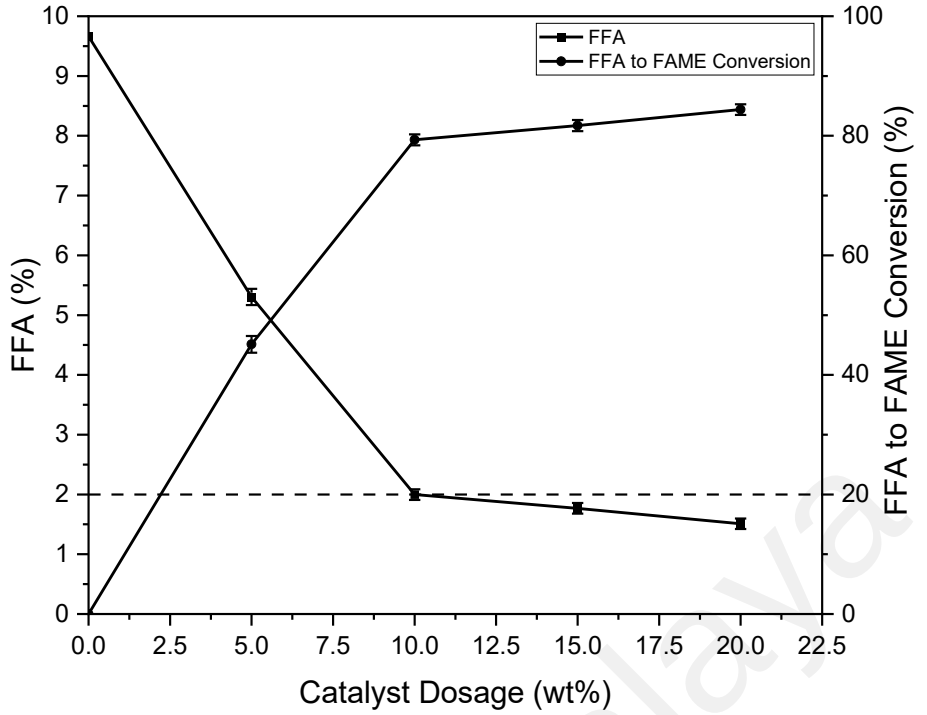

Figure 4.17: Effect of Fe_3O_4/PVA/PTSA catalyst loading on FFA content reduction and conversion.

4.4.6.2 Effect of Methanol Requirement

Methanol is supplied as a reactant in excess by molar ratio to enable the forward shift of the FFA esterification reaction to yield FAME. The effects of methanol ratio requirement on FFA conversion rate is presented in Figure 4.18. At an excess methanol:LPO molar ratio of 20:1, the final FFA content of 1.97 % was attained, corresponding to a 79.61 % FFA to FAME conversion. Increasing the methanol content to 25:1 molar ratio resulted in a slight increase in FFA conversion rate up to 81.07 %. Considering the economic significance of excessive methanol with respect to the minute FFA conversion percentage, the optimum methanol:LPO molar ratio was selected as 20:1. In comparison, the methanol molar ratio requirement in the use of PTSA as a homogeneous catalyst is halved at 10:1 (Hayyan *et al.*, 2010). However, excess methanol requirement is in good agreement with previous studies that used heterogeneous catalysts. (Ibrahim *et al.*, 2020a) utilized oil palm empty fruit bunches to synthesise novel magnetic

carbonaceous SAC for the esterification of palm fatty acid distillate. The magnetic catalyst enabled 96 % conversion of the palm fatty acid distillate feedstock at the optimized methanol requirement of 16:1 molar ratio. Rokhum *et al.* (2022) reported on the influence and optimization of a novel sugar-derived sulphonated aromatic carbon catalysts on oleic acid esterification, achieving 97.5 % conversion at the optimized conditions of 20:1 methanol molar ratio and 5 wt % catalyst loading.

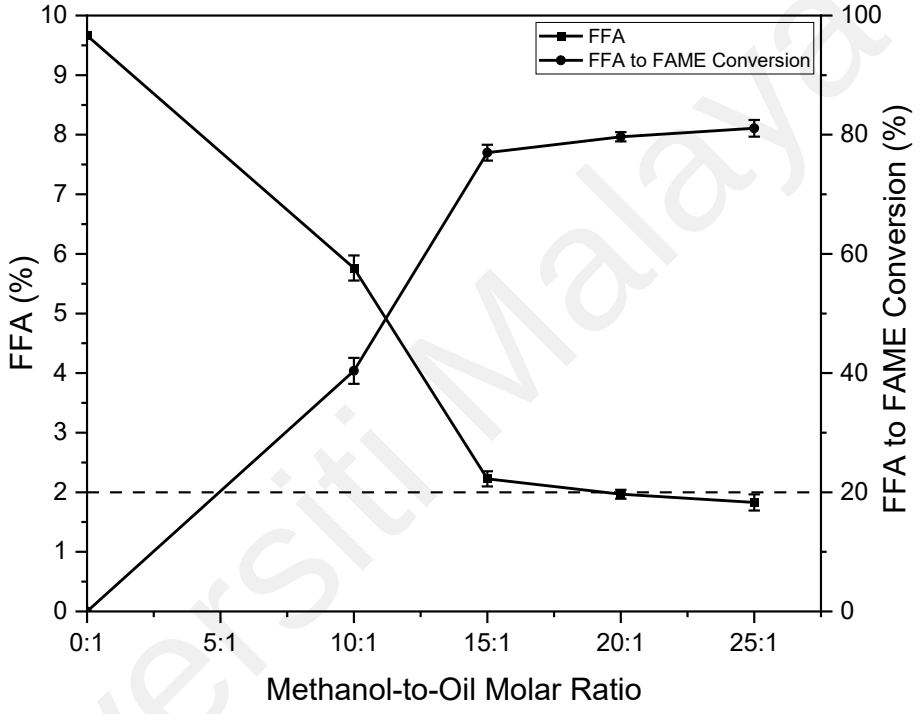

Figure 4.18: Effect of methanol requirement on FFA content reduction and conversion.

4.4.6.3 Effect of Contact Time

Compared to homogeneous mineral acid catalysts applied in biodiesel esterification reactions, heterogeneous catalysts typically require extended contact time (Racar *et al.*, 2023). Hence, the catalyst contact time should be optimized to reach reaction equilibrium due to the increased mass transfer resistance and reduced surface area. The optimization of catalyst contact time is presented in Figure 4.19. The FFA content was reduced down

to 2.00 % at the 5th hour of the reaction, and a slight reduction improvement in FFA content was recorded at 1.84 % at the 6th hour. Durations of optimal catalyst contact time from 3 – 8 h were reported in literature utilizing various forms of heterogeneous catalysts. Sulphonated carbon catalysts derived from *Sargassum horneri* biomass were optimized for a high oleic acid conversion of 96.4 % at a reaction time of 3 h (Cao *et al.*, 2021). (Xie and Wang, 2020) synthesised polymeric 1-vinyl-3-(3-sulphopropyl)imidazolium hydrogen sulphate as acidic ionic liquids supported on Fe_3O_4/SiO_2 magnetic composites which yielded high oil conversion at 93.3 % under optimal reaction time of 6 h. Sulphonated ZnO-β-zeolite catalysts were reported to exhibit high catalytic performance (96.9 % WCO conversion) in the simultaneous esterification and transesterification of waste cooking oil under optimal reaction time of 8 h (Yusuf *et al.*, 2023).

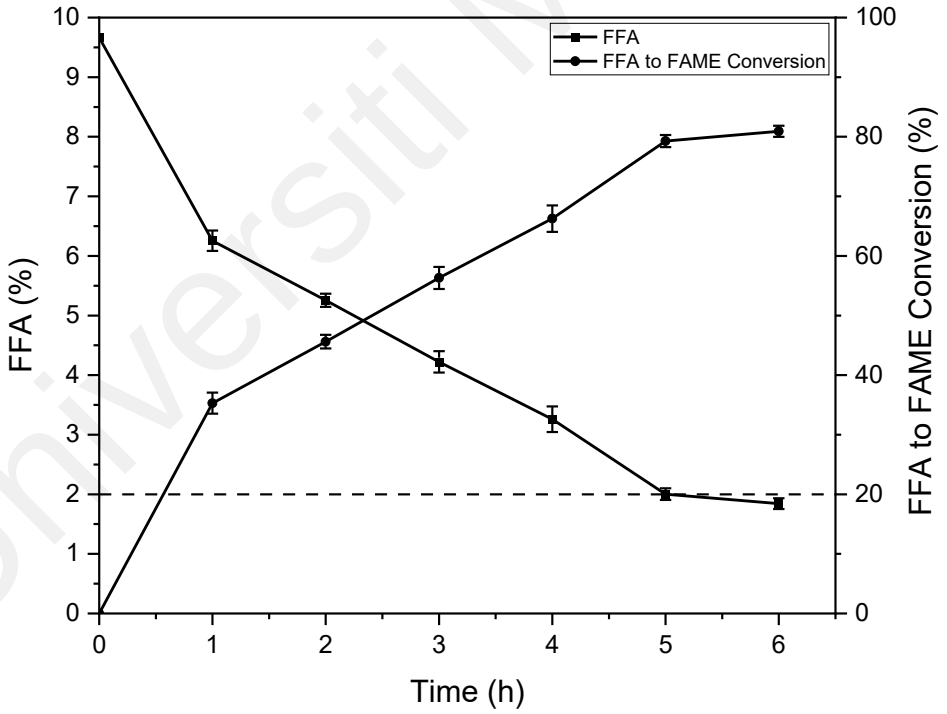

Figure 4.19: Effect of Fe_3O_4/PVA/PTSA catalyst contact time on FFA content reduction and conversion.

4.4.6.4 Effect of Reaction Temperature

Higher reaction temperatures are required for FFA esterification reactions catalysed by heterogeneous catalysts (Maleki *et al.*, 2022). The influence of reaction temperature on the reduction of FFA content is presented in Figure 4.20, and showed that the FFA conversion increased with increasing temperature from 40 – 70 °C. At 60 °C, the FFA was reduced to 1.96 %, with no significant reduction observed for 70 °C reaction temperature, indicating that the reaction equilibrium has been reached. Comparatively, phosphomolybdic acid were impregnated onto bismuth-based MOFs to yield SACs for the esterification of oleic acid (Zhang *et al.*, 2023). The esterification reaction was conducted in a sealed high-pressure autoclave that allowed reaction temperatures to be optimized between 120 – 170 °C. As the reaction was conducted at atmospheric pressure in this study, the reaction temperature was optimized around the boiling point of methanol. Similarly, the optimal reaction temperature was reported as 75 °C in the (trans)esterification of waste cooking oil in a glass batch reactor using a novel sulphonated Fe-Al-TiO_2 magnetic nanocomposite (Gardy *et al.*, 2018).

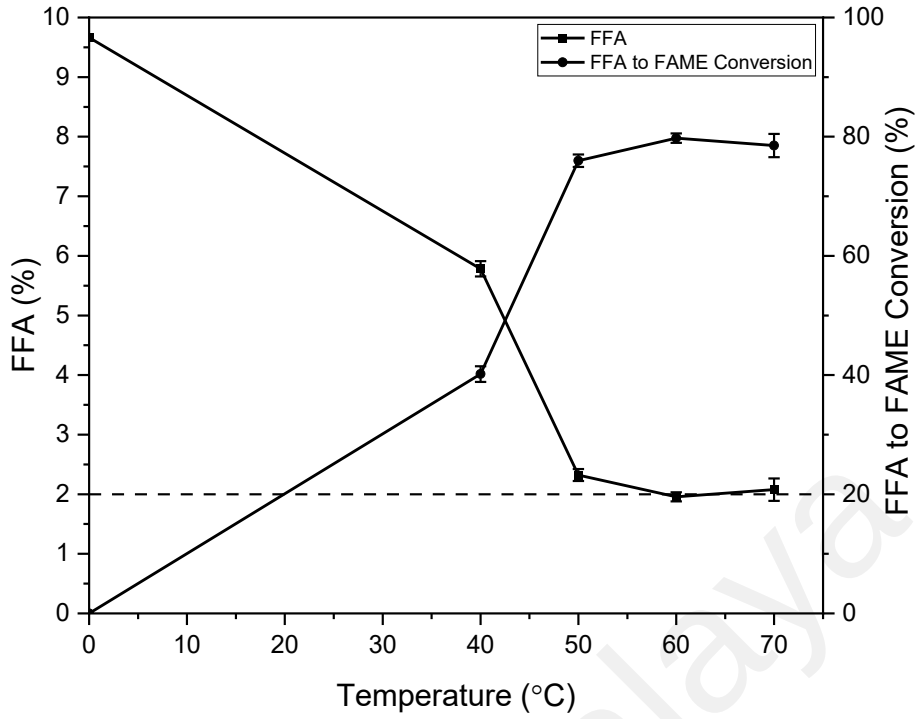

Figure 4.20: Effect of reaction temperature on FFA content reduction and conversion.

4.4.6.5 Validation of Reaction Conditions and Catalyst Recyclability

The reaction conditions determined in the optimum experiment conditions were: 10 wt% acid catalyst loading, 20:1 methanol:LPO molar ratio of methanol loading, and 5 h contact time at 60 °C. The reaction conditions were revalidated and yielded a treated LPO sample with an FFA content value of 1.95 % (79.81 % FFA conversion). Subsequently, the catalyst recyclability study was conducted to evaluate the reusability of the Fe_3O_4/PVA/PTSA SAC. Upon completion of the first reaction run, the catalyst was easily recovered using an external magnet, and washed continually for several times using distilled water, and dried in a vacuum oven for 24 h. Subsequently, Fe_3O_4/PVA/PTSA catalyst was transferred to a fresh batch of LPO for the second used and succeeding reaction runs. The catalyst recyclability performance for five continuous reaction cycles is presented in Figure 4.21. The Fe_3O_4/PVA/PTSA catalyst maintained a relatively high FFA conversion rate in the first three runs, demonstrating slight gradual decrease in FFA

conversion from 79.81 to 78.89 %. In the succeeding fourth and fifth reaction runs, the FFA conversion drops to 75.15 and 65.65 % respectively. The decrease in FFA conversion rate may be attributed to catalytic deactivation by water, by-product formation from the esterification reaction. To overcome this issue, the catalyst may be regenerated by re-sulphonation using PTSA (Cao *et al.*, 2021).

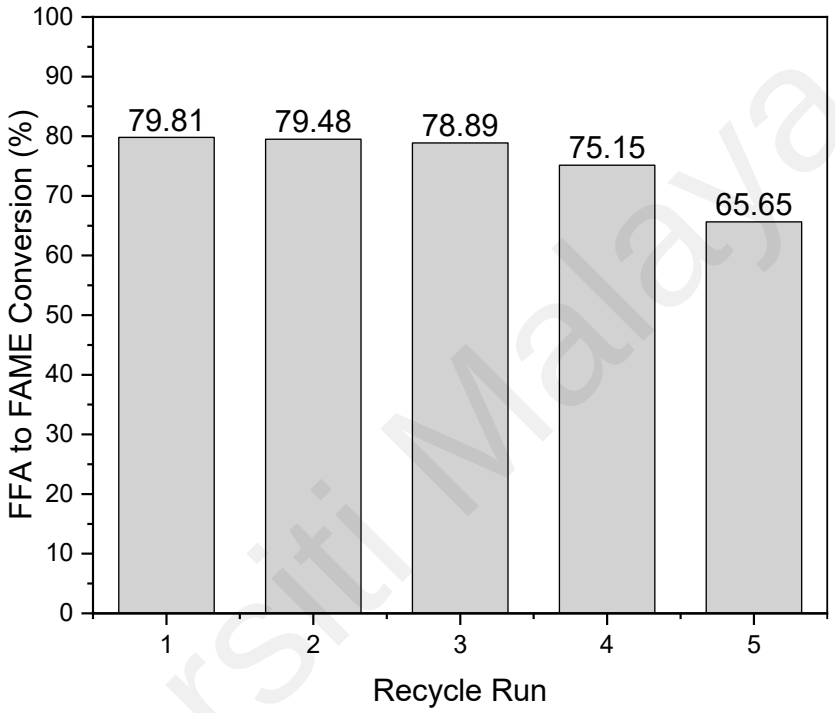

Figure 4.21: Evaluation of recyclability performance of Fe_3O_4/PVA/PTSA in FFA conversion.

4.4.7 Evaluation of Reaction Kinetics and Thermodynamic Studies

The reaction kinetics and thermodynamic studies were presented for the FFA esterification reaction using Fe_3O_4/PVA/PTSA at the optimum reaction conditions at reaction temperatures of 40, 50 and 60 °C. Given that significant excess of methanol (20:1 molar ratio to oil) was used, and assuming the methanol concentration remained constant, the empirical data was fitted according to the pseudo first order kinetics based on a simple rate expression of the kinetic model (Hayyan *et al.*, 2023a; Wang *et al.*, 2023b). By

plotting the rate constant (k) values against temperature, the activation energy (E_a) and frequency factor (A) was determined through the linearized form of the Arrhenius equation (Equation 4.7).

Figure 4.22 (a) depicts the Arrhenius plot with satisfactory coefficients of determination values ($R^2 > 0.9$) obtained. Here, the reaction kinetic factors of E_a and A values were calculated as 43.72 kJ/mol and 3.586×10^4 min^{-1} respectively. The E_a values were in agreement with literature values on the esterification of low value oils using heterogeneous SACs between the range of 18.11 – 64.60 kJ/mol (Olagbende *et al.*, 2021; Zhang *et al.*, 2021).

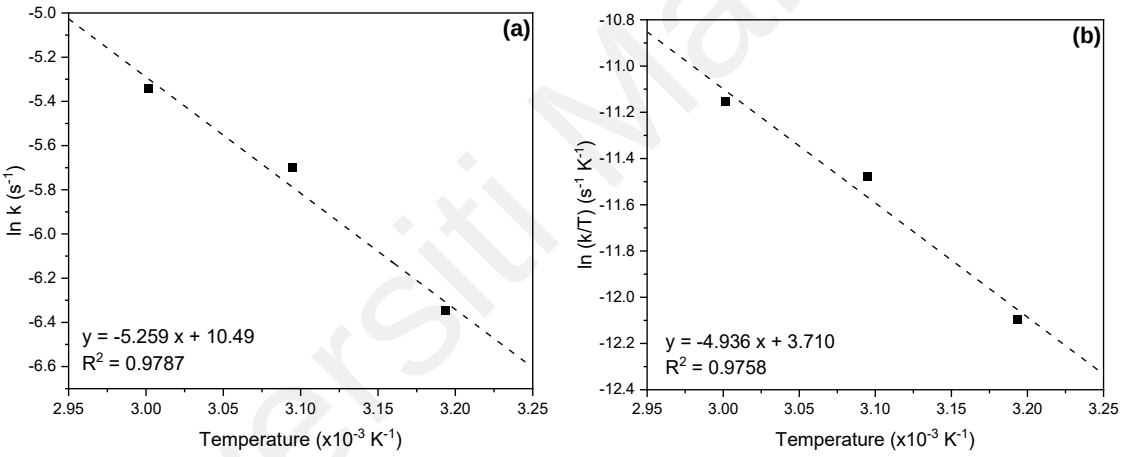

Figure 4.22: (a) Arrhenius plot; and (b) Eyring–Polanyi plot of temperature dependency in FFA esterification using Fe_3O_4/PVA/PTSA catalyst.

Subsequently, the thermodynamic factors of the esterification reaction were studied through the Eyring-Polanyi model (Equation 4.8 – 4.10). The linearized plot of the Eyring-Polanyi model is expressed as Equation 4. The Eyring-Polanyi plot is illustrated in Figure 4.22 (b), showing satisfactory fitting based on the coefficients of determination values ($R^2 > 0.9$), and the thermodynamic parameters were presented in Table 4.4. Based on the results, FFA esterification reaction using Fe_3O_4/PVA/PTSA was calculated as positive $\Delta H°$, negative $\Delta S°$ and positive $\Delta G°$ values, which corresponds to the

thermodynamics of the reaction process being dictated as endothermic, non-spontaneous and endergonic across the analysed temperature, respectively. The positive enthalpy values ($\Delta H° > 0$) dictate the requirement of external heat input for main product generation (FAME yield), attributed the optimal of reaction temperatures in FFA esterification. The results of this study were within range and in agreement with the thermodynamic parameters of SACs previously reported on the acid-catalysed esterification of FFA (Lieu *et al.*, 2016; Roslan *et al.*, 2022; Tang *et al.*, 2020).

Table 4.4: Values of thermodynamic factors for the FFA esterification reactions catalysed by Fe_3O_4/PVA/PTSA catalyst.

Standard enthalpy, $\Delta H°$ (kJ/mol)	Entropy of activation, $\Delta S°$ (kJ/mol)	Gibbs Free Energy, $\Delta G°$ (kJ/mol)			Coefficient of Determination, R^2
		313.15 K	323.15 K	333.15 K	
41.04	-0.167	93.24	94.91	96.57	0.9758

CHAPTER 5: CONCLUSION AND FUTURE RECOMMENDATIONS

5.1 Conclusion

In the works of this thesis, novel API-based DESs comprising paracetamol and sulfonic acids of BZSA and SSA were synthesized and firstly reported. These novel DESs were studied as homogeneous acid catalyst for the FFA esterification of LPO. The DESs were characterized using conventional spectroscopic methods using FTIR and the Hammett acidity function through UV-Vis spectroscopy. API-based DESs were determined to have high acidic according to the low Hammett acidity values (H_0), and the incorporation of paracetamol was observed to reduce the DES acidity. At the optimized reaction conditions of 1.5 wt% DES catalyst dosage, 8:1 methanol-to-oil molar ratio, 50 °C reaction temperature for 50 min reaction time, the [3BZSA:PCM] DES achieved high FFA conversion at 86.4 %. On the other hand, at the optimized conditions of 2.5 wt% DES catalyst dosage, 16:1 methanol-to-oil molar ratio, 60 °C reaction temperature for 90 min reaction time, the [3SSA:PCM] DES achieved similarly high FFA conversion at 86.0 %. The reaction kinetics study was conducted for the catalytic reaction using [3BZSA:PCM] and [3SSA:PCM] DESs, and the activation energy and frequency factor for the reactions were determined to be 40.91 and 50.89 kJ/mol and 9.028×10^4 and 2.056×10^6 min^{-1} respectively. The thermodynamic studies revealed that the DES acid-catalysed reactions were thermodynamically endothermic ($\Delta H° > 0$), non-spontaneous ($\Delta S° < 0$ and $\Delta G° > 0$), and endergonic. In line with previous studies, the API-based DESs exhibited weak recyclability, having a reduction of more than 50 % FFA conversion on the third recycling run.

Subsequently, the acidic DESs were supported on Fe_3O_4/PVA magnetic composites to yield heterogeneous SACs for the esterification of FFA in LPO. The screening results

reveal that PTSA was compatible with the Fe_3O_4/PVA support material based on the catalytic activity in FFA esterification, and that the pristine sulphonic acid components exhibited greater FFA conversion compared to the DES system. Subsequently, Fe_3O_4/PVA/PTSA was selected as the best performing catalyst for further optimization in reaction conditions. At reaction conditions of 10 wt% catalyst loading, 20:1 methanol-to-oil molar ratio, 5 h of contact time and at 60 °C, the LPO was pretreated to the FFA content value of 1.95 %, corresponding to an FFA conversion of 79.81 %. Additionally, the catalyst was recycled for five successive runs with fair stability and acceptable FFA conversion (> 65 %). The reaction kinetics revealed that the FFA esterification reaction using Fe_3O_4/PVA/PTSA follows the pseudo first order rate of reaction, requiring an activation energy of 43.72 kJ/mol. This study demonstrated the feasibility of certain sulphonic acids and DESs to be supported on the Fe_3O_4/PVA magnetic composite, with Fe_3O_4/PVA/PTSA being the viable catalyst choice for the pretreatment of low-quality oils through FFA esterification.

5.2 Future Recommendations and Considerations

The results from this thesis report on the synthesis of new DESs and the attempt on configuring it as a heterogeneous and homogeneous catalyst and forms as for the application in the methanolysis esterification of high FFA content oils. Further studies in the following domains are put forth in consideration.

The discovery of DESs synthesised from APIs paves the way for more DESs to be discovered and synthesized using different types of HBA/HBD constituents. Through the Hammett acidity function, the resultant DESs were recorded to exhibit lower acidity compared to its pristine acid components, and this was attributed to the low acidity of paracetamol, despite it being a key component to form the DES compound with the

relevant sulphonic acids. Hence, different types of chemical moieties can be studied for the formation of DESs that does not reduce the acidity, but in turn increases the acidity of the DESs for the purpose of catalytic applications. Furthermore, the use of COSMO-RS to screen potential constituents can be conducted and discovered more novel DESs that can contribute to the development of DESs for FFA esterification and other chemical processes, such as solvent extraction and electrochemical solutions.

In this study, it is deduced that pristine sulfonic acids are more viable to be supported onto the Fe_3O_4/PVA magnetic composite compared to its DES configuration. This was hypothesized to be due to the stronger interactions between the DESs compounds compared to the PVA chains of the magnetic composite material. Therefore, other types of heterogeneous support materials can be studied for its efficacy as catalyst support materials instead of Fe_3O_4/PVA. For example, ordered porous materials such as mesoporous silicas and MOFs that offer to improvements in terms of the acid compatibility may be studied as a further recommendation to comprehensively incorporate the DES moieties into the catalyst composites, and study its effect in catalytic efficiencies in the reaction environments of FFA esterification.

Furthermore, other types of low-quality feedstocks with similar or higher FFA content can be studied for the production of biodiesel, such as UCOs, low-value crude oils and sludge oils. The stability of the catalysts can be further evaluated in harsher esterification reaction conditions required to pretreat feedstock that contain high levels of impurities. Additionally, the study of FFA esterification using these novel DESs can be advanced in different operating behaviour of the reactor, such as continuous flow reactors. The reaction conditions in different reactor configurations require another set of optimization data, and can be further studied to provide insight into the functionality of DESs as catalyst in FFA esterification processes.

REFERENCES

Abranches, D. O., & Coutinho, J. A. P. (2022). Type V deep eutectic solvents: Design and applications. *Current Opinion in Green and Sustainable Chemistry, 35*, 100612.

Ahmad Farid, M. A., Hassan, M. A., Taufiq-Yap, Y. H., Ibrahim, M. L., Hasan, M. Y., Ali, A. A. M., Othman, M. R., & Shirai, Y. (2018). Kinetic and thermodynamic of heterogeneously K3PO4/AC-catalysed transesterification via pseudo-first order mechanism and Eyring-Polanyi equation. *Fuel, 232*, 653-658.

Ahmed, R., & Huddersman, K. (2022). Review of biodiesel production by the esterification of wastewater containing fats oils and grease (FOGs). *Journal of Industrial and Engineering Chemistry, 110*, 1-14.

Aissaoui, T., Benguerba, Y., & AlNashef, I. M. (2017). Theoretical investigation on the microstructure of triethylene glycol based deep eutectic solvents: COSMO-RS and TURBOMOLE prediction. *Journal of Molecular Structure, 1141*, 451-456.

Al-Sakkari, E. G., Abdeldayem, O. M., El-Sheltawy, S. T., Abadir, M. F., Soliman, A., Rene, E. R., & Ismail, I. (2020). Esterification of high FFA content waste cooking oil through different techniques including the utilization of cement kiln dust as a heterogeneous catalyst: A comparative study. *Fuel, 279*, 118519.

Ali, R. M., Elkatory, M. R., & Hamad, H. A. (2020). Highly active and stable magnetically recyclable CuFe2O4 as a heterogenous catalyst for efficient conversion of waste frying oil to biodiesel. *Fuel, 268*, 117297.

Ali, S., Khan, S. A., Eastoe, J., Hussaini, S. R., Morsy, M. A., & Yamani, Z. H. (2018). Synthesis, characterization, and relaxometry studies of hydrophilic and hydrophobic superparamagnetic Fe3O4 nanoparticles for oil reservoir applications. *Colloids and Surfaces A: Physicochemical and Engineering Aspects, 543*, 133-143.

Alioui, O., Benguerba, Y., & Alnashef, I. M. (2020). Investigation of the CO2-solubility in deep eutectic solvents using COSMO-RS and molecular dynamics methods. *Journal of Molecular Liquids, 307*, 113005.

AlOmar, M. K., Hayyan, M., Alsaadi, M. A., Akib, S., Hayyan, A., & Hashim, M. A. (2016). Glycerol-based deep eutectic solvents: Physical properties. *Journal of Molecular Liquids, 215*, 98-103.

Álvarez, M. S., Longo, M. A., Rodríguez, A., & Deive, F. J. (2024). The role of deep eutectic solvents in catalysis. A vision on their contribution to homogeneous, heterogeneous and electrocatalytic processes. *Journal of Industrial and Engineering Chemistry, 132*, 36-49.

Amesho, K. T. T., Lin, Y.-C., Mohan, S. V., Halder, S., Ponnusamy, V. K., & Jhang, S.-R. (2023). Deep eutectic solvents in the transformation of biomass into biofuels and fine chemicals: a review. *Environmental Chemistry Letters, 21*(1), 183-230.

Andreani, L., & Rocha, J. D. (2012). Use of ionic liquids in biodiesel production: a review. *Brazilian Journal of Chemical Engineering, 29*(1), 1-13.

Andrijanto, E., Dawson, E. A., & Brown, D. R. (2012). Hypercrosslinked polystyrene sulphonic acid catalysts for the esterification of free fatty acids in biodiesel synthesis. *Applied Catalysis B: Environmental, 115-116*, 261-268.

AOCS. (2017). *Official Methods and Recommended Practices of the AOCS*. Urbana, Illinois: American Oil Chemists Society.

Aroso, I. M., Paiva, A., Reis, R. L., & Duarte, A. R. C. (2017). Natural deep eutectic solvents from choline chloride and betaine – Physicochemical properties. *Journal of Molecular Liquids, 241*, 654-661.

Awogbemi, O., & Kallon, D. V. V. (2023). Application of machine learning technologies in biodiesel production process—A review. *Frontiers in Energy Research, 11*.

Ayoub, S. S. (2021). Paracetamol (acetaminophen): A familiar drug with an unexplained mechanism of action. *Temperature, 8*(4), 351-371.

Azmi, S., Klimek, A., & Frackowiak, E. (2023). Why electrochemical capacitor electrolytes should not be ignored? *Electrochimica Acta, 452*, 142347.

Azmi, S., Koudahi, M. F., & Frackowiak, E. (2022). Reline deep eutectic solvent as a green electrolyte for electrochemical energy storage applications. *Energy & Environmental Science, 15*(3), 1156-1171.

Ba-Abbad, M. M., Benamour, A., Ewis, D., Mohammad, A. W., & Mahmoudi, E. (2022). Synthesis of Fe3O4 Nanoparticles with Different Shapes Through a Co-Precipitation Method and Their Application. *JOM, 74*(9), 3531-3539.

Bai, H., Tian, J., Talifu, D., Okitsu, K., & Abulizi, A. (2022). Process optimization of esterification for deacidification in waste cooking oil: RSM approach and for biodiesel production assisted with ultrasonic and solvent. *Fuel, 318*, 123697.

Basumatary, S. F., Brahma, S., Hoque, M., Das, B. K., Selvaraj, M., Brahma, S., & Basumatary, S. (2023). Advances in CaO-based catalysts for sustainable biodiesel synthesis. *Green Energy and Resources, 1*(3), 100032.

Berrios, M., Siles, J., Martín, M. A., & Martín, A. (2007). A kinetic study of the esterification of free fatty acids (FFA) in sunflower oil. *Fuel, 86*(15), 2383-2388.

Booramurthy, V. K., Kasimani, R., Subramanian, D., & Pandian, S. (2020). Production of biodiesel from tannery waste using a stable and recyclable nano-catalyst: An optimization and kinetic study. *Fuel, 260*, 116373.

Camilo, G. L., Queiroz, A., Ribeiro, A. E., Gomes, M. C. S., & Brito, P. (2024). Review of biodiesel production using various feedstocks and its purification through several methodologies, with a specific emphasis on dry washing. *Journal of Industrial and Engineering Chemistry, 136*, 1-15.

Cao, D., Liu, Q., Jing, W., Tian, H., Yan, H., Bi, W., Jiang, Y., & Chen, D. D. Y. (2020). Insight into the Deep Eutectic Solvent Extraction Mechanism of Flavonoids from Natural Plant. *ACS Sustainable Chemistry & Engineering, 8*(51), 19169-19177.

Cao, M., Peng, L., Xie, Q., Xing, K., Lu, M., & Ji, J. (2021). Sulfonated Sargassum horneri carbon as solid acid catalyst to produce biodiesel via esterification. *Bioresource Technology, 324*, 124614.

Cao, Y., Li, Y., Sun, M., Xu, Y., & Chen, L. (2023). Unexpectedly Superhigh Toxicity of Superbase-Derived Deep Eutectic Solvents albeit High Efficiency for CO2 Capture and Conversion. *Industrial & Engineering Chemistry Research, 62*(7), 3338-3347.

Cárdenas, J., Orjuela, A., Sánchez, D. L., Narváez, P. C., Katryniok, B., & Clark, J. (2021). Pre-treatment of used cooking oils for the production of green chemicals: A review. *Journal of Cleaner Production, 289*, 125129.

Cavelius, P., Engelhart-Straub, S., Mehlmer, N., Lercher, J., Awad, D., & Brück, T. (2023). The potential of biofuels from first to fourth generation. *PLOS Biology, 21*(3), e3002063.

Chai, M., Tu, Q., Lu, M., & Yang, Y. J. (2014). Esterification pretreatment of free fatty acid in biodiesel production, from laboratory to industry. *Fuel Processing Technology, 125*, 106-113.

Changmai, B., Sudarsanam, P., & Rokhum, S. L. (2020). Biodiesel production using a renewable mesoporous solid catalyst. *Industrial Crops and Products, 145*, 111911.

Chen, C., Qu, S., Guo, M., Lu, J., Yi, W., Liu, R., & Ding, J. (2021). Waste limescale derived recyclable catalyst and soybean dregs oil for biodiesel production: Analysis and optimization. *Process Safety and Environmental Protection, 149*, 465-475.

Chen, C., Wang, F., Li, Q., Wang, Y., & Ma, J. (2022). Embedding of SO3H-functionalized ionic liquids in mesoporous MIL-101(Cr) through polyoxometalate bridging: A robust heterogeneous catalyst for biodiesel production. *Colloids and Surfaces A: Physicochemical and Engineering Aspects, 648*, 129432.

Chen, J., Ni, Y., Zhang, P., Liang, X., & Fang, S. (2023). Acidic natural deep eutectic solvents as dual solvents and catalysts for the solubilization and deglycosylation of soybean isoflavone extracts: Genistin as a model compound. *Food Chemistry, 406*, 134999.

Chutia, G. P., & Phukan, K. (2024). Facile synthesis of Fe3O4@biochar@SO3H as magnetically separable Bronsted acid nanocatalyst for biodiesel production from different oil feedstocks. *Industrial Crops and Products, 215*, 118578.

Correa, D. F., Beyer, H. L., Possingham, H. P., Thomas-Hall, S. R., & Schenk, P. M. (2017). Biodiversity impacts of bioenergy production: Microalgae vs. first generation biofuels. *Renewable and Sustainable Energy Reviews, 74*, 1131-1146.

Cui, Y., Li, C., Yin, J., Li, S., Jia, Y., & Bao, M. (2017). Design, synthesis and properties of acidic deep eutectic solvents based on choline chloride. *Journal of Molecular Liquids, 236*, 338-343.

da Luz Corrêa, A. P., Bastos, R. R. C., Rocha Filho, G. N. d., Zamian, J. R., & Conceição, L. R. V. d. (2020). Preparation of sulfonated carbon-based catalysts from murumuru kernel shell and their performance in the esterification reaction. *RSC Advances, 10*(34), 20245-20256.

Dabbawala, A. A., Park, J. J., Valekar, A. H., Mishra, D. K., & Hwang, J.-S. (2015). Arenesulfonic acid functionalized ordered mesoporous silica as solid acid catalyst for solvent free dehydration of sorbitol to isosorbide. *Catalysis Communications, 69*, 207-211.

de Jesus, S. S., & Maciel Filho, R. (2022). Are ionic liquids eco-friendly? *Renewable and Sustainable Energy Reviews, 157*, 112039.

Deshmukh, S., Kumar, R., & Bala, K. (2019). Microalgae biodiesel: A review on oil extraction, fatty acid composition, properties and effect on engine performance and emissions. *Fuel Processing Technology, 191*, 232-247.

Devaraj Naik, B., & Udayakumar, M. (2021). Optimization studies on esterification of waste cooking oil using sulfated montmorillonite clay acidic catalyst. *Materials Today: Proceedings, 46*, 9855-9861.

Đorđević, B. S., Kostić, M. D., Todorović, Z. B., Stamenković, O. S., Veselinović, L. M., & Veljković, V. B. (2023). Triethanolamine-based deep eutectic solvents as cosolvents in biodiesel production from black mustard (Brassica nigra L.) seed oil. *Chemical Engineering Research and Design, 195*, 526-536.

dos Santos, M. R. M., Teleken, J. G., Tavares, F., & da Silva, E. A. (2022). Biodiesel purification by novel green solvent based on choline chloride: Deep eutectic solvent. *Journal of Advanced Manufacturing and Processing, 4*(2), e10111.

El-Nagar, R. A. (2023). Dicationic ionic liquids (DILs) as rapid esterification catalyst of butyric fatty acid. *Scientific Reports, 13*(1), 18635.

El Achkar, T., Greige-Gerges, H., & Fourmentin, S. (2021). Basics and properties of deep eutectic solvents: a review. *Environmental Chemistry Letters, 19*(4), 3397-3408.

Elsheikh, Y. A., Man, Z., Bustam, M. A., Yusup, S., & Wilfred, C. D. (2011). Brønsted imidazolium ionic liquids: Synthesis and comparison of their catalytic activities as pre-catalyst for biodiesel production through two stage process. *Energy Conversion and Management, 52*(2), 804-809.

Encinar, J. M., Nogales-Delgado, S., & Sánchez, N. (2021). Pre-esterification of high acidity animal fats to produce biodiesel: A kinetic study. *Arabian Journal of Chemistry, 14*(4), 103048.

Encinar, J. M., Pardal, A., & Sánchez, N. (2016). An improvement to the transesterification process by the use of co-solvents to produce biodiesel. *Fuel, 166*, 51-58.

Esmaeili, H. (2022). A critical review on the economic aspects and life cycle assessment of biodiesel production using heterogeneous nanocatalysts. *Fuel Processing Technology, 230*, 107224.

Farobie, O., & Hartulistiyoso, E. (2022). Palm Oil Biodiesel as a Renewable Energy Resource in Indonesia: Current Status and Challenges. *BioEnergy Research, 15*(1), 93-111.

Fazelinia, F., Bayat, M., Nasri, S., Kamalzare, M., & Maleki, A. (2023). Chitosan@Tannic Acid-Supported Fe3O4 Magnetic Bionanocomposite as Green and Recyclable Catalyst for the Synthesis of Benzo[g]thiazolo[3,2-a]quinolones Based on Nitroketene N,S-Acetal. *Catalysis Surveys from Asia, 27*(4), 391-405.

Feng, J., Loussala, H. M., Han, S., Ji, X., Li, C., & Sun, M. (2020). Recent advances of ionic liquids in sample preparation. *TrAC Trends in Analytical Chemistry, 125*, 115833.

Foteinis, S., Chatzisymeon, E., Litinas, A., & Tsoutsos, T. (2020). Used-cooking-oil biodiesel: Life cycle assessment and comparison with first- and third-generation biofuel. *Renewable Energy, 153*, 588-600.

Gandhi, V. G., Mishra, M. K., Rao, M. S., Kumar, A., Joshi, P. A., & Shah, D. O. (2011). Comparative study on nano-crystalline titanium dioxide catalyzed photocatalytic degradation of aromatic carboxylic acids in aqueous medium. *Journal of Industrial and Engineering Chemistry, 17*(2), 331-339.

Ganesan, S., Nadarajah, S., Chee, X. Y., Khairuddean, M., & Teh, G. B. (2020). Esterification of free fatty acids using ammonium ferric sulphate-calcium silicate as a heterogeneous catalyst. *Renewable Energy, 153*, 1406-1417.

Gardy, J., Osatiashtiani, A., Céspedes, O., Hassanpour, A., Lai, X., Lee, A. F., Wilson, K., & Rehan, M. (2018). A magnetically separable SO4/Fe-Al-TiO2 solid acid catalyst for biodiesel production from waste cooking oil. *Applied Catalysis B: Environmental, 234*, 268-278.

Gaurav, A., Dumas, S., Mai, C. T. Q., & Ng, F. T. T. (2019). A kinetic model for a single step biodiesel production from a high free fatty acid (FFA) biodiesel feedstock over a solid heteropolyacid catalyst. *Green Energy & Environment, 4*(3), 328-341.

Gaurav, K., Neeti, K., & Singh, R. (2024). Microalgae-based biodiesel production and its challenges and future opportunities: A review. *Green Technologies and Sustainability, 2*(1), 100060.

Gomes, J. M., Silva, S. S., & Reis, R. L. (2019). Biocompatible ionic liquids: fundamental behaviours and applications. *Chemical Society Reviews, 48*(15), 4317-4335.

Gómez, A. V., Tadini, C. C., Biswas, A., Buttrum, M., Kim, S., Boddu, V. M., & Cheng, H. N. (2019). Microwave-assisted extraction of soluble sugars from banana puree with natural deep eutectic solvents (NADES). *LWT, 107*, 79-88.

Gouda, S. P., Dhakshinamoorthy, A., & Rokhum, S. L. (2022). Metal-organic framework as a heterogeneous catalyst for biodiesel production: A review. *Chemical Engineering Journal Advances, 12*, 100415.

Gu, L., Huang, W., Tang, S., Tian, S., & Zhang, X. (2015). A novel deep eutectic solvent for biodiesel preparation using a homogeneous base catalyst. *Chemical Engineering Journal, 259*, 647-652.

Gupta, P., & Paul, S. (2014). Solid acids: Green alternatives for acid catalysis. *Catalysis Today, 236*, 153-170.

Halimatussadiah, A., Nainggolan, D., Yui, S., Moeis, F. R., & Siregar, A. A. (2021). Progressive biodiesel policy in Indonesia: Does the Government's economic proposition hold? *Renewable and Sustainable Energy Reviews, 150*, 111431.

Han, S., Yang, J., & Huang, H. (2022). Novel self-solidifying double-site acidic ionic liquid as efficient and reusable catalyst for green biodiesel synthesis. *Fuel, 315*, 122815.

Hao, L., Wang, M., Shan, W., Deng, C., Ren, W., Shi, Z., & Lü, H. (2017). L-proline-based deep eutectic solvents (DESs) for deep catalytic oxidative desulfurization (ODS) of diesel. *Journal of Hazardous Materials, 339*, 216-222.

Hatami, B., Ebrahimi, A. A., Ehrampoush, M. H., Salmani, M. H., Tamaddon, F., & Mokhtari, M. (2022). An efficient heterogeneous solid acid catalyst derived from sewage sludge for the catalytic transformation of sludge into biodiesel: Preparation, characterization, and arylation process modeling. *Journal of Cleaner Production, 355*, 131809.

Hayyan, A., Alam, M. Z., Mirghani, M. E. S., Kabbashi, N. A., Hakimi, N. I. N. M., Siran, Y. M., & Tahiruddin, S. (2010). Sludge palm oil as a renewable raw material for biodiesel production by two-step processes. *Bioresource Technology, 101*(20), 7804-7811.

Hayyan, A., Ali Hashim, M., & Hayyan, M. (2014a). Agro-industrial acidic oil as a renewable feedstock for biodiesel production using (1R)-(–)-camphor-10-sulfonic acid. *Chemical Engineering Science, 116*, 223-227.

Hayyan, A., Ali Hashim, M., Mjalli, F. S., Hayyan, M., & AlNashef, I. M. (2013a). A novel phosphonium-based deep eutectic catalyst for biodiesel production from industrial low grade crude palm oil. *Chemical Engineering Science, 92*, 81-88.

Hayyan, A., Hadj-Kali, M. K., Salleh, M. Z. M., Hashim, M. A., Rubaidi, S. R., Hayyan, M., Zulkifli, M. Y., Rashid, S. N., Mirghani, M. E. S., Ali, E., & Basirun, W. J. (2020). Characterization of Tetraethylene glycol-based deep eutectic solvents and their potential application for dissolving unsaturated fatty acids. *Journal of Molecular Liquids, 312*, 113284.

Hayyan, A., Hashim, M. A., Hayyan, M., Mjalli, F. S., & AlNashef, I. M. (2013b). A novel ammonium based eutectic solvent for the treatment of free fatty acid and synthesis of biodiesel fuel. *Industrial Crops and Products, 46*, 392-398.

Hayyan, A., Hashim, M. A., Hayyan, M., Mjalli, F. S., & AlNashef, I. M. (2014b). A new processing route for cleaner production of biodiesel fuel using a choline chloride based deep eutectic solvent. *Journal of Cleaner Production, 65*, 246-251.

Hayyan, A., Hizaddin, H. F., Abed, K. M., Mjalli, F. S., Hashim, M. A., Abo-Hamad, A., Saleh, J., Aljohani, A. S. M., Alharbi, Y. M., Alhumaydhi, F. A., Ahmad, A. A., Yeow, A. T. H., Aldeehani, A. K., Alajmi, F. D. H., & Al Nashef, I. (2022). Encapsulated deep eutectic solvent for esterification of free fatty acid. *Biomass Conversion and Biorefinery, 12*(9), 3725-3735.

Hayyan, A., Mjalli, F. S., Hashim, M. A., Hayyan, M., AlNashef, I. M., Al-Wahaibi, T., & Al-Wahaibi, Y. M. (2014c). A Solid Organic Acid Catalyst for the Pretreatment of Low-Grade Crude Palm Oil and Biodiesel Production. *International Journal of Green Energy, 11*(2), 129-140.

Hayyan, A., Qing, F. L. W., Salleh, M. Z. M., Basirun, W. J., Hamid, M. D., Saleh, J., Aljohani, A. S. M., Alhumaydhi, F. A., Zulkifli, M. Y., Abdulmonem, W. A., Yeow, A. T. H., Nor, M. R. M., Hashim, M. A., & Al-Sabahi, J. N. (2023a). Encapsulated paracetamol-based eutectic solvents for the treatment of low-grade palm oil mixed with microalgae oil. *Industrial Crops and Products, 195*, 116322.

Hayyan, A., Rashid, S. N., Hayyan, M., Zulkifliy, M. Y., Hashim, M. A., & Osman, N. A. (2017). Synthesis of novel eutectic catalyst for the esterification of crude palm oil mixed with sludge palm oil. *Journal of Oil Palm Research, 29*(3), 373-379.

Hayyan, A., Yeow, A. T. H., Abed, K. M., Jeffrey Basirun, W., Boon Kiat, L., Saleh, J., Wen Han, G., Chia Min, P., Aljohani, A. S. M., Zulkifli, M. Y., Alajmi, F. D. H., Alhumaydhi, F. A., Kadmouse Aldeehani, A., & Ali Hashim, M. (2021). The development of new homogenous and heterogeneous catalytic processes for the treatment of low grade palm oil. *Journal of Molecular Liquids, 344*, 117574.

Hayyan, M., Aissaoui, T., Hashim, M. A., AlSaadi, M. A., & Hayyan, A. (2015). Triethylene glycol based deep eutectic solvents and their physical properties. *Journal of the Taiwan Institute of Chemical Engineers, 50*, 24-30.

Hayyan, M., Hashim, M. A., Al-Saadi, M. A., Hayyan, A., AlNashef, I. M., & Mirghani, M. E. S. (2013c). Assessment of cytotoxicity and toxicity for phosphonium-based deep eutectic solvents. *Chemosphere, 93*(2), 455-459.

Hayyan, M., Hayyan, A., Hafizi, A. D. M., Basirun, W. J., Yeow, A. T. H., Salleh, M. Z. M., Saputra, H., Saleh, J., Alkandari, K. H., Hashim, M. A., & Alsaadi, M. A. (2023b). Phosphonium-based deep eutectic solvents: Physicochemical properties and application in Zn-air battery. *Chemical Engineering and Processing - Process Intensification, 185*, 109310.

Hayyan, M., Mbous, Y. P., Looi, C. Y., Wong, W. F., Hayyan, A., Salleh, Z., & Mohd-Ali, O. (2016). Natural deep eutectic solvents: cytotoxic profile. *SpringerPlus, 5*(1), 913.

Hazmi, B., Rashid, U., Kawi, S., Mokhtar, W. N. A. W., Yaw, T. C. S., Moser, B. R., & Alsalme, A. (2022). Palm fatty acid distillate esterification using synthesized heterogeneous sulfonated carbon catalyst from plastic waste: Characterization,

catalytic efficacy and stability, and fuel properties. *Process Safety and Environmental Protection, 162*, 1139-1151.

He, L., Qin, S., Chang, T., Sun, Y., & Gao, X. (2013). Biodiesel synthesis from the esterification of free fatty acids and alcohol catalyzed by long-chain Brønsted acid ionic liquid. *Catalysis Science & Technology, 3*(4), 1102-1107.

Hizaddin, H. F., Wazeer, I., Huzaimi, N. A., El Blidi, L., Hashim, M. A., Lévêque, J.-M., & Hadj-Kali, M. K. (2022). Extraction of Phenolic Compound from Model Pyrolysis Oil Using Deep Eutectic Solvents: Computational Screening and Experimental Validation. *Separations, 9*(11).

Hu, Z., Xian, F., Guo, Z., Lu, C., Du, X., Cheng, X., Zhang, S., Dong, S., Cui, G., & Chen, L. (2020). Nonflammable Nitrile Deep Eutectic Electrolyte Enables High-Voltage Lithium Metal Batteries. *Chemistry of Materials, 32*(8), 3405-3413.

Huang, Z., ChenYang, Y., Wang, X., Cai, R., & Han, B. (2024). Biodiesel synthesis through soybean oil transesterification using choline-based amino acid ionic liquids as catalysts. *Industrial Crops and Products, 208*, 117869.

Ibrahim, A. S. I., Gözmen, B., & Sönmez, Ö. (2024). Esterification of oleic acid using CoFe2O4@MoS2 solid acid catalyst under microwave irradiation. *Fuel, 371*, 131988.

Ibrahim, N. A., Rashid, U., Choong, T. S. Y., & Nehdi, I. A. (2020a). Synthesis of nanomagnetic sulphonated impregnated Ni/Mn/Na2SiO3 as catalyst for esterification of palm fatty acid distillate. *RSC Advances, 10*(10), 6098-6108.

Ibrahim, R. K., Hayyan, M., Alsaadi, M. A., Ibrahim, S., Hayyan, A., & Hashim, M. A. (2017). Diethylene glycol based deep eutectic solvents and their physical properties. *Studia Universitatis Babes-Bolyai Chemia, 62*(4), 433-450.

Ibrahim, R. K., Hayyan, M., AlSaadi, M. A., Ibrahim, S., Hayyan, A., & Hashim, M. A. (2019). Physical properties of ethylene glycol-based deep eutectic solvents. *Journal of Molecular Liquids, 276*, 794-800.

Ibrahim, S. F., Asikin-Mijan, N., Ibrahim, M. L., Abdulkareem-Alsultan, G., Izham, S. M., & Taufiq-Yap, Y. H. (2020b). Sulfonated functionalization of carbon derived corncob residue via hydrothermal synthesis route for esterification of palm fatty acid distillate. *Energy Conversion and Management, 210*, 112698.

Ijardar, S. P., Singh, V., & Gardas, R. L. (2022). Revisiting the Physicochemical Properties and Applications of Deep Eutectic Solvents. *Molecules, 27*(4).

Jha, D., Haider, M. B., Kumar, R., & Balathanigaimani, M. S. (2020). Extractive desulfurization of fuels using diglycol based deep eutectic solvents. *Journal of Environmental Chemical Engineering, 8*(5), 104182.

Jiang, W., Zhu, K., Li, H., Zhu, L., Hua, M., Xiao, J., Wang, C., Yang, Z., Chen, G., Zhu, W., Li, H., & Dai, S. (2020). Synergistic effect of dual Brønsted acidic deep eutectic solvents for oxidative desulfurization of diesel fuel. *Chemical Engineering Journal, 394*, 124831.

Jisieike, C. F., Ishola, N. B., Latinwo, L. M., & Betiku, E. (2023). Crude rubber seed oil esterification using a solid catalyst: Optimization by hybrid adaptive neuro-fuzzy inference system and response surface methodology. *Energy, 263*, 125734.

Kalhor, P., & Ghandi, K. (2021). Deep Eutectic Solvents as Catalysts for Upgrading Biomass. *Catalysts, 11*(2).

Kalla, R. M. N., Kim, M.-R., & Kim, I. (2018). Sulfonic Acid-Functionalized, Hyper-Cross-Linked Porous Polyphenols as Recyclable Solid Acid Catalysts for Esterification and Transesterification Reactions. *Industrial & Engineering Chemistry Research, 57*(34), 11583-11591.

Kamalzare, M., Ahghari, M. R., Bayat, M., & Maleki, A. (2021). Fe3O4@chitosan-tannic acid bionanocomposite as a novel nanocatalyst for the synthesis of pyranopyrazoles. *Scientific Reports, 11*(1), 20021.

Kefas, H. M., Yunus, R., Rashid, U., & Taufiq-Yap, Y. H. (2018). Modified sulfonation method for converting carbonized glucose into solid acid catalyst for the esterification of palm fatty acid distillate. *Fuel, 229*, 68-78.

Ketzer, F., & de Castilhos, F. (2021). An assessment on kinetic modeling of esterification reaction from oleic acid and methyl acetate over USY zeolite. *Microporous and Mesoporous Materials, 314*, 110890.

Khan, A. S., Ibrahim, T. H., Rashid, Z., Khamis, M. I., Nancarrow, P., & Jabbar, N. A. (2021a). COSMO-RS based screening of ionic liquids for extraction of phenolic compounds from aqueous media. *Journal of Molecular Liquids, 328*, 115387.

Khan, I. W., Naeem, A., Farooq, M., din, I. U., Ghazi, Z. A., & Saeed, T. (2021b). Reusable Na-SiO2@CeO2catalyst for efficient biodiesel production from non-edible wild olive oil as a new and potential feedstock. *Energy Conversion and Management, 231*, 113854.

Kibar, M. E., Hilal, L., Çapa, B. T., Bahçıvanlar, B., & Abdeljelil, B. B. (2023). Assessment of Homogeneous and Heterogeneous Catalysts in Transesterification Reaction: A Mini Review. *ChemBioEng Reviews, 10*(4), 412-422.

Kosuru, S. M. Y., Delhiwala, Y., Koorla, P. B., & Mekala, M. (2024). A review on the biodiesel production: Selection of catalyst, Pre-treatment, Post treatment methods. *Green Technologies and Sustainability, 2*(1), 100061.

Krishnan, S. G., Pua, F.-l., & Zhang, F. (2021). A review of magnetic solid catalyst development for sustainable biodiesel production. *Biomass and Bioenergy, 149*, 106099.

Kumar, S., Kumar, M., & Singh, A. (2021). Synthesis and characterization of iron oxide nanoparticles (Fe2O3, Fe3O4): a brief review. *Contemporary Physics, 62*(3), 144-164.

Kurchania, R., Sawant, S. S., & Ball, R. J. (2014). Synthesis and Characterization of Magnetite/Polyvinyl Alcohol Core–Shell Composite Nanoparticles. *Journal of the American Ceramic Society, 97*(10), 3208-3215.

Kushwaha, T., Ao, S., Ngaosuwan, K., Assabumrungrat, S., Gurunathan, B., & Rokhum, S. L. (2023). Esterification of oleic acid to biodiesel using biowaste-based solid acid catalyst under microwave irradiation. *Environmental Progress & Sustainable Energy, 42*(6), e14170.

Lanjekar, K. J., & Rathod, V. K. (2021). Green extraction of Glycyrrhizic acid from Glycyrrhiza glabra using choline chloride based natural deep eutectic solvents (NADESs). *Process Biochemistry, 102*, 22-32.

Li, H., Han, Z., Liu, F., Li, G., Guo, M., Cui, P., Zhou, S., & Yu, M. (2021a). Esterification catalyzed by an efficient solid acid synthesized from PTSA and UiO-66(Zr) for biodiesel production. *Faraday Discussions, 231*(0), 342-355.

Li, M., Chen, J., Li, L., Ye, C., Lin, X., & Qiu, T. (2021b). Novel multi–SO3H functionalized ionic liquids as highly efficient catalyst for synthesis of biodiesel. *Green Energy & Environment, 6*(2), 271-282.

Li, P., Yang, C., Jiang, Z., Jin, Y., & Wu, W. (2023a). Lignocellulose pretreatment by deep eutectic solvents and related technologies: A review. *Journal of Bioresources and Bioproducts, 8*(1), 33-44.

Li, Q., Ma, C., Di, J., Ni, J., & He, Y.-C. (2022). Catalytic valorization of biomass for furfuryl alcohol by novel deep eutectic solvent-silica chemocatalyst and newly constructed reductase biocatalyst. *Bioresource Technology, 347*, 126376.

Li, Y., Luo, J., Shan, S., & Cao, Y. (2023b). High toxicity of amino acid-based deep eutectic solvents. *Journal of Molecular Liquids, 370*, 121044.

Lieu, T., Yusup, S., & Moniruzzaman, M. (2016). Kinetic study on microwave-assisted esterification of free fatty acids derived from Ceiba pentandra Seed Oil. *Bioresource Technology, 211*, 248-256.

Liu, F., Ma, X., Li, H., Wang, Y., Cui, P., Guo, M., Yaxin, H., Lu, W., Zhou, S., & Yu, M. (2020a). Dilute sulfonic acid post functionalized metal organic framework as a heterogeneous acid catalyst for esterification to produce biodiesel. *Fuel, 266*, 117149.

Liu, W., Wang, F., Meng, P., & Zang, S.-Q. (2020b). Sulfonic Acids Supported on UiO-66 as Heterogeneous Catalysts for the Esterification of Fatty Acids for Biodiesel Production. *Catalysts, 10*(11).

Liu, X., Zhu, F., Zhang, R., Zhao, L., & Qi, J. (2021). Recent progress on biodiesel production from municipal sewage sludge. *Renewable and Sustainable Energy Reviews, 135*, 110260.

Liu, Y., Lotero, E., & Goodwin, J. G. (2006). Effect of water on sulfuric acid catalyzed esterification. *Journal of Molecular Catalysis A: Chemical, 245*(1), 132-140.

Liu, Y., Wang, Y., Cao, Y., Chen, X., Yu, Q., Wang, Z., & Yuan, Z. (2020c). One-Pot Synthesis of Cyclic Biofuel Intermediates from Biomass in Choline Chloride/Formic Acid-Based Deep Eutectic Solvents. *ACS Sustainable Chemistry & Engineering, 8*(18), 6949-6955.

Liu, Y., Yan, H., Liu, J., Dong, W., Cao, Z., Hu, X., & Zhou, Z. (2020d). Acidic deep eutectic solvents with long carbon chains as catalysts and reaction media for biodiesel production. *Renewable Energy, 162*, 1842-1853.

Lomba, L., Werner, Á., Giner, B., & Lafuente, C. (2023). Deep Eutectic Solvents Formed by Glycerol and Xylitol, Fructose and Sorbitol: Effect of the Different Sugars in Their Physicochemical Properties. *Molecules, 28*(16).

Lowe, B., Gardy, J., & Hassanpour, A. (2022). The Role of Sulfated Materials for Biodiesel Production from Cheap Raw Materials. *Catalysts, 12*(2).

Lu, W., Xu, Z., Li, M., Ma, Y., & Xiao, Z. (2022). Deep eutectic solvent (DES) assisted deacidification of acidic oil and retaining catalyst activity: Variables optimization and catalyst characterization. *Industrial Crops and Products, 183*, 114990.

Luo, N., Yang, Z., Tang, F., Wang, D., Feng, M., Liao, X., & Yang, X. (2019). Fe3O4/Carbon Nanodot Hybrid Nanoparticles for the Indirect Colorimetric Detection of Glutathione. *ACS Applied Nano Materials, 2*(6), 3951-3959.

Luz, P. T. S. d., Moraes, B. F. d., Ferreira, R. K., Melo, C. C. d., Oliveira, A. d. N. d., Costa, A. A. F. d., Costa, C. E. F. d., Rocha Filho, G. N. d., Osman, S. M., Luque, R., & Nascimento, L. A. S. d. (2024). Design of activated bentonite-based catalysts for the esterification of residual free fatty acids from palm oil. *Catalysis Today, 441*, 114886.

Ma, W., & Row, K. H. (2021). pH-induced deep eutectic solvents based homogeneous liquid-liquid microextraction for the extraction of two antibiotics from environmental water. *Microchemical Journal, 160*, 105642.

Mahajan, A., & Gupta, P. (2020). Carbon-based solid acids: a review. *Environmental Chemistry Letters, 18*(2), 299-314.

Mahdi, H. I., Ramlee, N. N., da Silva Duarte, J. L., Cheng, Y.-S., Selvasembian, R., Amir, F., de Oliveira, L. H., Wan Azelee, N. I., Meili, L., & Rangasamy, G. (2023). A comprehensive review on nanocatalysts and nanobiocatalysts for biodiesel production in Indonesia, Malaysia, Brazil and USA. *Chemosphere, 319*, 138003.

Maleki, A., Niksefat, M., Rahimi, J., & Hajizadeh, Z. (2019). Design and preparation of Fe3O4@PVA polymeric magnetic nanocomposite film and surface coating by sulfonic acid via in situ methods and evaluation of its catalytic performance in the synthesis of dihydropyrimidines. *BMC Chemistry, 13*(1), 19.

Maleki, B., Ashraf Talesh, S. S., & Mansouri, M. (2022). Comparison of catalysts types performance in the generation of sustainable biodiesel via transesterification of various oil sources: a review study. *Materials Today Sustainability, 18*, 100157.

Malode, S. J., Prabhu, K. K., Mascarenhas, R. J., Shetti, N. P., & Aminabhavi, T. M. (2021). Recent advances and viability in biofuel production. *Energy Conversion and Management: X, 10*, 100070.

Mamtani, K., Farid, M. M., & Shahbaz, K. (2023). Application of Quaternary Ammonium-Based Deep Eutectic Solvents as Catalysts for the Glycerolysis of Free Fatty Acids. *Energy & Fuels, 37*(11), 7848-7855.

Mamtani, K., Shahbaz, K., & Farid, M. M. (2021). Deep eutectic solvents – Versatile chemicals in biodiesel production. *Fuel, 295*, 120604.

Mandari, V., & Devarai, S. K. (2022). Biodiesel Production Using Homogeneous, Heterogeneous, and Enzyme Catalysts via Transesterification and Esterification Reactions: a Critical Review. *BioEnergy Research, 15*(2), 935-961.

Maquirriain, M. A., Querini, C. A., & Pisarello, M. L. (2021). Glycerine esterification with free fatty acids: Homogeneous catalysis. *Chemical Engineering Research and Design, 171*, 86-99.

Marchel, M., Cieśliński, H., & Boczkaj, G. (2022). Thermal Instability of Choline Chloride-Based Deep Eutectic Solvents and Its Influence on Their Toxicity─ Important Limitations of DESs as Sustainable Materials. *Industrial & Engineering Chemistry Research, 61*(30), 11288-11300.

Marchetti, J. M. (2022). Optimization of the esterification reaction of free fatty acids present in waste salmon oil. *Biofuels, Bioproducts and Biorefining, 16*(5), 1297-1303.

Martínez, G. M., Townley, G. G., & Martínez-Espinosa, R. M. (2022). Controversy on the toxic nature of deep eutectic solvents and their potential contribution to environmental pollution. *Heliyon, 8*(12), e12567.

Masri, A. N., Abdul Mutalib, M. I., Aminuddin, N. F., & Lévêque, J. M. (2018). Novel SO3H-functionalized dicationic ionic liquids – A comparative study for esterification reaction by ultrasound cavitation and mechanical stirring for biodiesel production. *Separation and Purification Technology, 196*, 106-114.

Masri, A. N., Abdul Mutalib, M. I., Yahya, W. Z. N., Aminuddin, N. F., & Leveque, J. M. (2020). Rapid esterification of fatty acid using dicationic acidic ionic liquid catalyst via ultrasonic-assisted method. *Ultrasonics Sonochemistry, 60*, 104732.

Mat Aron, N. S., Khoo, K. S., Chew, K. W., Show, P. L., Chen, W.-H., & Nguyen, T. H. P. (2020). Sustainability of the four generations of biofuels – A review. *International Journal of Energy Research, 44*(12), 9266-9282.

Melero, J. A., Morales, G., Iglesias, J., Paniagua, M., Hernández, B., & Penedo, S. (2013). Efficient conversion of levulinic acid into alkyl levulinates catalyzed by sulfonic mesostructured silicas. *Applied Catalysis A: General, 466*, 116-122.

Melián-Cabrera, I. (2021). Catalytic Materials: Concepts to Understand the Pathway to Implementation. *Industrial & Engineering Chemistry Research, 60*(51), 18545-18559.

Mendaros, C. M., Go, A. W., Nietes, W. J. T., Gollem, B. E. J. O., & Cabatingan, L. K. (2020). Direct sulfonation of cacao shell to synthesize a solid acid catalyst for the esterification of oleic acid with methanol. *Renewable Energy, 152*, 320-330.

Mohammad Fauzi, A. H., & Amin, N. A. S. (2012). An overview of ionic liquids as solvents in biodiesel synthesis. *Renewable and Sustainable Energy Reviews, 16*(8), 5770-5786.

Mohan, M., Keasling, J. D., Simmons, B. A., & Singh, S. (2022). In silico COSMO-RS predictive screening of ionic liquids for the dissolution of plastic. *Green Chemistry, 24*(10), 4140-4152.

Mok, C. F., Ching, Y. C., Abu Osman, N. A., Muhamad, F., Mohd Junaidi, M. U., & Choo, J. H. (2020). Preparation and characterization study on maleic acid cross-linked poly(vinyl alcohol)/chitin/nanocellulose composites. *Journal of Applied Polymer Science, 137*(35), 49044.

Muhammad, N., Elsheikh, Y. A., Mutalib, M. I. A., Bazmi, A. A., Khan, R. A., Khan, H., Rafiq, S., Man, Z., & khan, I. (2015). An overview of the role of ionic liquids in biodiesel reactions. *Journal of Industrial and Engineering Chemistry, 21*, 1-10.

Murshid, G., Mjalli, F. S., Naser, J., Al-Zakwani, S., & Hayyan, A. (2019). Novel diethanolamine based deep eutectic mixtures for carbon dioxide (CO2) capture: synthesis and characterisation. *Physics and Chemistry of Liquids, 57*(4), 473-490.

Naghmash, M. A., El-Molla, S. A., & Mahmoud, H. R. (2022). Synthesis and characterization of novel chlorinated SnO2 nanomaterials for biodiesel production via stearic acid esterification with methanol. *Advanced Powder Technology, 33*(4), 103532.

Naji, S. Z., Tye, C. T., & Abd, A. A. (2021). State of the art of vegetable oil transformation into biofuels using catalytic cracking technology: Recent trends and future perspectives. *Process Biochemistry, 109*, 148-168.

Nayak, S. N., Nayak, M. G., & Bhasin, D. C. P. (2021). Parametric, kinetic, and thermodynamic studies of microwave-assisted esterification of Kusum oil. *Fuel Communications, 8*, 100018.

Nejrotti, S., Antenucci, A., Pontremoli, C., Gontrani, L., Barbero, N., Carbone, M., & Bonomo, M. (2022). Critical Assessment of the Sustainability of Deep Eutectic Solvents: A Case Study on Six Choline Chloride-Based Mixtures. *ACS Omega, 7*(51), 47449-47461.

Ofoefule, A. U., Esonye, C., Onukwuli, O. D., Nwaeze, E., & Ume, C. S. (2019). Modeling and optimization of African pear seed oil esterification and transesterification using artificial neural network and response surface methodology comparative analysis. *Industrial Crops and Products, 140*, 111707.

Olagbende, O. H., Falowo, O. A., Latinwo, L. M., & Betiku, E. (2021). Esterification of Khaya senegalensis seed oil with a solid heterogeneous acid catalyst: Modeling, optimization, kinetic and thermodynamic studies. *Cleaner Engineering and Technology, 4*, 100200.

Omar, K. A., & Sadeghi, R. (2022). Physicochemical properties of deep eutectic solvents: A review. *Journal of Molecular Liquids, 360*, 119524.

Omar, K. A., & Sadeghi, R. (2023). Database of deep eutectic solvents and their physical properties: A review. *Journal of Molecular Liquids, 384*, 121899.

Organisation for Economic Cooperation and Development. (2016). OECD-FAO Agricultural Outlook 2016-2025.

Pan, H., Li, H., Liu, X.-F., Zhang, H., Yang, K.-L., Huang, S., & Yang, S. (2016). Mesoporous polymeric solid acid as efficient catalyst for (trans)esterification of crude Jatropha curcas oil. *Fuel Processing Technology, 150*, 50-57.

Panchal, B., Chang, T., Qin, S., Sun, Y., Wang, J., & Bian, K. (2020). Optimization of soybean oil transesterification using an ionic liquid and methanol for biodiesel synthesis. *Energy Reports, 6*, 20-27.

Parveez, G. K. A., Leow, S.-S., Kamil, N. N., Madihah, A. Z., Ithnin, M., Ng, M. H., Yusof, Y. A., & Idris, Z. (2024). Oil Palm Economic Performance in Malaysia and R&D Progress In 2023. *Journal of Oil Palm Research, 36*(2), 171-186.

Perez, G. A. P., & Dumont, M.-J. (2021). Polyvinyl sulfonated catalyst and the effect of sulfonic sites on the dehydration of carbohydrates. *Chemical Engineering Journal, 419*, 129573.

Picchio, M. L., Minudri, D., Mantione, D., Criado-Gonzalez, M., Guzmán-González, G., Schmarsow, R., Müller, A. J., Tomé, L. C., Minari, R. J., & Mecerreyes, D. (2022). Natural Deep Eutectic Solvents Based on Choline Chloride and Phenolic Compounds as Efficient Bioadhesives and Corrosion Protectors. *ACS Sustainable Chemistry & Engineering, 10*(25), 8135-8142.

Picciolini, E., Pastore, G., Del Giacco, T., Ciancaleoni, G., Tiecco, M., & Germani, R. (2023). aquo-DESs: Water-based binary natural deep eutectic solvents. *Journal of Molecular Liquids, 383*, 122057.

Qin, H., Hu, X., Wang, J., Cheng, H., Chen, L., & Qi, Z. (2020). Overview of acidic deep eutectic solvents on synthesis, properties and applications. *Green Energy & Environment, 5*(1), 8-21.

Qin, H., Song, Z., Zeng, Q., Cheng, H., Chen, L., & Qi, Z. (2019). Bifunctional imidazole-PTSA deep eutectic solvent for synthesizing long-chain ester IBIBE in reactive extraction. *AIChE Journal, 65*(2), 675-683.

Qiu, Y., & Wang, L. (2022). Imidazolium ionic liquids as potential persistent pollutants in aqueous environments: Indirect photochemical degradation kinetics and mechanism. *Environmental Research, 211*, 113031.

Racar, M., Šoljić Jerbić, I., Glasovac, Z., & Jukić, A. (2023). Guanidine catalysts for biodiesel production: Activity, process modelling and optimization. *Renewable Energy, 202*, 1046-1053.

Rahimi, J., Taheri-Ledari, R., Niksefat, M., & Maleki, A. (2020). Enhanced reduction of nitrobenzene derivatives: Effective strategy executed by Fe3O4/PVA-10%Ag as a versatile hybrid nanocatalyst. *Catalysis Communications, 134*, 105850.

Rahman, M. S., Roy, R., Jadhav, B., Hossain, M. N., Halim, M. A., & Raynie, D. E. (2021). Formulation, structure, and applications of therapeutic and amino acid-based deep eutectic solvents: An overview. *Journal of Molecular Liquids, 321*, 114745.

Rashid, S. N., Hayyan, A., & Hashim, M. A. (2017). Production of Fatty Acid Methyl Ester from Low Grade Palm Oil Using Eutectic Solvent Based on Benzyltrimethylammonium Chloride. *IOP Conference Series: Materials Science and Engineering, 210*(1), 012012.

Rechnia-Gorący, P., Malaika, A., & Kozłowski, M. (2018). Acidic activated carbons as catalysts of biodiesel formation. *Diamond and Related Materials, 87*, 124-133.

Ridwan, I., Chinwanitcharoen, C., & Tamura, K. (2021). A new biodiesel production by water addition to supercritical tert-butyl methyl ether using a plug flow reactor. *Fuel, 305*, 121512.

Rodriguez Rodriguez, N., Machiels, L., & Binnemans, K. (2019). p-Toluenesulfonic Acid-Based Deep-Eutectic Solvents for Solubilizing Metal Oxides. *ACS Sustainable Chemistry & Engineering, 7*(4), 3940-3948.

Rokhum, S. L., Changmai, B., Kress, T., & Wheatley, A. E. H. (2022). A one-pot route to tunable sugar-derived sulfonated carbon catalysts for sustainable production of biodiesel by fatty acid esterification. *Renewable Energy, 184*, 908-919.

Roman, F. F., Ribeiro, A. E., Queiroz, A., Lenzi, G. G., Chaves, E. S., & Brito, P. (2019). Optimization and kinetic study of biodiesel production through esterification of oleic acid applying ionic liquids as catalysts. *Fuel, 239*, 1231-1239.

Roslan, N. A., Zainal Abidin, S., Abdullah, N., Osazuwa, O. U., Abdul Rasid, R., & Yunus, N. M. (2022). Esterification reaction of free fatty acid in used cooking oil using sulfonated hypercrosslinked exchange resin as catalyst. *Chemical Engineering Research and Design, 180*, 414-424.

Russo, F., Tiecco, M., Galiano, F., Mancuso, R., Gabriele, B., & Figoli, A. (2022). Launching deep eutectic solvents (DESs) and natural deep eutectic solvents (NADESs), in combination with different harmless co-solvents, for the preparation of more sustainable membranes. *Journal of Membrane Science, 649*, 120387.

Saidi, M., Safaripour, M., Ameri, F. A., & Jomeh, M. E. (2023). Application of sulfonated biochar-based magnetic catalyst for biodiesel production: Sensitivity analysis and process optimization. *Chemical Engineering and Processing - Process Intensification, 190*, 109419.

Saimon, N. N., Jusoh, M., Ngadi, N., & Zakaria, Z. Y. (2020). Kinetic Study of Esterification of Palm Fatty Acid Distillate Using Sulfonated Glucose Prepared via Microwave-Assisted Heating Method. *Chemical Engineering Transactions, 78*, 403-408.

Salleh, M. Z. M., Hadj-Kali, M. K., Hashim, M. A., & Mulyono, S. (2018). Ionic liquids for the separation of benzene and cyclohexane – COSMO-RS screening and experimental validation. *Journal of Molecular Liquids, 266*, 51-61.

Sander, A., Petračić, A., Vrsaljko, D., Parlov Vuković, J., Hršak, P., & Jelavić, A. (2024). Continuous Purification of Biodiesel with Deep Eutectic Solvent in a Laboratory Karr Column. *Separations, 11*(3).

Saravanan, A., Senthil Kumar, P., Jeevanantham, S., Karishma, S., & Vo, D.-V. N. (2022). Recent advances and sustainable development of biofuels production from lignocellulosic biomass. *Bioresource Technology, 344*, 126203.

Serrano, M., Marchetti, J.-M., Martínez, M., & Aracil, J. (2015). Biodiesel production from waste salmon oil: kinetic modeling, properties of methyl esters, and economic feasibility of a low capacity plant. *Biofuels, Bioproducts and Biorefining, 9*(5), 516-528.

Shahbaz, K., Mjalli, F. S., Hashim, M. A., & AlNashef, I. M. (2010). Using Deep Eutectic Solvents for the Removal of Glycerol from Palm Oil-Based Biodiesel. *Journal of Applied Sciences, 10*(24), 3349-3354.

Shahbaz, K., Mjalli, F. S., Hashim, M. A., & AlNashef, I. M. (2011a). Eutectic solvents for the removal of residual palm oil-based biodiesel catalyst. *Separation and Purification Technology, 81*(2), 216-222.

Shahbaz, K., Mjalli, F. S., Hashim, M. A., & AlNashef, I. M. (2011b). Using Deep Eutectic Solvents Based on Methyl Triphenyl Phosphunium Bromide for the Removal of Glycerol from Palm-Oil-Based Biodiesel. *Energy & Fuels, 25*(6), 2671-2678.

ShenavaeiZare, T., Khoshsima, A., & ZareNezhad, B. (2021). Production of biodiesel through nanocatalytic transesterification of extracted oils from halophytic safflower and salicornia plants in the presence of deep eutectic solvents. *Fuel, 302*, 121171.

Silva, E., Oliveira, F., Silva, J. M., Matias, A., Reis, R. L., & Duarte, A. R. C. (2020). Optimal Design of THEDES Based on Perillyl Alcohol and Ibuprofen. *Pharmaceutics, 12*(11).

Singh, D., Sharma, D., Soni, S. L., Sharma, S., Kumar Sharma, P., & Jhalani, A. (2020). A review on feedstocks, production processes, and yield for different generations of biodiesel. *Fuel, 262*, 116553.

Singh, K., Shibu, R. P., Mehra, S., & Kumar, A. (2023). Insights into the physicochemical properties of newly synthesized benzyl triethylammonium chloride-based deep eutectic solvents. *Journal of Molecular Liquids, 386*, 122589.

Singh, N., Saluja, R. K., Rao, H. J., Kaushal, R., Gahlot, N. K., Suyambulingam, I., Sanjay, M. R., Divakaran, D., & Siengchin, S. (2024). Progress and facts on biodiesel generations, production methods, influencing factors, and reactors: A comprehensive review from 2000 to 2023. *Energy Conversion and Management, 302*, 118157.

Siow, H. S., Sudesh, K., Murugan, P., & Ganesan, S. (2021). Mealworm (Tenebrio molitor) oil characterization and optimization of the free fatty acid pretreatment via acid-catalyzed esterification. *Fuel, 299*, 120905.

Soontarapa, K., Ampairojanawong, R., & Palakul, T. (2023). Esterification and transesterification of palm fatty acid distillate in chitosan membrane reactor. *Fuel, 339*, 126918.

Srikumar, K., Tan, Y. H., Kansedo, J., Tan, I. S., Mubarak, N. M., Ibrahim, M. L., Yek, P. N. Y., Foo, H. C. Y., Karri, R. R., & Khalid, M. (2024). A review on the environmental life cycle assessment of biodiesel production: Selection of catalyst and oil feedstock. *Biomass and Bioenergy, 185*, 107239.

Sun, L.-B., Liu, X.-Q., & Zhou, H.-C. (2015). Design and fabrication of mesoporous heterogeneous basic catalysts. *Chemical Society Reviews, 44*(15), 5092-5147.

Swami, P., Rathod, S., Choudhari, P., Patil, D., Patravale, A., Nalwar, Y., Sankpal, S., & Hangirgekar, S. (2023). Fe3O4@SiO2@TDI@DES: A novel magnetically separable catalyst for the synthesis of oxindoles. *Journal of Molecular Structure, 1292*, 136079.

Syazwani, O. N., Rashid, U., Mastuli, M. S., & Taufiq-Yap, Y. H. (2019). Esterification of palm fatty acid distillate (PFAD) to biodiesel using Bi-functional catalyst synthesized from waste angel wing shell (Cyrtopleura costata). *Renewable Energy, 131*, 187-196.

Szulczyk, K. R., Yap, C. S., & Ho, P. (2021). The economic feasibility and environmental ramifications of biodiesel, bioelectricity, and bioethanol in Malaysia. *Energy for Sustainable Development, 61*, 206-216.

Tamjidi, S., Kamyab Moghadas, B., & Esmaeili, H. (2022). Ultrasound-assisted biodiesel generation from waste edible oil using CoFe2O4@GO as a superior and reclaimable nanocatalyst: Optimization of two-step transesterification by RSM. *Fuel, 327*, 125170.

Tan, X., Sudarsanam, P., Tan, J., Wang, A., Zhang, H., Li, H., & Yang, S. (2021). Sulfonic acid-functionalized heterogeneous catalytic materials for efficient biodiesel production: A review. *Journal of Environmental Chemical Engineering, 9*(1), 104719.

Tang, W., Gao, M., Zhang, B., Wang, X., Wu, C., Wang, Q., & Liu, S. (2023). Performance and deactivation mechanism of a carbon-based solid acid catalyst in the esterification of soybean saponin acid oil. *Journal of Environmental Chemical Engineering, 11*(3), 109797.

Tang, Z.-E., Lim, S., Pang, Y.-L., Shuit, S.-H., & Ong, H.-C. (2020). Utilisation of biomass wastes based activated carbon supported heterogeneous acid catalyst for biodiesel production. *Renewable Energy, 158*, 91-102.

Taysun, M. B., Sert, E., & Atalay, F. S. (2016). Physical properties of benzyl tri-methyl ammonium chloride based deep eutectic solvents and employment as catalyst. *Journal of Molecular Liquids, 223*, 845-852.

Teh, S. S., & Lau, H. L. N. (2023). Phytonutrient content and oil quality of selected edible oils upon twelve months storage. *Journal of the American Oil Chemists' Society*.

Testa, M. L., & La Parola, V. (2021). Sulfonic Acid-Functionalized Inorganic Materials as Efficient Catalysts in Various Applications: A Minireview. *Catalysts, 11*(10).

Thoai, D. N., Tongurai, C., Prasertsit, K., & Kumar, A. (2019). Review on biodiesel production by two-step catalytic conversion. *Biocatalysis and Agricultural Biotechnology, 18*, 101023.

Thul, M., Pantawane, A., Lin, W., Lin, Y.-J., Su, P.-F., Tseng, S.-A., Wu, H.-R., Ho, W.-Y., & Luo, S.-Y. (2021). Tunable aryl imidazolium ionic liquids (TAIILs) as environmentally benign catalysts for the esterification of fatty acids to biodiesel fuel. *Catalysis Communications, 149*, 106243.

Triolo, A., Lo Celso, F., & Russina, O. (2023). Liquid structure of a water-based, hydrophobic and natural deep eutectic solvent: The case of thymol-water. A Molecular Dynamics study. *Journal of Molecular Liquids, 372*, 121151.

Troter, D. Z., Todorović, Z. B., Đokić-Stojanović, D. R., Stamenković, O. S., & Veljković, V. B. (2016). Application of ionic liquids and deep eutectic solvents in biodiesel production: A review. *Renewable and Sustainable Energy Reviews, 61*, 473-500.

Troter, D. Z., Todorović, Z. B., Đokić-Stojanović, D. R., Veselinović, L. M., Zdujić, M. V., & Veljković, V. B. (2018). Choline chloride-based deep eutectic solvents in CaO-catalyzed ethanolysis of expired sunflower oil. *Journal of Molecular Liquids, 266*, 557-567.

Ullah, H., Wilfred, C. D., & Shaharun, M. S. (2019). Ionic liquid-based extraction and separation trends of bioactive compounds from plant biomass. *Separation Science and Technology, 54*(4), 559-579.

Ullah, Z., Bustam, M. A., & Man, Z. (2015). Biodiesel production from waste cooking oil by acidic ionic liquid as a catalyst. *Renewable Energy, 77*, 521-526.

Uslu, S., Maki, D. F., & Al-Gburi, A. S. K. (2023). Synthesis of spirulina microalgae biodiesel, and experimental research of its effects on compression ignition engine responses with iron II-III oxide (Fe3O4) nanoparticle supplementation. *Energy Conversion and Management, 293*, 117457.

Usmani, Z., Sharma, M., Tripathi, M., Lukk, T., Karpichev, Y., Gathergood, N., Singh, B. N., Thakur, V. K., Tabatabaei, M., & Gupta, V. K. (2023). Biobased natural deep eutectic system as versatile solvents: Structure, interaction and advanced applications. *Science of The Total Environment, 881*, 163002.

Vasić, K., Hojnik Podrepšek, G., Knez, Ž., & Leitgeb, M. (2020). Biodiesel Production Using Solid Acid Catalysts Based on Metal Oxides. *Catalysts, 10*(2).

Wang, B., Wang, B., Shukla, S. K., & Wang, R. (2023a). Enabling Catalysts for Biodiesel Production via Transesterification. *Catalysts, 13*(4).

Wang, H., Zhou, H., Yan, Q., Wu, X., & Zhang, H. (2023b). Superparamagnetic nanospheres with efficient bifunctional acidic sites enable sustainable production of biodiesel from budget non-edible oils. *Energy Conversion and Management, 297*, 117758.

Wang, P., Tian, B., Ge, Z., Feng, J., Wang, J., Yang, K., Sun, P., & Cai, M. (2023c). Ultrasound and deep eutectic solvent as green extraction technology for recovery of phenolic compounds from Dendrobium officinale leaves. *Process Biochemistry, 128*, 1-11.

Wang, W., & Lee, D.-J. (2021). Lignocellulosic biomass pretreatment by deep eutectic solvents on lignin extraction and saccharification enhancement: A review. *Bioresource Technology, 339*, 125587.

Wang, Y.-T., Yang, X.-X., Xu, J., Wang, H.-L., Wang, Z.-B., Zhang, L., Wang, S.-L., & Liang, J.-L. (2019). Biodiesel production from esterification of oleic acid by a sulfonated magnetic solid acid catalyst. *Renewable Energy, 139*, 688-695.

Wang, Y., Meng, X., Tian, Y., Kim, K. H., Jia, L., Pu, Y., Leem, G., Kumar, D., Eudes, A., Ragauskas, A. J., & Yoo, C. G. (2021). Engineered Sorghum Bagasse Enables a Sustainable Biorefinery with p-Hydroxybenzoic Acid-Based Deep Eutectic Solvent. *ChemSusChem, 14*(23), 5235-5244.

Wang, Y., Wang, D., Tan, M., Jiang, B., Zheng, J., Tsubaki, N., & Wu, M. (2015). Monodispersed Hollow SO3H-Functionalized Carbon/Silica as Efficient Solid Acid Catalyst for Esterification of Oleic Acid. *ACS Applied Materials & Interfaces, 7*(48), 26767-26775.

Williamson, S. T., Shahbaz, K., Mjalli, F. S., AlNashef, I. M., & Farid, M. M. (2017). Application of deep eutectic solvents as catalysts for the esterification of oleic acid with glycerol. *Renewable Energy, 114*, 480-488.

Xia, X., Wan, R., Wang, P., Huo, W., Dong, H., & Du, Q. (2018). Toxicity of imidazoles ionic liquid [C16mim]Cl to Hela cells. *Ecotoxicology and Environmental Safety, 162*, 408-414.

Xie, W., & Li, J. (2023). Magnetic solid catalysts for sustainable and cleaner biodiesel production: A comprehensive review. *Renewable and Sustainable Energy Reviews, 171*, 113017.

Xie, W., & Wang, H. (2020). Immobilized polymeric sulfonated ionic liquid on core-shell structured Fe3O4/SiO2 composites: A magnetically recyclable catalyst for simultaneous transesterification and esterifications of low-cost oils to biodiesel. *Renewable Energy, 145*, 1709-1719.

Xie, W., & Wang, H. (2021). Grafting copolymerization of dual acidic ionic liquid on core-shell structured magnetic silica: A magnetically recyclable Brönsted acid catalyst for biodiesel production by one-pot transformation of low-quality oils. *Fuel, 283*, 118893.

Xu, H., Ou, L., Li, Y., Hawkins, T. R., & Wang, M. (2022). Life Cycle Greenhouse Gas Emissions of Biodiesel and Renewable Diesel Production in the United States. *Environmental Science & Technology, 56*(12), 7512-7521.

Yu, G., Jin, D., Zhang, F., Li, Q., Zhou, Z., & Ren, Z. (2022). Oxidation-extraction desulfurization of fuel with a novel green acidic deep eutectic solvent system. *Fuel, 329*, 125495.

Yu, J., Wang, Y., Sun, L., Xu, Z., Du, Y., Sun, H., Li, W., Luo, S., Ma, C., & Liu, S. (2021). Catalysis Preparation of Biodiesel from Waste Schisandra chinensis Seed Oil with the Ionic Liquid Immobilized in a Magnetic Catalyst: Fe3O4@SiO2@[C4mim]HSO4. *ACS Omega, 6*(11), 7896-7909.

Yusuf, B. O., Oladepo, S. A., & Ganiyu, S. A. (2023). Biodiesel Production from Waste Cooking Oil via β-Zeolite-Supported Sulfated Metal Oxide Catalyst Systems. *ACS Omega, 8*(26), 23720-23732.

Zahan, K. A., & Kano, M. (2018). Biodiesel Production from Palm Oil, Its By-Products, and Mill Effluent: A Review. *Energies, 11*(8).

Zapata, F., López-Fernández, A., Ortega-Ojeda, F., Quintanilla, G., García-Ruiz, C., & Montalvo, G. (2021). Introducing ATR-FTIR Spectroscopy through Analysis of Acetaminophen Drugs: Practical Lessons for Interdisciplinary and Progressive Learning for Undergraduate Students. *Journal of Chemical Education, 98*(8), 2675-2686.

Zavarize, D. G., Vieira, G. E. G., & de Oliveira, J. D. (2023). Kinetics of free fatty acids esterification in waste frying oil using novel carbon-based acid heterogeneous catalyst derived from Amazonian Açaí seeds – Role of experimental conditions on a simpler pseudo first-order reaction mechanism. *Catalysis Communications, 180*, 106716.

Zhang, H., Gao, J., Zhao, Z., Chen, G. Z., Wu, T., & He, F. (2016). Esterification of fatty acids from waste cooking oil to biodiesel over a sulfonated resin/PVA composite. *Catalysis Science & Technology, 6*(14), 5590-5598.

Zhang, J., Li, S., Yao, L., Yi, Y., Shen, L., Li, Z., & Qiu, H. (2022). Responsive switchable deep eutectic solvents: A review. *Chinese Chemical Letters*, 107750.

Zhang, Q., Lei, Y., Li, L., Lei, J., Hu, M., Deng, T., Zhang, Y., & Ma, P. (2023). Construction of the novel PMA@Bi-MOF catalyst for effective fatty acid esterification. *Sustainable Chemistry and Pharmacy, 33*, 101038.

Zhang, Q., Luo, Q., Wu, Y., Yu, R., Cheng, J., & Zhang, Y. (2021). Construction of a Keggin heteropolyacid/Ni-MOF catalyst for esterification of fatty acids. *RSC Advances, 11*(53), 33416-33424.

Zhang, T., Shahbaz, K., & Farid, M. M. (2020). Glycerolysis of free fatty acid in vegetable oil deodorizer distillate catalyzed by phosphonium-based deep eutectic solvent. *Renewable Energy, 160*, 363-373.

Zhao, H., & Baker, G. A. (2013). Ionic liquids and deep eutectic solvents for biodiesel synthesis: a review. *Journal of Chemical Technology & Biotechnology, 88*(1), 3-12.

Zheng, B., Chen, L., He, L., Wang, H., Li, H., Zhang, H., & Yang, S. (2024). Facile synthesis of chitosan-derived sulfonated solid acid catalysts for realizing highly effective production of biodiesel. *Industrial Crops and Products, 210*, 118058.

Zhou, R., Ye, B., & Hou, Z. (2023). Synthesis of acetylglycerols over hierarchical porous sulfonated polymeric solid acid. *Fuel, 354*, 129325.

Zhu, J., Jiang, W., Yuan, Z., Lu, J., & Ding, J. (2024). Esterification of tall oil fatty acid catalyzed by Zr4+-CER in fixed bed membrane reactor. *Renewable Energy, 221*, 119760.

Zhuo, Y., Cheng, H.-L., Zhao, Y.-G., & Cui, H.-R. (2024). Ionic Liquids in Pharmaceutical and Biomedical Applications: A Review. *Pharmaceutics, 16*(1).